



University
of Glasgow

Giaedi, Abubaker Ammar (1986) A study on the effect of stress level on the vibration frequency of structures. PhD thesis

<http://theses.gla.ac.uk/6738/>

Copyright and moral rights for this thesis are retained by the author

A copy can be downloaded for personal non-commercial research or study, without prior permission or charge

This thesis cannot be reproduced or quoted extensively from without first obtaining permission in writing from the Author

The content must not be changed in any way or sold commercially in any format or medium without the formal permission of the Author

When referring to this work, full bibliographic details including the author, title, awarding institution and date of the thesis must be given.

**" A STUDY ON THE EFFECT OF STRESS LEVEL
ON THE VIBRATION FREQUENCY OF STRUCTURES"**

By

ABUBAKER AMMAR GIAEDI

**Thesis presented for the degree of
Doctor of Philosophy to the Faculty of Engineering
University of Glasgow
Department of Aeronautics and Fluid-Mechanics**



IMAGING SERVICES NORTH

Boston Spa, Wetherby
West Yorkshire, LS23 7BQ
www.bl.uk

BEST COPY AVAILABLE.

VARIABLE PRINT QUALITY

TO THE MEMORY OF MY PARENTS

AMMAR ALMABROUK GIAEDI

&

FATIMA OMAR IMTAIR

ACKNOWLEDGMENTS

I would like to emphasise my deepest gratitude to my supervisor Mr T. H. Cain for his consistent supervision, heuteric advice, useful discussions, and valuable suggestions all the way throughout this research work.

Many thanks to the head of the Aeronautics and Fluid-Mechanics Department, Professor B. E. Richards, for accepting me in his department and for his interest towards the progress of the research activities in the department.

Thanks are due to Alfatah University for the financial support it provided to allow my studies to reach this stage.

Thanks are due to all the technicians who helped in preparing the necessary equipment and material related to this research assignment.

Many thanks are due to my wife Ftaiem, to my children: Haifa, Hala, Wyle, and Anas for the pleasant time they provided me with during our stay in this country.

A. A. Giaedi

October 1986

ABSTRACT

The apparently different physical problems of forced vibrations and elastic stability are both cases of a single phenomenon, the more general expression being the mode of vibration relation with the axial applied load.

This thesis studies the relationship between the frequency of vibration of a loaded structure and the magnitude of the applied loads and its application to the analysis of elastic stability.

In the case of a flat plate, it will be shown that the square of the frequency ratio is very close to being linearly related to the applied inplane loads, and this relation can be extended to include two dimensional and three dimensional frameworks having axial symmetry and subjected to purely axial loads. Experimental and analytical results have been obtained which agree closely with the theoretical predictions (exact or approximate).

A literature review on this subject has disclosed that earlier experimental work appears to contradict the expected results obtained from the theory, especially when three dimensional structures were analysed and tested. A few experiments done in the past years studied only the two dimensional cases with relative success but those dealing with space frames and plate structures led to different conclusions being drawn.

The accuracy of these earlier experiments is questionable and so the results obtained have to be considered critically.

Many components forming the flight vehicle structure are susceptible to various types of aeroelastic instability of which the most noticeable is flutter. However, flutter analyses are, to a large extent, dependent on predictions of vibration frequencies. Characteristics of different structural elements, in particular, three dimensional frames, and plates subjected to inplane loadings and having various constraint situations, could be obtained experimentally as well as theoretically in order to solve for the dynamic problem.

The problem of determining the natural vibration characteristics of isotropic and, more generally, orthotropic rectangular plates in the absence of inplane loads, for various boundary conditions, has been the subject of numerous theoretical and experimental investigations during the past years, but the effect of inplane loads on the natural frequency of simply supported and fully or partially clamped plates has been studied almost entirely analytically, due to difficulties which arose when attempting experimental investigations.

This research will deal with the direct effect of the stress level due to axial loads applied on the axially symmetrical and rigidly jointed space frame structure as well as the isotropic rectangular flat plate (details of the plate analysis are shown in part II of this manuscript) while under forced vibration, and subjected to different boundary conditions.

Experimental results obtained in this investigation are compared firstly with closed-form theoretical results, and then checked against analytical results obtained via computer analysis using the Finite Element Method. Finally, the results are checked against any available results, exact or approximate obtained by other investigators.

An application of the Finite Element Method constitutes an important part of this work by providing the analytical solution to the problem. This method is made as simple and economic as possible by improving on the assembly routines making them easy to check, analyse, and assemble.

The elements chosen for this method of computer analysis are two node bars for the space frame structure, and rectangular elements with four nodes located at the corners for the isotropic plate structure. The node numbering is made in such a way to save space in memory and time of assembly, execution, and space allocation.

This research work leads to a different interpretation of other researchers's experimental and analytical results on both physical and mathematical grounds.

Analytical graphs for each case are suggested to be used in the analytical solution of similar problems if subjected to similar conditions.

Finally, the present experimental method is applied to a cantilevered monocoque beam structure, and a theoretical analyses is done based on the Finite Element Method. Both methods (experimental and analytical) gave a further confirmation of results obtained previously both analytically and experimentally.

TABLE OF CONTENTS

Subject	Page Number
ACKNOWLEDGEMENTS	i
ABSTRACT	ii
TABLE OF CONTENTS	vi
LIST OF SYMBOLS USED IN PART I	x
LIST OF SYMBOLS USED IN PART II	xi

PART I

Stability and Vibrations of 3-D Frame Structures
Subjected to Axial Loads

CHAPTER 1

Background on Frame Analysis

1.1 INTRODUCTION	2
1.2 CONCEPT OF STABILITY	3
1.3 BUCKLING OF FRAME STRUCTURES	6
1.4 MODES OF BUCKLING OF FRAMES	8
1.5 METHODS USED TO FIND THE CRITICAL LOAD	10
1.6 LITERATURE REVIEW	11

CHAPTER 2

Experiment Preparation and Equipment Used

2.1 INTRODUCTION	17
2.2 MATERIAL PROPERTIES	18
2.3 BUCKLING LOAD ESTIMATION	19
2.4 APPARATUS USED	20
2.5 EXPERIMENTAL SET UP PROCEDURE	23

CHAPTER 3

Matrix Analysis and Computer Methods

3.1 DIFFERENCE BETWEEN STIFFNESS AND FLEXIBILITY METHODS	26
3.2 MATRICES AND THE FINITE ELEMENT METHOD	27
3.3 ELEMENTS USED FOR MATRIX ANALYSIS	28
3.3.1 STRESS-STRAIN RELATION	29
3.3.2 WORK AND ENERGY	29
3.3.3 COORDINATE TRANSFORMATIONS	30

Subject	Page Number
3.3.4 DIRECTION COSINE TABLES	31
3.4 CONCEPT OF THE MEMBER STIFFNESS MATRIX	33
3.4.1 ELASTIC STIFFNESS MATRIX	35
3.4.2 GEOMETRIC STIFFNESS MATRIX	39
3.5 CONSISTENT MASS MATRIX	43
3.6 COMPUTATIONS OF BUCKLING LOAD AND NATURAL FREQUENCY OF THE FRAME	45

CHAPTER 4

Experimental and Computer Results

4.1 EXPERIMENTAL RESULTS	46
4.1.1 EXPERIMENTAL GRAPHS	48
4.1.2 OBSERVATIONS ON THE EXP. GRAPHS	51
4.2 FINITE ELEMENT RESULTS COMPARED WITH EXPERIMENTS	56
4.2.1 ANALYTICAL OBSERVATIONS	57
4.2.2 ANALYTICAL GRAPHS	58
4.2.3 COMPARATIVE GRAPHS DISCUSSION	59
4.2.4 COMPARATIVE GRAPHS	60
4.2.5 COMPUTER FLOW CHART	62
4.3 CONCLUSIONS AND DISCUSSIONS	63
REFERENCES	66

PART II

Stability and Vibration of Isotropic Plates and Application

CHAPTER 5

Background and Literature Review

5.1 INTRODUCTION	71
5.2 LITERATURE REVIEW "Plate Buckling"	72
5.3 PLATE STABILITY	74
5.4 CALCULUS OF VARIATION "Applied Cases"	79
5.4.1 STABILITY OF SIMPLY SUPPORTED PLATES	79
5.4.2 PLATE STABILITY UNDER DIFFERENT B.C'S	83
5.5 LITERATURE REVIEW "Plate Vibration"	90
5.6 VIBRATION OF RECTANGULAR PLATES	93
5.6.1 ORTHOTROPIC CONSIDERATIONS	93
5.6.2 ISOTROPIC CONSIDERATIONS	95

CHAPTER 6

The Finite Element Method

6.1 REVIEW	100
6.2 COMPARISON BETWEEN F.E.M. AND OTHER METHODS	102
6.3 GENERAL STEPS TOWARDS THE F.E.M. PROGRAMS	103

Subject	Page number
6.4 FINITE ELEMENTS AND RECTANGULAR PLATES	104
6.4.1 ISOTROPIC PLATE FLOW CHART	110

CHAPTER 7

Concept of Matrix Methods in Plate Analysis

7.1 GENERAL THEORY	111
7.2 DISPLACEMENT FUNCTIONS	113
7.3 STIFFNESS DETERMINATION BASED ON THE ASSUMED DISPLACEMENT FUNCTION	114
7.3.1 GEOMETRIC STIFFNESS MATRIX	119
7.3.2 ELASTIC STIFFNESS MATRIX	120
7.3.3 OTHER GEOMETRIC AND ELASTIC STIFFNESS DEVELOPMENT	122
7.4 MASS MATRIX DETERMINATION	123
7.4.1 MASS MATRIX BASED ON COMPATIBLE DISPLACEMENT	125

CHAPTER 8

Experiments and Equipment Used

8.1 INTRODUCTION	127
8.2 PLATE MODELS	128
8.3 EQUIPMENT USED	131
8.4 EXPERIMENT PROCEDURE	133
8.5 SOME IMPORTANT OBSERVATIONS	134
8.6 EXTENDED USE OF THE EXPERIMENTAL SET UP	135
8.6.1 MONOCOQUE FLOW CHART	137

CHAPTER 9

Correlation between Experimental and Theoretical Analysis

CORRELATION BETWEEN EXPERIMENTS AND THEORY	138
--	-----

CHAPTER 10

Conclusions and Future Prospects

CONCLUSIONS	154
FUTURE PROSPECTS	159
REFERENCES	160

Subject

Page number

APPENDICES

APPENDIX 1	MATHEMATICAL MODEL	169
APPENDIX 2	LINEAR REGRESSION PROSEDURE	174
APPENDIX 3	SPACE FRAME EXPERIMENTAL GRAPHS	178
APPENDIX 4	RESULTS FROM OTHER SOURCES	193
APPENDIX 5	DETERMINATION OF THE ELASTIC AND THE GEOMETRIC STIFFNESS MATRICES	202

LIST OF SYMBOLS USED IN PART I

A	Cross sectional area of the space frame bar..
[A]	Global (total) stiffness matrix.
[B]	Mass and Inertia matrix.
[C]	Total stiffness matrix used in equation 1.15.
c	End fixity coefficient.
d	Diameter of the bar forming the space frame.
d_i	Displacements of the nodes.
E	Young's or Axial Elastic Modulus.
E_{ij}	Elastic stiffness matrix $i=1,12$ and $j=1,12$.
e	Extension of the bar.
G_{ij}	Geometric stiffness matrix.
I	Moment of Inertia.
K	Frequency factor, $K=2\pi^2L^2f_0/a$, $a^2=EI/\rho$.
K_z	Radius of gyration
L	Length of the bar.
l_1, m_1, n_1	Direction cosines.
L_1, L_2	Original and new bar lengths.
m	Mass per unit length.
P	Applied loads.
P_0	Reference load.
P_e	Euler load.
P_{cr}	Critical load.
t	time.
U	Strain energy.
u_i	Nodal displacements and rotations, $i=1,12$.
$\{X\}, \{\ddot{X}\}$	Displacement and acceleration vectors, see eq.1.1.
α	Angle the bars form with the horizontal plane.
$\gamma = \rho AL$	Specific weight.
ρ	Material density.
ξ	Spring constant, see section 1.6.
$\omega = 2\pi f$	Circular frequency.
ω_0	Fundamental (resonant) frequency.
ν	Poisson's ratio.
λ	Eigenvalue.

LIST OF SYMBOLS USED IN PART II

a	Plate length.
b	Plate width.
A_m }	
A_{mn} }	
B_m }	Coefficients of integration, see equation 5.26.
C_m }	
D_m }	
C	Side ratio boundary condition dependent.
D	Plate rigidity.
D_x }	
D_y }	Orthotropic constants
D_{xy} }	
N_{xcr}	Critical load.
K	Buckling stress coefficient, see figure -8-.
m	Half waves in the X-direction.
n	Half waves in the Y-direction.
t	Plate thickness.
u_i, U_i	Nodal displacements $i=1,2$.
U	Strain energy of the plate.
V	Potential energy.
$(U + V)$	Total energy.
W	Deflection function.
$\lambda_x = a/m$	Buckle ratio in the X-direction.
$\lambda_y = b/n$	Buckle ratio in the Y-direction.
ω	Circular frequency.
ρ	Material density.
τ_m }	
}	Coefficients used in equations 5.27 and 5.28.
ϕ_m }	

PART I

**STABILITY AND VIBRATION OF THREE
DIMENSIONAL FRAME STRUCTURE
SUBJECTED TO AXIAL LOADS**

CHAPTER 1

BACKGROUND ON FRAME ANALYSIS

1.1 Introduction

Knowledge of structural stability is of paramount importance to practising structural engineers. In many instances, see references [19] and [21], buckling is the primary consideration in the design of various structural configurations.

Structural engineers often have to study and investigate the dynamical behavior of structures with many degrees of freedom. For example, in the design of frame structures, plates, or shells, the engineer would wish to know the natural frequency of vibration of the system in hand in order to estimate the likelihood of resonance due to external loads.

It is therefore imperative to study both the analytical and the experimental aspects of the problem.

The emphasis in presenting the Finite Element Method of analysis is to determine that it facilitates computational work and is capable of producing results with reasonable accuracy when compared with the exact solutions.

The elastic theory of small deflection assumptions [23] as well as the theories of undamped vibrations [17] and [22] were

used for these analyses. The basic equation of motion to be solved are simplified to have the following mathematical form:

$$[A] \{X\} + \lambda [B] \{\ddot{X}\} = 0 \quad \text{eq. 1.1}$$

Where [A] represents the global stiffness matrix of the structure (elastic and geometric), and [B] represents the mass matrix of the structure including all inertia effects, λ 's are the eigenvalues, $\{X\}$ and $\{\ddot{X}\}$ are the displacement and the acceleration vectors.

The experimental study of model structures is a useful complement to analysis. It is applicable to complicated structures if handled with the needed attention and care.

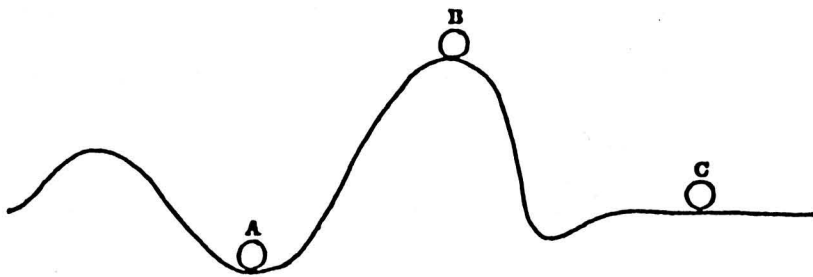
1.2 Concept of Stability

As the external loads are applied quasi-statically, the elastic structure deforms while the static equilibrium is maintained. If, at any level of the external loading, when an infinitesimal external transient disturbance is applied, the structure reacts by simply performing oscillations about the deformed equilibrium state, the equilibrium is said to be stable. The disturbances could be defined in the form of displacement or force.

It is emphasized that when the disturbance is applied, the level of the external loads is kept constant [23].

On the other hand, if the elastic structure either remains in the disturbed position or tends to diverge from the deformed

equilibrium state, the equilibrium is said to be unstable. The least value of the external load corresponding to this condition is the "critical load" or "buckling load". This can be illustrated by the following sketch:



Stability concept

Figure -1-

This system consists of a ball of mass m resting at different points on the surface with zero curvature normal to the plane of the figure. Points of zero slope on the surface denote positions of static equilibrium (points A, B, and C).

However, the character of equilibrium at these points is substantially different. At A, if the system is given an infinitesimal disturbance and released, the ball will simply oscillate about the static equilibrium position A. Such equilibrium position is called stable. At point B, if the process of disturbing is repeated, the mass will tend to move away from the static equilibrium position. Such an equilibrium position B is called unstable.

Finally, at point C, if the system is disturbed, the ball will tend to remain in the disturbed position. Such an equilibrium is called the neutral equilibrium.

In structures or structural elements, the loss of stability is associated with the tendency of the configuration to pass from one deformation pattern to another, the buckling mode. For instance, a long slender column loaded axially will, at the critical condition, pass from the straight configuration (pure compression) to the combined compression and bending state. Similarly, a perfect thin spherical shell under external hydrostatic pressure, at the critical condition, passes from pure membrane state to a combined compression and bending state.

This characteristic of elastic structures has been recognised for many years and it was the first to be used to solve stability problems. Now it allows the analyst to reduce the problem to an eigenvalue problem which is easier to handle by digital computers, since the application of buckling criteria is essential for the designer especially when safety and economy are of prime concern.

Mathematical similarity between the elastic stability and vibration of a structure may be demonstrated by considering the example of a forced vibration relation and the stability of an initially curved beam member, as shown in [4] and [12].

Suppose that the static-deflection function of a uniform beam is expanded in a series of terms corresponding to the modes of vibration. Then it is known that, under a harmonic load, the shape of the deflection curve for a forced vibration with frequency ω is obtained by multiplying all terms of the static-deflection function by:

$$[1/(1 - (\omega/\omega_0)^2)] \qquad \text{eq.1.2}$$

Similarly, it can be shown that if the shape of an initially curved column is expanded in a Fourier series, the shape of the deflection curve under the applied axial load P is obtained by multiplying all terms of the unloaded deflection function by:

$$\left[\frac{1}{1 - P/P_0} \right] \qquad \text{eq.1.3}$$

It is this similarity between the above two factors (eq's 1.2 and 1.3) that might lead one to seek the relation between the applied loads and the square ratio of the frequency of vibration of the structure.

This suspicion will be corroborated for the case of three dimensional frames and isotropic plates axially loaded and subjected to various boundary conditions.

1.3 Buckling of Framed Structures

In aerospace, mechanical, and civil engineering, frames of various types are widely used in main or auxiliary structural configurations. Examples could be found in a helicopter fuselage, an engine mounting, bridges, and multistorey buildings, see [21] and [23]. These frames are subjected to different kinds of loadings, concentrated and distributed, which, in many cases, may cause buckling of an element or group of elements of the frame. Usually, the frame members are rigidly connected to each other as well as to the other structural parts, so that deformation in one element will cause deformations in the neighbouring elements. This may result in loss of stiffness of the whole structure.

Knowledge of the critical buckling load is essential for the design phases of both simple and complex structures.

The theoretical analysis of stability of two dimensional frames is well established so far as structures consisting of members subjected to essentially axial loading are concerned. The discussion of this section will deal primarily with such and similar systems. However, not a great effort has been made, so far, to study the stability of three dimensional frame structures or other complex structural geometries.

In a framework, the members (as a rule) should be rigidly connected to one another at the joints. As a consequence of this, no single compression member can buckle without all the other members in the frame being deformed, in other words, the elastic restraint at the end of a given compression member depends not only on the members immediately connected to it but also on each and every member of the entire system.

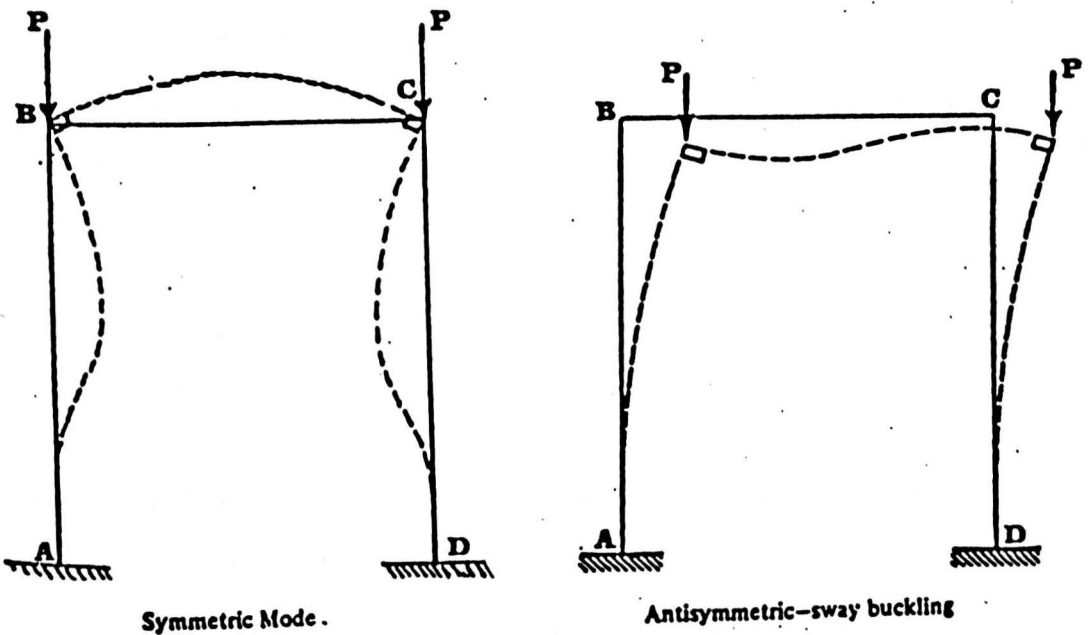
This explains why, when the critical load of a member is of interest, the whole frame will be analysed and investigated as one single unit.

So far as the literature survey is concerned (see section 1.6) all experimental and analytical results found were for two dimensional frames only, and these emphasized correctly [6], for the structural configuration considered, the existence of a linear relationship between the natural frequency ratio squared and the applied axial loads. But very little could be found concerning the same phenomenon for three dimensional frames, which are of great importance in modern antennas and space applications.

The objective of this research work is to enlighten this situation by experimental and theoretical analysis, since the space frame is the most general type of framed structures. The individual member of the space frame may carry a combination of axial force, torsional moment, and bending moments in both principal directions. It is assumed that each member is straight along the axis and that its cross section is uniform throughout its length.

1.4 Modes of Buckling of Frames

Consider the following figure, assuming that the loads are applied in such a way as to avoid any bending moments (the same assumption is used for the three dimensional framework). This is additional to the assumption of small deformation elastic theory [21] in the analysis.



Buckling modes of portal frames

Figure -2-

Cases 1 and 2 show that it is self evident that the buckling takes place when the applied load P is equal to the critical load of the column P_{cr} . It is also clear that the upper end of each column is elastically restrained by the beam which is rigidly connected to the columns, the critical load therefore depends not only on the column stiffness, but also on the stiffness of the beam.

Assumptions can be made on the rigidity of the beam. As shown in the first case, if it is infinitely rigid, then we get four times the Euler load of a column as the critical load for the member. If instead the assumption is made that the beam is infinitely flexible, then the critical value of the load P will be approximately half of the previous one. That is to say:

$$2.05 P_e < P_{cr} < 4P_e \quad \text{eq.1.4}$$

where $P_e = \pi^2 EI/l^2$ is the Euler load.

The same line of thought can be applied to frames whose upper joints are free to move laterally, and the previous relation becomes:

$$0.25 P_e < P_{cr} < P_e \quad \text{eq.1.5}$$

Comparing the above two results, one notices that the buckling load required for the symmetrical buckling case is larger than that required for the antisymmetrical one regardless of the stiffness of the members. It can be concluded therefore, that the above portal frame will always be inclined to buckle sideways

unless it is forced to buckle otherwise, and this is true for multistorey frames [19] if based on the same assumptions.

1.5 Methods Used to Find the Critical Load

The critical load can be calculated analytically by different methods some of which are summarised in this section. For further details on these methods, one can refer to a specific literature study on this subject if needed. Some of the commonly used methods are presented here based on their historical backgrounds:

- 1) Energy Methods.
- 2) Finite Difference Method.
- 3) Finite Strip Method.
- 4) Finite Element Method.

Some of these methods will be used in the analytical study of this research work, they will be illustrated and used to solve for the space frame and flat plate analyses.

The Finite Element Method based on the Matrix Analysis Method is selected for its proven computational advantages over the other methods.

1.6 Literature Review

The topic of the relationship between the stability and the vibration of structures has a long history. It has been the interest of many scientists since 1929, when Grauers first studied the rectangular plate subjected to vibration. However, no conclusions were drawn out of that study. In 1936, Stephens [20] provided some useful results although his analyses were incorrect, as will be explained later. He was one of the first to attempt this kind of analysis with relative success.

Chu [6] in 1949, had tested and confirmed the existence of a linear relation between the square of the frequency and the applied loads in the cases of a pin-jointed column and a two dimensional framework.

Even though most of Chu's work [6] was useful and reliable, there still remains much to learn about the three dimensional frames and other more complicated structures (plates and shells).

Stephens, in his 1936 paper, was one of the first scientists to present experimental methods for determining:

- 1) The degree of end restraint of a structural member.
- 2) The magnitude of the load by frequency measurement.

He used D'Alembert's principal to obtain the vibration and deflection equations but, considered only the transverse translational inertia, neglecting effects due to any rotary inertias which might arise. This is considered to restrict his approach to only one class of deflection behaviour.

Starting from the partial differential equation of motion:

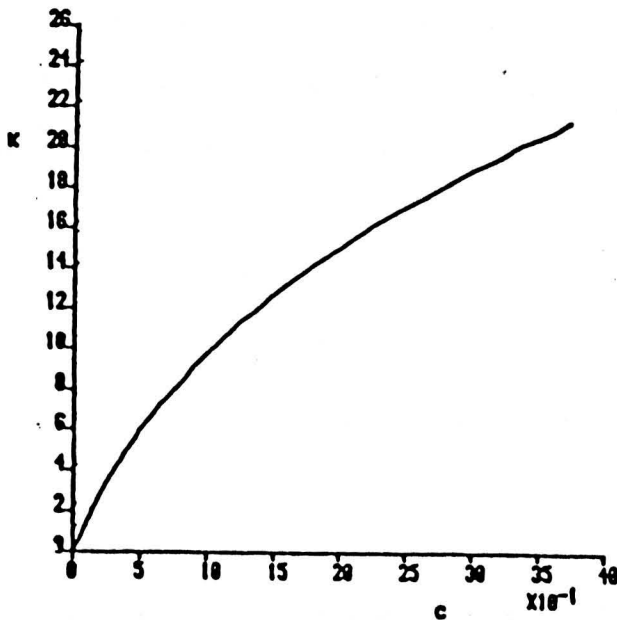
$$m^2 \frac{\partial^4 Y}{\partial X^4} + \frac{\partial^2 Y}{\partial t^2} = 0 \quad \text{eq.1.6}$$

which includes all material properties, deflections, and the time variations, leads to a straight-forward solution of the above linear fourth order partial differential equation as:

$$Y = A \cos \omega t + B \sin \omega t \quad \text{eq.1.7}$$

where, A and B are functions of X, and ω , and $\omega = 2 \pi f$.

Applying the boundary conditions he evaluated the unknowns A and B, and obtained a graph relating K to c, which is reproduced in figure-3-.



Stephen c-K relation, ref.[20]

Figure -3-

Where, c is the end fixity coefficient, K is the frequency factor, $2\pi L^2 f_0/a$, and $a = \sqrt{EI/\rho}$.

However, Stephens's relationship between K and c is not unique, since there may be more than one value of K corresponding to each value of c . This might be expected from the physics of the problem, the following argument to illustrate it is made as follows:

It is feasible for two identical bars with differently restrained ends to have the same fixity coefficient c . However, different modes of vibration and hence, different frequencies would be anticipated.

We considered a strut elastically restrained at each end, and assumed the restraint to be such as to give an end fixity coefficient c equals to 2.047 (one end fixed, the other pinned). The value of K for such a strut could be calculated. Assuming the same spring constant on both sides and the length of the strut to be $2L$, and taking the origin of the coordinates at the midpoint of the strut, then the boundary conditions will be:

$$Y = 0 \quad \text{at} \quad X = \pm L$$

and
$$EIY'' = \mp \xi Y' \quad \text{at} \quad X = \pm L$$

where ξ is the spring constant.

According to Lurie [13] the general buckling solution of the fourth order ordinary differential equation is of the type :

$$Y = A \cos \beta X + B \sin \beta X + D X + F \quad \text{eq.1.8}$$

where $\beta^2 = \frac{P}{EI}$ and $P = c \frac{\pi^2 EI}{4L^2}$

By applying the boundary conditions the unknowns could be found easily and :

$$\beta = \frac{\pi \sqrt{c}}{2L} \quad \text{eq.1.9}$$

$$\alpha = \pi EI \frac{\sqrt{c}}{2L} \cot \frac{\pi \sqrt{c}}{2} \quad \text{eq.1.10}$$

But, from Timoshenko and Young [22] the general solution to the free vibration equation is given as:

$$Y = A \cos \lambda X + B \sin \lambda X + D \cosh \lambda X + F \sinh \lambda X \quad \text{eq.1.11}$$

where $\lambda^4 = \frac{m \omega^2}{EI}$ and m is the mass per unit length.

By applying the above boundary conditions:

$$\text{Then, } \alpha = \frac{2EI\lambda}{\tan \lambda L + \tanh \lambda L} \quad \text{eq.1.12}$$

Since α should be the same for both cases, then:

$$\frac{2 EI\lambda}{\tan \lambda L + \tanh \lambda L} = \frac{\pi EI \sqrt{c}}{2L} \cot \frac{\pi \sqrt{c}}{2} \quad \text{eq.1.13}$$

Now, using the value of $c = 2.047$, then we find that-

$$K = (2\lambda L)^2 = 14.258 \quad \text{eq.1.14}$$

According to Stephens [20], $K = 15.421$, which does not agree with equation 1.14. This may allow us to conclude that the single relation between c and K as accepted by Stephens in his earlier work [20] is not justifiable, and it suggests that the values on the curve might be higher.

Lurie [12] 1952, did verify Chu's work [6], checked the simply supported column using experimental tests, both (Lurie and Chu) obtained a good agreement for the plane frame analysis, but for the rectangular plate tests the extrapolated critical value appears to be lower than the exact (theoretical) value. The linear relationship between applied loads and the square of the frequency is no longer obtainable by Lurie for the isotropic plates and, to a certain extent, even for space frames, which leaves one suspecting either the accuracy of the instrumentations used or in the interpretation of conclusions drawn and results obtained.

In 1955, Bishop [4] provided a numerical technique based on related tables to calculate the natural frequencies of vibrating plane frames. Some experiments were conducted to check the natural frequency of the plane frames, and his method was shown to facilitate the determination of the principal modes of vibrations. He admitted [4] that the natural frequency equations become extremely complicated as the number of beams embodied in the structure is increased.

Bishop's method is claimed to be exact as far as the elementary theory [21] of beam vibration is concerned, but this method is indeed in contrast with the well known energy method based on Lord Rayleigh's principle [17]. This energy principle is known to produce only an approximate solution, but a reliable one.

Bishop's method, when tested on symmetric and antisymmetric portal frames, found the first six natural frequencies which were in very good agreement with his own previous analysis.

Nevertheless, all his and other previous analyses as well as the related tests were of extreme importance to the research on the frame structures at that period of time, but, unfortunately, for the space frame structures this method did not demonstrate its power to solve the dynamic problem (buckling and vibration combined).

In 1964, Gladwell [8] solved the same problem as that done by Bishop [4] using another method, based on an assumed mode shape instead of Bishop's tables, and setting all his analysis in a matrix form. This matrix formulation has the advantage over all the previous analyses if digital computers are to be used.

Stability and inertia matrices were emphasised in an equation of the type:

$$(C - \omega^2 A) U = 0 \quad \text{eq.1.15}$$

Where, by the stability matrix C is meant the total of the elastic and the geometric matrices, and by the inertia matrix A the mass and inertia of the main structure, so that equation 1.15 is similar to equation 1.1.

Kinetic and Potential energy were evaluated successfully, and it was demonstrated that, especially when the structure tends to be geometrically more complicated, the matrix form is more convenient to use.

CHAPTER 2

EXPERIMENTAL PREPARATION AND EQUIPMENT USED

2.1 Introduction

Over the years, a few investigations had been conducted to correlate theory and experiments. Chu [6] was one of the first in trying to verify the relation between the applied loads and the frequency of vibrations; his investigation dealt only with two dimensional frames and portal frames. Although he obtained a linear relationship between the axial applied loads versus the square of the frequency ratio, these results were criticised by Lurie [11] in 1951 as being not so conclusive and general as one expects to achieve. Lurie [12] in a later paper stated that, from energy considerations, this relation could not describe the true behaviour which relates the two phenomena of buckling and vibration. However, no further discussions were obtained to sustain these conclusions.

Lurie [11] produced similar results as Chu [6] for the same portal frame structure and then he attempted other types of two dimensional structures (rigidly jointed trusses) for which he reported different conclusions. Furthermore, Lurie tried the same experiment on an isotropic plate subjected to axial loads and

caused to vibrate, concluding, again, that a nonlinear relation exists between the applied loads and the square of the frequency of vibration ratio.

One of the objectives of the present experimental work on three dimensional structures (space frames and isotropic plates) is to find a reliable relationship between theoretical predictions and experimental verifications, and to give the possible reasons behind the discrepancies found between theory and experiments.

Sources of error in experimentation can be numerous; one should be careful at all stages of an experiment, by giving full attention to most particulars.

Provided this is done, attention can be devoted to interpreting the results obtained from the graphs produced from the data obtained by both theory and experimentation.

2.2 Material Properties

As one of the sources of error mentioned in the above section (2.1), the material properties could, if not verified carefully, lead to differences between the final analytical and theoretical results.

Property tests on the material used in these experiments gave a density and an elastic modulus which differed slightly from the values quoted in the literature.

Direct tension tests were conducted on a material specimen using an Instron Tensile Machine connected to an XY-Recorder Type 26000 A3 by Bryans Industries to verify the material properties before testing starts.

2.3 Buckling Load Estimation

After deciding on the geometry of the space frame (see figure 7) to be tested, one could easily produce a rough estimate of its static buckling load by assuming the applied loads to act along the vertical axis of the frame so that each bar is loaded axially and, hence, each bar is subjected to the same amount of stress.

The buckling value for this space frame was estimated to be about 360 Newtons. The need to experimentally achieve equal axial loads in each member of the space frame led to the use of a spherical bearing located at the point of intersection of the axes of the members.

To help in avoiding some problems which could have been the cause of some of the errors in previous works, problems such as the mass of the load associated with the main mass of the structure, and the presence of some undesired bending or torsional moments due to the load position being some distance away from the point of application of the applied load to the structure, especially when the system is vibrating, a spring is introduced to carry the applied loads, transmitting them to the point of the axes intersection. This spring is suspended from the spherical bearing.

The point of the application of the load is very important if the presence of bending or torsional moments is undesired. When present, surely they will change the experimental conditions and results.

In studying the problem as conducted by Lurie [12] on the two dimensional rigid jointed truss and the isotropic plate, it was realised that part of the claim of nonlinear behaviour of the structure may have been caused on the one hand, by some bending moments due to the position of the applied loads, or, on the other hand, by the mass of the main structure being effectively increased by the applied load masses.

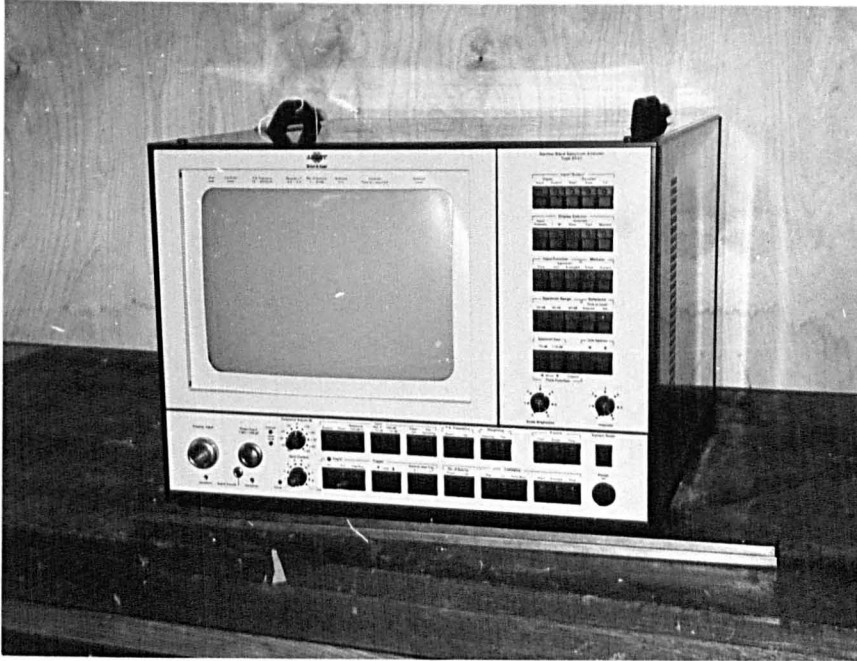
2.4 Apparatus Used

Since accuracy is a major objective of this research work, all the instruments used have been tested and calibrated. Some of these instruments had been calibrated by the manufacturer, but others had to be calibrated in the laboratory. The instruments used are:

- 1) A Narrow Band Spectrum Analyser Type 2031, see figure-4-, which has been designed and tested by the manufacturer according to class II of IEC Publications 348. The spectral analysis takes place in 400 constant bandwidth lines across a frequency range which is selectable from 0_10 Hz to 0_20 KHz. The analysis takes place in real time for the whole frequency range.

The results produced could be averaged exponentially or linearly prior to displaying them on an 11 inches display screen, which may also be used to show the time function and the instantaneous spectrum. The instrument could hold the maximum spectrum when desired by the analyst, it is also supplied with a memory and could be connected to a computer and a plotter to plot stored data and analyse it.

The N.B.S.A. analyses the frequency by Fourier Transform Procedure (FTP) in the form of Discrete Fourier Transform (DFT) for a finite number of discrete samples.



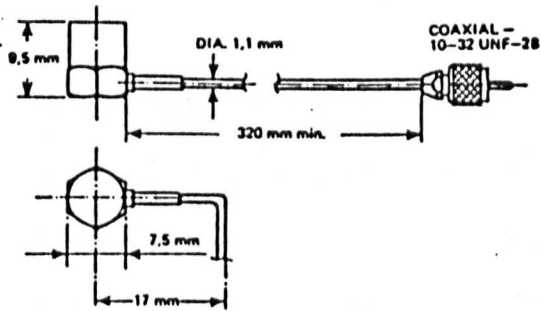
Narrow Band Spectrum Analyser

Figure -4-

2) An Exciter is used in contact with the structure through a transmitter, and activated by either a Function Generator Type TWG 501, or, for more precise harmonic waves, by a Beat Frequency Oscillator Type 1022. The input frequency of vibration could be varied continuously.

3) Philips Multimeter Type PM 2521 Automatic, to check the input frequency.

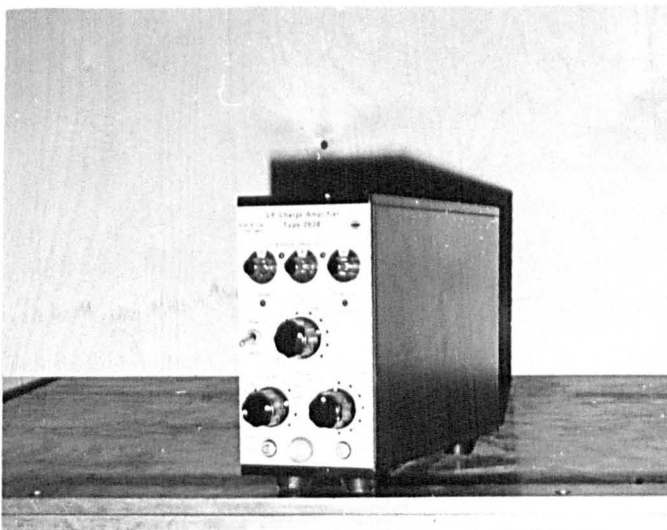
4) A light-weight piezo-electric Accelerometer Type B&K 4375, made of titanium, with given manufacturer calibration and other specifications as shown below:



Accelerometer used

Figure-5-

5) The accelerometer is connected to a Low Frequency Charge Amplifier of Type B & K 2628, which has been calibrated and checked earlier in the laboratory. This charge amplifier is directly connected to the Narrow Band Spectrum Analyser, both instruments form the output of the system.



Charge amplifier

Figure-6-

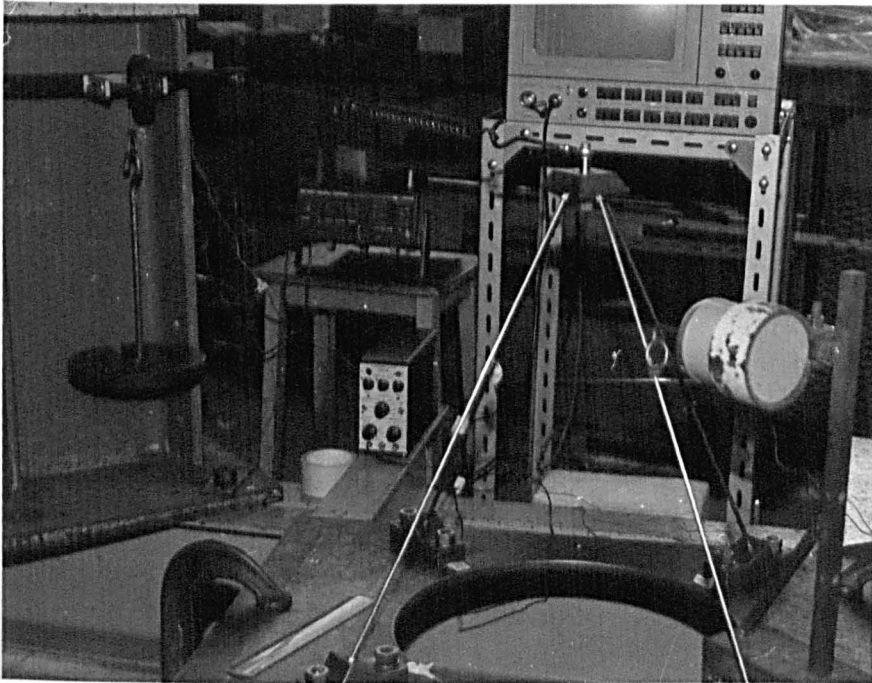
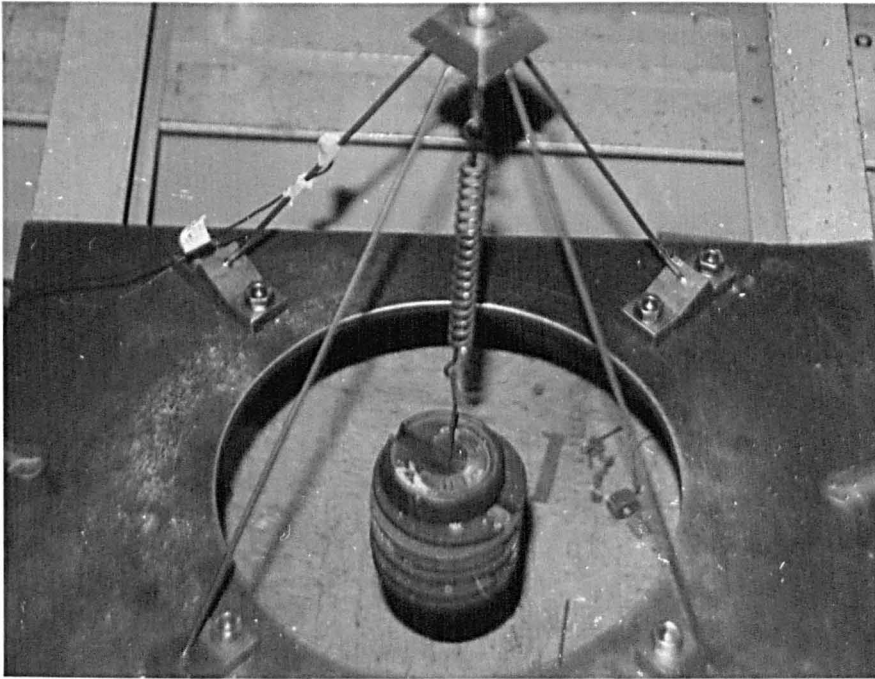
6) Strain gauges of Type N11_FA_8_120_23 of resistance of about 120 Ω are located at various positions of the structure (use of these strain gauges is necessary in the case of the plate structures only). These strain gauges are connected to an extension box.

7) An extension box, Peekel type 5UD; only a quarter bridge gauge is needed for the analyses, this box is connected to a strain gauge reader.

8) A strain gauge instrument, Peekel type 581 DNH, which reads each individual direct strain value.

2.5 Experimental Set Up Procedure

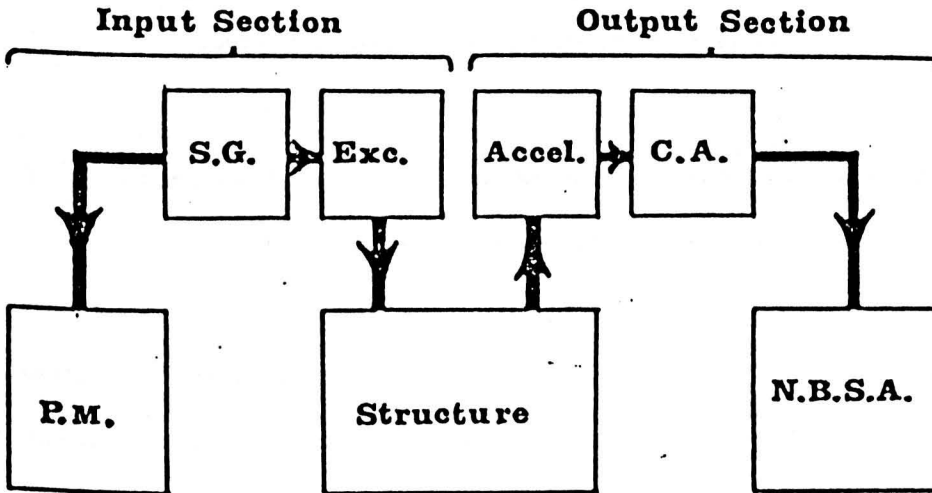
The space frame structure to be tested is formed of four solid bars made of brass type BS 2874 M_Extruded, 470 mm long, and 4.75 mm in diameter. All the four bars are rigidly connected at one end to a joint fitting in which a bearing is housed at the calculated point of intersection of the axes of the bars. The bearing supports a short link to which the spring is connected. The other end of each frame bar is rigidly fixed to a horizontal steel foundation plate with a circular hole at its centre to accommodate the load to pass freely. The shape of the complete space frame structure is shown in figure- 7 -



The space frame used

Figure - 7 -

A schematic sketch diagram of the space frame structure and all equipment connected to it is shown in the figure below:



Schematic diagram of the experimental set up

Figure-8-

- * S.G. = Signal Generator.
- * EXC. = Exciter.
- * ACCEL.= Accelerometer.
- * C.A. = Charge Amplifier.
- * P.M. = Phillips Multimeter.
- * N.B.S.A. = Narrow Band Spectrum Analyser.

CHAPTER 3

MATRIX ANALYSIS AND COMPUTER METHOD

3.1 Difference between Stiffness and Flexibility Methods

The ready availability of digital computers has revolutionised the analysis and, to a lesser extent, the design of complex structures. They can be programmed to perform extremely complex calculations with the minimum input of base data. Matrix structural analysis based on the displacement method is particularly suited to exploit the power of computers, see ref [1] and [3].

One of the advantages of the displacement (stiffness) method over the force (flexibility) method is that it is more conducive to computer programming. Once the analytical model of a structure has been defined, no further engineering decisions are required in the displacement (stiffness) method in order to carry out the analysis. In this respect it differs from the flexibility method, although the two methods have similar mathematical forms.

In the flexibility method the unknown quantities are redundant actions that must be arbitrarily chosen; but in the stiffness method the unknowns are the joint displacements which are automatically specified in the structure. Thus, in the displacement method the number of unknowns to be calculated is the

same as the number of independent components of displacement associated with the node (joint) system of the structure.

Another attractive aspect of the stiffness method is that the technique varies very little as the structural form is changed from the two dimensional frame to the three dimensional frame or to even more complex structures such as plates or shells, while the flexibility method could widely vary.

3.2 Matrices Use in the Finite Element Method

It is the responsibility of the design engineer to devise arrangements and proportions of members that can withstand economically and efficiently the conditions anticipated during the life-time of the structure. The central aspect of this function is the calculation of the distribution of stresses within the structure and the displacement state of the system. It is useful to show and describe modern methods of performing this kind of calculation, in particular for a structure such as those used here (space frame and plate) under elastic linear behaviour where elementary theory assumptions are used, see [2] and [3].

It is recognized that for anything other than a one dimensional structure it is not likely to be easy to give an exact solution, therefore it is imperative to use numerical methods such as Finite Element Method or Finite Strip Method, where the basic concept is that any continua can be modeled analytically by subdividing it into elements, each of which can be assumed to have the same form of displacement function, considering, of course, the right set of boundary conditions.

Obviously the Finite Element Method and Matrix Analysis are complementary. The methods of matrix algebra are used to facilitate the analysis of the numerous equations resulting from the application of the Finite Element Method of representing a structure. This relation is used in the theoretical analysis of this work.

3.3 Elements Used for Matrix Analysis

The main purpose of this work is the development and use of the stiffness matrix for a twelve degrees of freedom member as representative of an element of the space frame and as shown below:

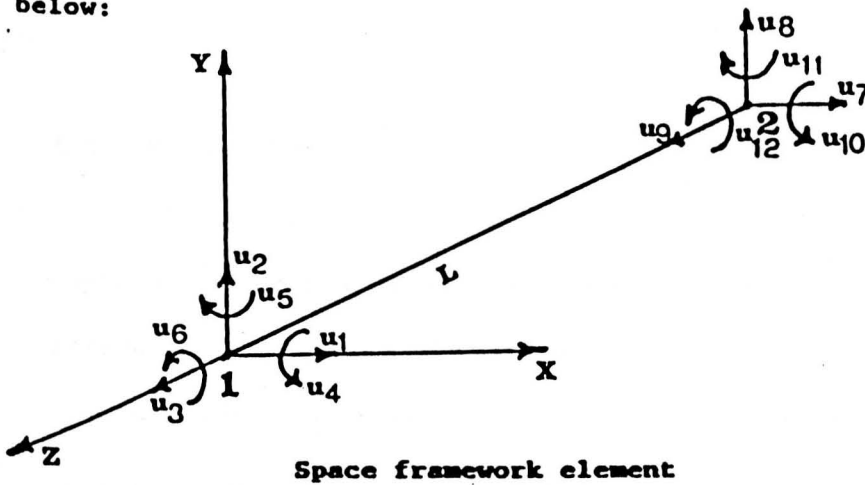


Figure-9-

The construction of the matrix requires an understanding of the stress-strain behaviour in the structure, furthermore it is facilitated by the use of energy principles and theorems. These concepts could have been thoroughly studied but, since they are described in many texts, only a brief discussion is presented here.

3.3.1 Stress-Strain Relation

Homogeneity and isotropy assumptions of the material used lead to the stress-strain relationship being defined by three properties which are:

- i_ E, Young's Modulus which is the ratio of direct stress to corresponding strain in a uniaxially stressed element.
- ii_ G, Shear Modulus, representing the ratio of shearing stresses to shearing strains.
- iii_ ν , Poisson's Ratio, as the numerical value of the ratio of transverse strain to axial strain in the deformed uniaxially stressed element.

3.3.2 Work and Energy

The relationship between force and displacement at a point could be represented by the work done on a structure by the external forces when the point is given unit displacement. The strain energy the structure can gain for a given displacement is presented in the following equation:

$$U = 1/2 [F]\{\Delta\} \qquad \text{eq.3.1}$$

Which is equal to the work done on the structure. Equation 3.1 is true if the assumed linear relationship between stress and strain holds, in other words, if the small deflection theory assumptions are used.

3.3.3 Coordinate Transformations

Very often in structural analysis, it is needed to resolve forces and couples into components along and perpendicular to the structure's axis. For the three dimensional structures a coordinate transformation procedure is applied. Direction cosines are the cosines of the angles between the member axis and the set of orthogonal reference axes, these will be used to form the transformation matrix needed. Usually they are denoted by letters such as l, m, n corresponding to $x-, y-, z-$ axes respectively. For three dimensional structures a transformation matrix of 3-rows by 3-columns is available in the literature. The direction vectors of the element axes are given in the following matrix which is the basis for the space frame transformation used to resolve both the forces and the couples.

$$\begin{bmatrix} d_1 \\ d_2 \\ d_3 \end{bmatrix} = \begin{bmatrix} l_1 & m_1 & n_1 \\ l_2 & m_2 & n_2 \\ l_3 & m_3 & n_3 \end{bmatrix} \quad \text{eq.3.2}$$

Where each of l_i, m_i, n_i ($i= 1,2,3$) represents the direction cosines of the orientations of the element axes (local axes) with respect to the reference axes (global axes).

3.3.4 Direction Cosine Tables for the 3-D Space Frame Used

Dividing each bar into two elements for simplicity, where both parts of each bar will have the same direction cosines as will be shown in the following tables. All values agree with orthogonality conditions. It is necessary that for each set a transformation matrix is assigned, but for the computer analysis this could be done automatically when dealing with many elements.

$$R_{1,5} = \begin{bmatrix} 0 & -0.866 & 0.5 \\ 0 & 0.5 & 0.866 \\ -1.0 & 0 & 0 \end{bmatrix}$$

$$R_{2,6} = \begin{bmatrix} -0.5 & -0.866 & 0 \\ 0.866 & -0.5 & 0 \\ 0 & 0 & 1.0 \end{bmatrix}$$

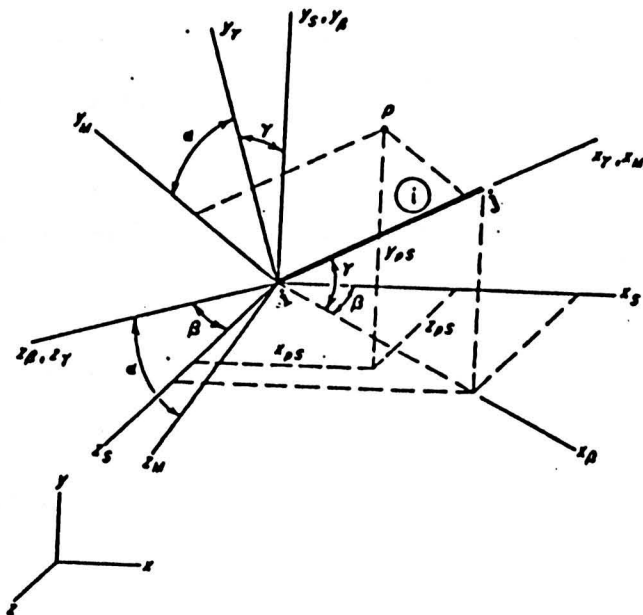
$$R_{3,7} = \begin{bmatrix} 0 & -0.866 & -0.5 \\ 0 & 0.5 & -0.866 \\ -1.0 & 0 & 0 \end{bmatrix}$$

$$R_{4,8} = \begin{bmatrix} 0.5 & -0.866 & 0 \\ 0.866 & 0.5 & 0 \\ 0 & 0 & 1.0 \end{bmatrix}$$

where, $R_{i,j}$ ($i= 1,2,3,4$, and $j= 5,6,7,8$) is the direction cosine matrix for elements i and j as shown above. The above are obtained from the general calculation of the direction cosines following the procedure based on an angle of orientation α , which denotes the angle between the two sets of axes having one axis in common.

$$R = \begin{bmatrix} C_x & & C_y & & C_z \\ -\frac{C_x C_y \cos \alpha - C_z \sin \alpha}{\sqrt{C_x^2 + C_z^2}} & \sqrt{C_x^2 + C_z^2} \cos \alpha & -\frac{C_y C_z \cos \alpha + C_x \sin \alpha}{\sqrt{C_x^2 + C_z^2}} \\ C_x C_y \sin \alpha - C_z \cos \alpha & -\sqrt{C_x^2 + C_z^2} \sin \alpha & \frac{C_y C_z \sin \alpha + C_x \cos \alpha}{\sqrt{C_x^2 + C_z^2}} \end{bmatrix}$$

Using the information of the above table, one could easily produce tables in R_{ij} as shown in the earlier tables, see Weaver et al. [23].



Rotation of axes for the space frame member

Figure-10-

3.4 Concept of the Member Elastic Stiffness Matrix

Essentially, the concept of the elastic stiffness matrix can be understood by considering the simple case of a pin-jointed element of the frame structure.

Assuming linear elasticity, one could use the following equations:

$$\text{from the equilibrium of forces: } F_1 + F_2 = 0 \quad \text{eq.3.4}$$

where F is a force in the direction of the element axis and positive in the sense 1-2.

$$\text{the net extension of the bar: } e = L_2 - L_1 \quad \text{eq.3.5}$$

where L_1 is the initial, unloaded length and L_2 is the final, loaded length.

$$\text{axial strain: } \epsilon_a = (L_2 - L_1)/L_1 \quad \text{eq.3.6}$$

$$\text{axial stress: } \sigma_a = E \epsilon_a \quad \text{eq.3.7}$$

$$\text{axial force: } F_2 = -F_1 = \sigma_a A \quad \text{eq.3.8}$$

having followed all above steps, one end up with:

$$\begin{Bmatrix} F_1 \\ F_2 \end{Bmatrix} = EA/L_1 \begin{bmatrix} 1 & -1 \\ -1 & 1 \end{bmatrix} \begin{Bmatrix} L_1 \\ L_2 \end{Bmatrix} \quad \text{eq.3.9}$$

If one uses the transformation matrix [R], this analysis could be extended to the three dimensional structures. Without getting into further details, the elastic stiffness, the geometric stiffness, and the mass matrices which were used for our computational Finite Element Analysis of the space frame structure have been reproduced in the following pages in a lower triangular matrix form.

All above matrix terms E_{ij} have the following values:

$$E_{11} = l_1^2 \rho^2 + 12 l_2^2 + 12 Cl_3^2$$

$$E_{21} = l_1 m_1 \rho^2 + 12 l_2 m_2 + 12 Cl_3 m_3$$

$$E_{22} = m_1^2 \rho^2 + 12 m_2^2 + 12 Cm_3^2$$

$$E_{31} = n_1 l_1 \rho^2 + 12 n_2 l_2 + 12 Cn_3 l_3$$

$$E_{32} = m_1 n_1 \rho^2 + 12 m_2 n_2 + 12 Cm_3 n_3$$

$$E_{33} = n_1^2 \rho^2 + 12 n_2^2 + 12 Cn_3^2$$

$$E_{41} = 6 Ll_2 l_3 - 6 LCl_2 l_3$$

$$E_{42} = 6 Ll_3 m_2 - 6 LCl_2 m_3$$

$$E_{43} = 6 Ln_2 l_3 - 6 LCl_2 n_3$$

$$E_{44} = l_1^2 L^2 q + 4 L^2 Cl_2^2 + 4 L^2 l_3^2$$

$$E_{51} = 6 Ll_2 m_3 - 6 LCl_3 m_2$$

$$E_{52} = 6 Lm_2 m_3 - 6 Lcm_2 m_3$$

$$E_{53} = 6 Ln_2 m_3 - 6 Lcm_2 n_3$$

$$E_{54} = l_1 m_1 L^2 q + 4 L^2 Cl_2 m_2 + 4 L^2 l_3 m_3$$

$$E_{55} = m_1^2 L^2 q + 4 L^2 Cm_2^2 + 4 L^2 m_3^2$$

$$E_{61} = 6 Ll_2 n_3 - 6 LCn_2 l_3$$

$$E_{62} = 6 Lm_2 n_3 - 6 LCm_3 n_2$$

$$E_{63} = 6 Ln_2 n_3 - 6 LCn_2 n_3$$

$$E_{64} = n_1 l_1 L^2 q + 4 L^2 Cn_2 l_2 + 4 L^2 n_3 l_3$$

$$E_{65} = m_1 n_1 L^2 q + 4 L^2 Cm_2 n_2 + 4 L^2 m_3 n_3$$

$$E_{66} = n_1^2 L^2 q + 4 L^2 Cn_2^2 + 4 L^2 n_3^2$$

$$E_{71} = -l_1^2 \rho^2 - 12 l_2^2 - 12 Cl_3^2$$

$$E_{72} = -l_1 m_1 \rho^2 - 12 l_2 m_2 - 12 Cl_3 m_3$$

$$E_{73} = -l_1 n_1 \rho^2 - 12 l_2 n_2 - 12 Cl_3 n_3$$

$$E_{74} = 6 LCl_2 l_3 - 6 Ll_2 l_3$$

$$E_{75} = 6 LCl_3 m_2 - 6 Ll_2 m_3$$

$$\begin{aligned}
E_{76} &= 6 LC_{13}n_2 - 6 Ll_2n_3 \\
E_{77} &= 1_1^2\rho^2 + 12 1_2^2 + 12 Cl_3^2 \\
E_{81} &= - 1_1m_1\rho^2 - 12 1_2m_2 - 12 Cl_3m_3 \\
E_{82} &= - m_1^2\rho^2 - 12 m_2^2 - 12 Cm_3^2 \\
E_{83} &= - n_1m_1\rho^2 - 12 m_2n_2 - 12 Cm_3n_3 \\
E_{84} &= 6 LC_{12}m_3 - 6 L 1_3m_2 \\
E_{85} &= 6 Lcm_2m_3 - 6 Lm_2m_3 \\
E_{86} &= 6 Lcm_3n_2 - 6 Lm_2n_3 \\
E_{87} &= 1_1m_1\rho^2 + 12 1_2m_2 + 12 Cl_3m_3 \\
E_{88} &= m_1^2\rho^2 + 12 m_2^2 + 12 Cm_3^2 \\
E_{91} &= - n_1l_1\rho^2 - 12 n_2l_2 - 12 Cn_3l_3 \\
E_{92} &= - m_1n_1\rho^2 - 12 m_2n_2 - 12 Cm_3n_3 \\
E_{93} &= - n_1^2\rho^2 - 12 n_2^2 - 12 Cn_3^2 \\
E_{94} &= 6 LC_{12}n_3 - 6 Ll_3n_2 \\
E_{95} &= 6 Lcm_2n_3 - 6 Lm_3n_2 \\
E_{96} &= 6 Lcn_2n_3 - 6 Ln_2n_3 \\
E_{97} &= n_1l_1\rho^2 + 12 n_2l_2 + 12 Cl_3n_3 \\
E_{98} &= m_1n_1\rho^2 + 12 m_2n_2 + 12 Cm_3n_3 \\
E_{99} &= n_1^2\rho^2 + 12 n_2^2 + 12 n_3^2 \\
E_{101} &= 6 Ll_2l_3 - 6 LC_{12}l_3 \\
E_{102} &= 6 Ll_3m_2 - 6 LC_{12}m_3 \\
E_{103} &= 6 Ll_3n_2 - 6 LC_{12}n_3 \\
E_{104} &= - L^2 1_1^2 q + 2 L^2 Cl_2^2 + 2 L^2 l_3^2 \\
E_{105} &= - L^2 1_1 m_1 q + 2 L^2 Cl_2 m_2 + 2 L^2 l_3 m_3 \\
E_{106} &= - L^2 1_1 n_1 q + 2 L^2 Cl_2 n_2 + 2 L^2 l_3 n_3 \\
E_{107} &= 6 LC_{12}l_3 - 6 Ll_2l_3
\end{aligned}$$

$$\begin{aligned}
E_{108} &= 6 LCl_2m_3 - 6 Ll_3m_2 \\
E_{109} &= 6 LCl_2n_3 - 6 Ll_3n_2 \\
E_{1010} &= L^2l_1^2q + 4 L^2Cl_2^2 + 4 L^2l_3^2 \\
E_{111} &= - 6 LCl_3m_2 + 6 Ll_2m_3 \\
E_{112} &= - 6 Lcm_2m_3 + 6 Lm_2m_3 \\
E_{113} &= - 6 Lcm_2n_3 + 6 Lm_3n_2 \\
E_{114} &= - L^2l_1m_1q + 2 L^2Cl_2m_2 + 2 L^2l_3m_3 \\
E_{115} &= - L^2m_1^2q + 2 L^2Cm_2^2 + 2 L^2m_3^2 \\
E_{116} &= - L^2m_1n_1q + 2 L^2Cm_2n_2 + 2 L^2m_3n_3 \\
E_{117} &= 6 LCl_3m_2 - 6 Ll_2m_3 \\
E_{118} &= 6 Lcm_2m_3 - 6 Lm_2m_3 \\
E_{119} &= 6 Lcm_2n_3 - 6 Lm_3n_2 \\
E_{1110} &= L^2l_1m_1q + 4 L^2Cl_2m_2 + 4 L^2l_3m_3 \\
E_{1111} &= L^2m_1^2q + 4 L^2Cm_2^2 + 4 L^2m_3^2 \\
E_{121} &= 6 Ln_3l_2 - 6 Lcn_2l_3 \\
E_{122} &= 6 Lm_2n_3 - 6 Lcm_3n_2 \\
E_{123} &= 6 Ln_2n_3 - 6 Lcn_2n_3 \\
E_{124} &= - L^2l_1n_1q + 2 L^2Cl_2n_2 + 2 L^2l_3n_3 \\
E_{125} &= - L^2m_1n_1q + 2 L^2Cm_2n_2 + 2 L^2m_3n_3 \\
E_{126} &= - L^2n_1^2q + 2 L^2Cn_2^2 + 2 L^2n_3^2 \\
E_{127} &= 6 LCl_3n_2 - 6 Ll_2n_3 \\
E_{128} &= 6 Lcm_3n_2 - 6 Lm_2n_3 \\
E_{129} &= 6 Lcn_2n_3 - 6 Ln_2n_3 \\
E_{1210} &= L^2l_1n_1q + 4 L^2Cl_2n_2 + 4 L^2l_3n_3 \\
E_{1211} &= L^2m_1n_1q + 4 L^2Cm_2n_2 + 4 L^2m_3n_3 \\
E_{1212} &= L^2n_1^2q + 4 L^2Cn_2^2 + 4 L^2n_3^2.
\end{aligned}$$

All above matrix terms have the following values:

$$G_{11} = 36 (l_2^2 + l_3^2)$$

$$G_{21} = 36 (l_2 m_2 + l_3 m_3)$$

$$G_{22} = 36 (m_2^2 + m_3^2)$$

$$G_{31} = 36 (l_2 n_2 + l_3 n_3)$$

$$G_{32} = 36 (m_2 n_2 + m_3 n_3)$$

$$G_{33} = 36 (n_2^2 + n_3^2)$$

$$G_{41} = 0$$

$$G_{42} = 3L (l_3 m_2 - l_2 m_3)$$

$$G_{43} = 3L (l_3 n_2 - l_2 n_3)$$

$$G_{44} = 4L^2 (l_2^2 + l_3^2)$$

$$G_{51} = 3L (l_2 m_3 - l_3 m_2)$$

$$G_{52} = 0$$

$$G_{53} = 3L (m_3 n_2 - m_2 n_3)$$

$$G_{54} = 4L^2 (l_2 m_2 + l_3 m_3)$$

$$G_{55} = 4L^2 (m_2^2 + m_3^2)$$

$$G_{61} = 3L (l_2 n_3 - l_3 n_2)$$

$$G_{62} = 3L (m_2 n_3 - m_3 n_2)$$

$$G_{63} = 0$$

$$G_{64} = 4L^2 (n_2 l_2 + n_3 l_3)$$

$$G_{65} = 4L^2 (m_2 n_2 + m_3 n_3)$$

$$G_{66} = 4L^2 (n_2^2 + n_3^2)$$

$$G_{71} = -36 (l_2^2 + l_3^2)$$

$$G_{72} = -36 (l_2 m_2 + l_3 m_3)$$

$$G_{73} = -36 (l_2 n_2 + l_3 n_3)$$

$$G_{74} = 0$$

$$G_{75} = 3L (l_3 m_2 - l_2 m_3)$$

$$G_{76} = 3L (1_3 n_2 - 1_2 n_3)$$

$$G_{77} = 36(1_2^2 + 1_3^2)$$

$$G_{81} = -36(1_2 m_2 + 1_3 m_3)$$

$$G_{82} = -36(m_2^2 + m_3^2)$$

$$G_{83} = -36(m_2 n_2 + m_3 n_3)$$

$$G_{84} = 3L (1_2 m_3 - 1_3 m_2)$$

$$G_{85} = 0$$

$$G_{86} = 3L (m_3 n_2 - m_2 n_3)$$

$$G_{87} = 36(1_2 m_2 + 1_3 m_3)$$

$$G_{88} = 36(m_2^2 + m_3^2)$$

$$G_{91} = -36(1_2 n_2 + 1_3 n_3)$$

$$G_{92} = -36(m_2 n_2 + m_3 n_3)$$

$$G_{93} = -36(n_2^2 + n_3^2)$$

$$G_{94} = 3L (1_2 n_3 - 1_3 n_2)$$

$$G_{95} = 3L (m_2 n_3 - m_3 n_2)$$

$$G_{96} = 0$$

$$G_{97} = 36(1_2 n_2 + 1_3 n_3)$$

$$G_{98} = 36(m_2 n_2 + m_3 n_3)$$

$$G_{99} = 36(n_2^2 + n_3^2)$$

$$G_{101} = 0$$

$$G_{102} = 3L (1_3 m_2 - 1_2 m_3)$$

$$G_{103} = 3L (1_3 n_2 - 1_2 n_3)$$

$$G_{104} = -L^2(1_2^2 + 1_3^2)$$

$$G_{105} = -L^2(1_2 m_2 + 1_3 m_3)$$

$$G_{106} = -L^2(1_2 n_2 + 1_3 n_3)$$

$$G_{107} = 0$$

$$G_{108} = 3L (1_2 m_3 - 1_3 m_2)$$

$$G_{109} = 3L (1_2 n_3 - 1_3 n_2)$$

$$G_{1010} = 4L^2 (1_2^2 + 1_3^2)$$

$$G_{111} = 3L (1_2 m_3 - 1_3 m_2)$$

$$G_{112} = 0$$

$$G_{113} = 3L (m_3 n_2 - m_2 n_3)$$

$$G_{114} = -L^2 (1_2 m_2 + 1_3 m_3)$$

$$G_{115} = -L^2 (m_2^2 + m_3^2)$$

$$G_{116} = -L^2 (m_2 n_2 + m_3 n_3)$$

$$G_{117} = 3L (1_3 m_2 - 1_2 m_3)$$

$$G_{118} = 0$$

$$G_{119} = 3L (m_2 n_3 - m_3 n_2)$$

$$G_{1110} = 4L^2 (1_2 m_2 + 1_3 m_3)$$

$$G_{1111} = 4L^2 (m_2^2 + m_3^2)$$

$$G_{121} = 3L (1_2 n_3 - 1_3 n_2)$$

$$G_{122} = 3L (m_2 n_3 - m_3 n_2)$$

$$G_{123} = 0$$

$$G_{124} = -L^2 (1_2 n_2 + 1_3 n_3)$$

$$G_{125} = -L^2 (m_2 n_2 + m_3 n_3)$$

$$G_{126} = -L^2 (n_2^2 + n_3^2)$$

$$G_{127} = 3L (1_3 n_2 - 1_2 n_3)$$

$$G_{128} = 3L (m_3 n_2 - m_2 n_3)$$

$$G_{129} = 0$$

$$G_{1210} = 4L^2 (1_2 n_2 + 1_3 n_3)$$

$$G_{1211} = 4L^2 (m_2 n_2 + m_3 n_3)$$

$$G_{1212} = 4L^2 (n_2^2 + n_3^2)$$

$$\begin{aligned}
m_{11} &= 1/3 \\
m_{22} &= (13/35 + 6I_z/5AL^2) \\
m_{33} &= (13/35 + 6I_y/5AL^2) \\
m_{44} &= J_x/3A \\
m_{55} &= (L^2/105 + 2I_y/15A) \\
m_{66} &= (L^2/105 + 2I_z/15A) \\
m_{77} &= m_{11} \\
m_{88} &= m_{22} \\
m_{99} &= m_{33} \\
m_{1010} &= m_{44} \\
m_{1111} &= m_{55} \\
m_{1212} &= m_{66} \\
m_{59} &= -(11L/210 + I_y/10AL) \\
m_{62} &= (11L/210 + I_z/10AL) \\
m_{71} &= 1/6 \\
m_{82} &= (9/70 - 6I_z/5AL^2) \\
m_{86} &= (13L/420 - I_z/10AL) \\
m_{99} &= (9/70 - 6I_y/5AL^2) \\
m_{95} &= (-13L/420 + I_y/10AL) \\
m_{104} &= J_x/6A \\
m_{119} &= (13L/420 - I_y/10AL) \\
m_{115} &= -(L^2/140 + I_y/30A) \\
m_{119} &= (11L/210 + I_y/10AL) \\
m_{122} &= (-13L/420 + I_z/10AL) \\
m_{126} &= -(L^2/140 + I_z/30A) \\
m_{128} &= -(11L/210 + I_z/10AL)
\end{aligned}$$

All the other values of \mathbf{n}_{ij} not specified here are of zero value. The direction cosines l_i, m_i, n_i have been illustrated in a matrix form according to each element position earlier.

It is worth emphasizing that I_x, I_y, I_z represent the mass moments of inertia for each element including all extra (linear and rotational) inertia effects on the structure produced by components forming the joints between the structure members.

3.6 Computation of the buckling load and the natural frequency:

Buckling load and natural frequency of vibration of the frame were computed by the F.E.M. No allowance was made for the slight increase in stiffness arising from the finite length of the joint fittings at the loaded and fixed nodes. Bearing in mind that the work in this section was primarily intended to establish principles and techniques, a very simple nodal pattern was used, resulting in each member of the framework being represented by two elements.

3.6.1 Computation of the static buckling load:

The computed values for the buckling load was 220 Newtons. This is very close indeed to the value obtained from the preliminary mathematical model analysis, as used to decide on the strength and stiffness of the loading spring and to estimate the frequency of vibration, see Appendix 1.

3.6.2 Natural frequency computations

In a similar computer analysis, the frequencies of the frame were obtained and the lowest amongst them (the natural or fundamental frequency) was obtained. The value of this frequency was 32 Hz. which is very close to both estimated and experimental values.

CHAPTER 4

EXPERIMENTAL AND COMPUTER RESULTS

4.1 Experimental Results

The experimental tests which have been conducted on the space frame structure, shown earlier in figure-7-, were made firstly, to find the resonant frequency of the structure in order to locate the position of any possible nodes to identify the structure modes of vibration. Various positions of both the exciter and the accelerometer were used and axial loads ranging from zero to slightly more than a half of the estimated buckling load were applied. The upper limit to loading was imposed in order to save the structure for possible confirmatory tests.

As would be expected, the frequencies of the primary (fundamental) and the higher modes of vibration were found easily, using the facility of the frequency analyser, figure-4-, which is able to produce a full spectra of natural frequencies.

Secondly, the tests were designed to study the nature of the relationship between the level of axial loading and the frequency of vibration of the frame structure. In presenting the results graphically the frequency ratio is based on the experimentally determined frequency at no load and the load ratio is based on the calculated buckling value in section 3.6.1.

The following graphs, figures 11 and 12, clearly establish that the relationship between the axially applied loads and the square of the primary frequency ratio is very close to being linear, as predicted by the theory and demonstrated numerically

for the primary mode of vibration by the approximate Finite Element Method which employs a displacement function based on simple bending theory.

Thirdly, the experiments helped in predicting the (exact) buckling load for the whole structure by extrapolating a straight line connecting the points in the following graphs until it reaches the value of $(\omega/\omega_0)^2 = 0$. At that point the critical load is obtained; this load is found to be very close to the exact one, within an acceptable error of 10% for both experimental and analytical results.

Linearity between loading applied axially and the square of the frequency ratio holds very well even for the higher modes of vibration, but these relationships cannot give the primary buckling value, but instead give higher buckling loads corresponding to higher order of buckling mode shapes .

It will be easy by inspecting the following graphs (more graphs are reported in Appendix 3) to find a nonlinear relationship between the loads applied and the square of the frequency ratio, as this is intentionally done experimentally and shown in related graphs, see figure-13-, in order to study the reasons behind the discrepancies reported earlier in the literature [11], [12], and [13]. Sources of non-linearity could be: misreading the instrument data, external noises mixed with the structure vibration, material internal non-linearity such as composite materials, and by deviating the applied loads from being axial to being applied laterally. All the above are possible sources of non-linearity in the relationship between applied loads and the square of the frequency ratio.

Basically, it is emphasised here that most of the results obtained produce a linear relationship between applied load level and the squared ratio of the frequency of vibration, and this contradicts results obtained in earlier analytical and experimental investigations [12].

The following figures illustrate the experimental graphs obtained at different stages of the set up of the loads applied to the structure.

Figure-11-, experiments 4 and 7, emphasise the existence of a linear relationship between the axially applied loads and the squared ratio of the frequency for the primary mode of vibration. Figure-12-, experiments 17 and 20, show the same phenomenon for a higher mode. A higher buckling load is obtained due to this higher mode of excitation. Figure-13-, experiments 21 and 22, show the non-linearity aspect as it appears to exist when applying the loading laterally instead of axially at the intersection point of the structural bars, which are rigidly connected to each other.

More of these experimental graphs are shown in Appendix 3 at the end of the manuscript.

4.1.1 Experimental Graphs

The graphs of figures-11- and -12- (more graphs are in Appendix 3) represent the experimental results obtained from the space frame analysis. The data of the first ten graphs, see table -1-, were taken at the fundamental frequency of vibration of the framed structure. The data for the next ten graphs were taken at approximately the second mode of vibration. In all these tests the

load was applied along the vertical axis of the structure and all bars forming the space frame are subjected to the same compressive loads. The data of the nonlinear graphs which are obtained by applying the loads laterally are of similar frequency and mode ranges.

To test the sensitivity of the experimental results to the positioning of the exciter and the accelerometer, different combinations of excited and instrumented bars were tried, as reported in table-1- below, in each case the exciter or accelerometer being placed at the mid-point of the bar. This table summarizes the arrangements used and gives the natural frequencies for the unloaded condition.

Experiment No.	Frequency obtained	Exciter on	Acceler. on
1	33.75 Hz.	3	1
2	30.00 Hz.	3	2
3	31.00 Hz.	4	2
4	30.00 Hz.	1	3
5	28.75 Hz.	4	1
6	32.50 Hz.	3	3
7	32.00 Hz.	3	4
8	32.00 Hz.	2	4
9	31.75 Hz.	4	3
10	32.00 Hz.	2	1
11	65.00 Hz.	3	1
12	53.00 Hz.	3	2
13	55.00 Hz.	4	2
14	60.00 Hz.	1	3
15	58.00 Hz.	4	1
16	65.00 Hz.	3	3
17	63.50 Hz.	3	4
18	64.00 Hz.	2	4
19	62.75 Hz.	4	3
20	64.00 Hz.	2	1

Table-1-

On the experimental set up, positioning of the exciter and accelerometer for the axial load case.

It is important to note that in the nonlinear graphs, see also Appendix 3, similar arrangements of exciter and accelerometer positioning have been followed. In figure-13- the sudden drop in the frequency ratio at about 55% of the buckling load computed for the axial case can be understood on physical grounds as the buckling of one bar can occur without the whole structure collapsing; the structure will still accept further loading before the final collapse since three out of four bars are still fully effective but, of course, the total (effective) stiffness of the structure has been significantly reduced.

Static strain measurements were made on the compression member to substantiate this phenomenon, figure-10a- shows a marked discontinuity in the strain-load relationship.

Although referring to a particular case, these results demonstrate the possibility of a nonlinear relationship existing between the applied loads and the ratio squared of the frequency of the structure if certain conditions are not met, such as; the applied load must be purely axial, the boundary conditions must not produce any subsidiary effects which can change the behaviour of the structure and the primary mode of the frequency of vibration must be easily obtained.

Detailed discussion of the experimental graphs will be given in the next section in order to study all features of these experimental results clearly.

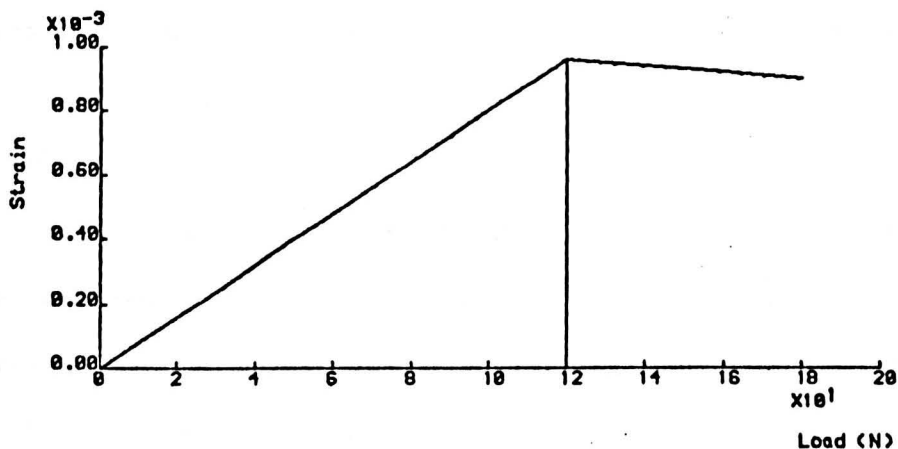


Figure-10a-

4.1.2 Observations on the Experimental Graphs

Analysing the experimental graphs in figures 11,12,13, and the graphs in Appendix 3, one can make the following observations:

Experiments 1,2,3,11,15,16,and 19 show a slight drop in the frequency immediately after the first load is applied, thereafter the system starts to stabilise. This is possibly due to some prestress in the structure which could be partly due to forces introduced when connecting the bars to the base plate, partly due to manufacturing prestresses due to heating processes, and partly due to certain boundary conditions.

Data of experiments 4 to 10, 12 to 14, 17 and 18 were taken at the best possible laboratory quietness and the loading was applied very slowly.

It is apparent from the above graphs, in both modes (primary modes and higher modes) of vibration used, that the relation between the applied axial loads and the squared ratio of the frequency is close enough to be considered linear, and to support further this assertion, a linear regression procedure was introduced to the experimental graphs to make the linearity more evident to the reader.

In the last graphs, experiments 21 to 27 obtained by loading the structure laterally, a similar drop in the frequency is observed at the early stages of loading and a sudden higher drop in the frequency is again observed when the load in the most heavily compressed bar is about 50 Newtons, and this is due to the early buckling of that bar leaving the structure to continue to

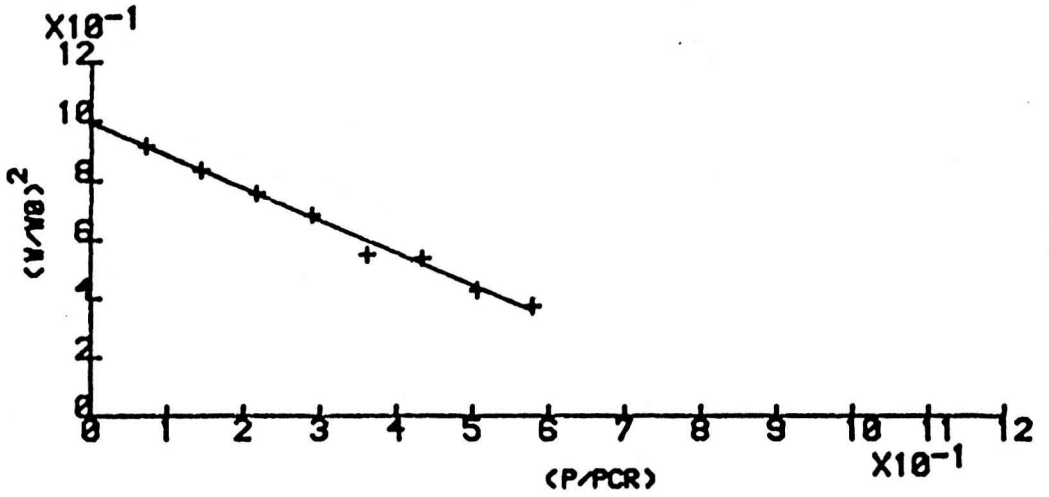
carry more loading at a lower stiffness. Some of the next points are observed to be at higher frequency values. This is due to the nature of this type of lateral loading in which some of the bars will be axially in tension, where an increase in stiffness is predicted, and the others will be axially loaded in compression, where a decrease in stiffness is obtained. If the first effect is greater than the second then, as a result, an increase in the frequency is seen.

Generally speaking, the variation of position of the exciter and the accelerometer do not appear to effect the results. Experiments 27 and 28 are made at the next higher frequency of vibration, show a continuing increase in the frequency as the load is applied. A study of the available literature suggests that this phenomenon has not been observed by other experimenters and no adequate explanation has been found in published theory. Possibly, since the structure is rigidly jointed at the point of the load application, bending moments have arisen from the antisymmetric load orientation which would have produced additional bending and torsional effects in the members.

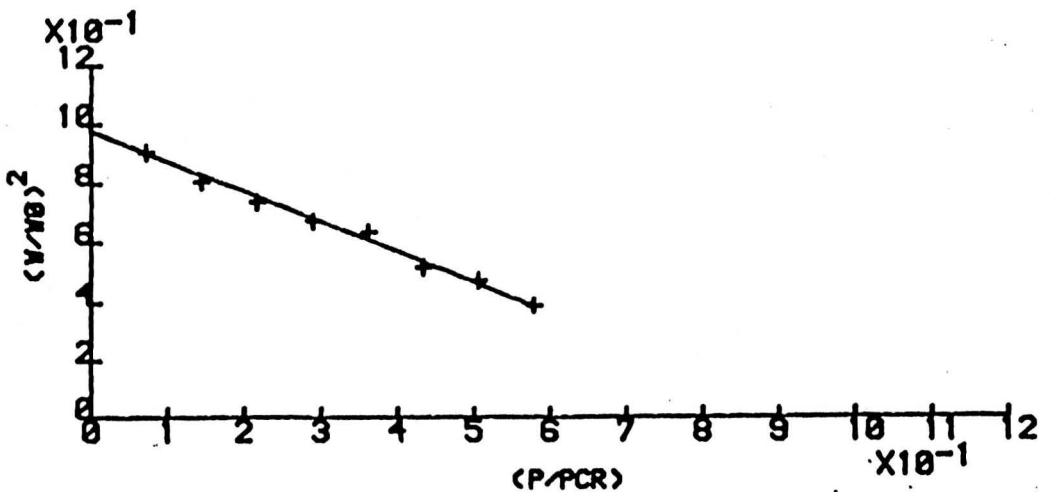
These speculations could account for the effective (total) stiffness increasing rather than decreasing linearly as the load level is increased.

The foregoing work was preliminary to the main object of this investigation which was to examine the behaviour of vibrating flat plate structures subjected to uniaxial loadings under different boundary conditions. Part II of this work deals with the experimental tests and finite element computational analysis of simple plate structures.

EXPERIMENTAL GRAPHS OF
 FREQUENCY-STRESS LEVEL RELATION OF THE
 AXIALLY LOADED SPACE FRAME STRUCTURE



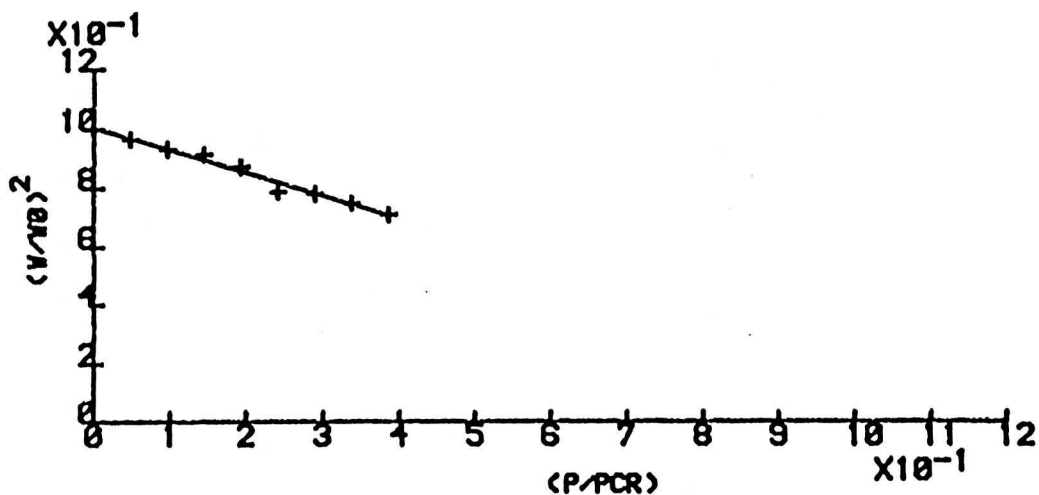
EXPERIMENT NO.4



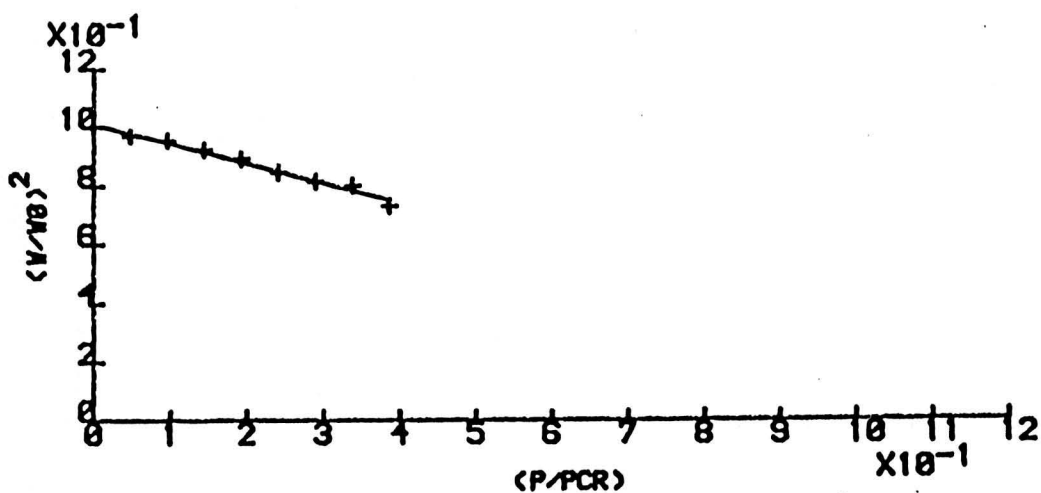
EXPERIMENT NO.7

FIGURE NO.11

EXPERIMENTAL GRAPHS OF
 FREQUENCY-STRESS LEVEL RELATION OF THE
 AXIALLY LOADED SPACE FRAME STRUCTURE



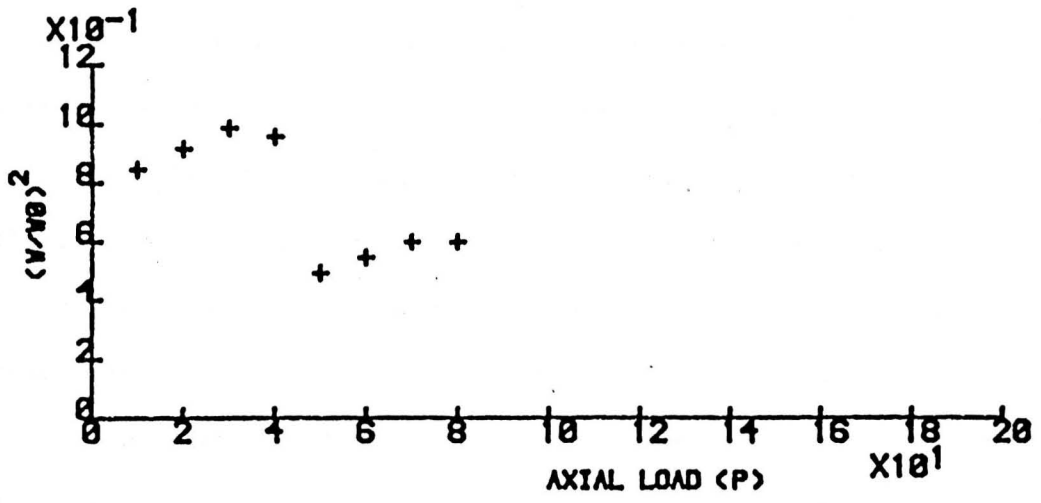
EXPERIMENT NO.17



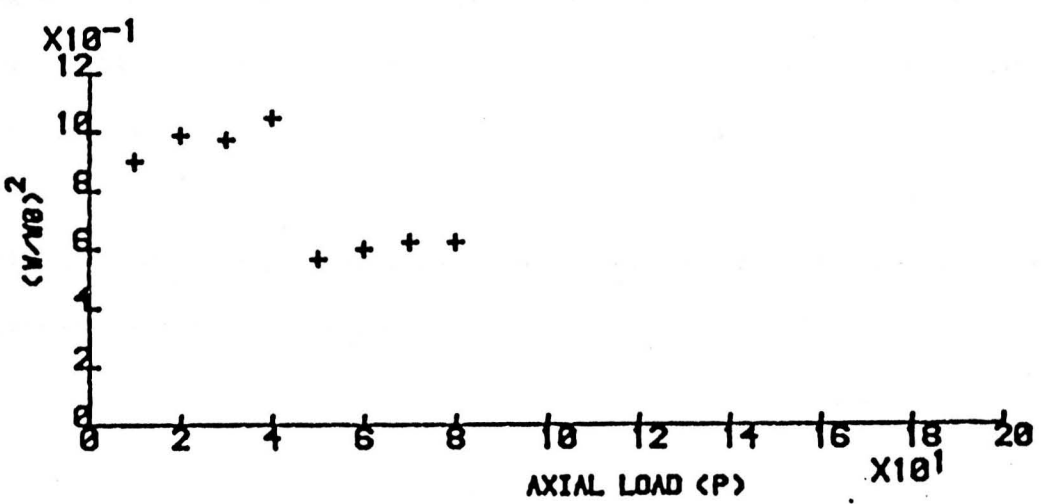
EXPERIMENT NO.20

FIGURE NO.12

EXPERIMENTAL GRAPHS OF
 FREQUENCY-STRESS LEVEL RELATION OF THE
 Laterally Loaded Space Frame Structure



EXPERIMENT NO.21



EXPERIMENT NO.22

FIGURE NO.13

4.2 Finite Element Results Compared with Experimental Results.

As explained earlier, a computer programme has been developed based on the Finite Element Method techniques using the stiffness method assumptions, where each bar of the three dimensional frame structure is divided into two equal parts. Matrices such as elastic, geometric, and mass have been calculated as shown earlier in chapter 3. These matrices are used in the programme to calculate the eigenvalues and associated eigenvectors.

The results of the computer analysis for the frequency of vibration for the loaded space frame structure (dynamic analysis) have produced an almost linear relationship similar to that obtained by experimental means and predicted by the theory (exact or approximate). When experimental results and computer results are compared on the same graphs, it is found that a close agreement does exist, the only very slight difference reported here being that the analytical results(Finite Element Method) produce a lower-bound solution while the experimental ones are of a slightly upper- bound solution. Extrapolating to $(w/w_0)^2 = 0$ gives a buckling load which is close to that obtained in the static computer analysis.

4.2.1 Analytical Observations

From figure -14-, the first graph represents the analytical solution for the relation between the applied axial loads and the squared ratio of the frequency at the lowest possible mode of vibration of the structure. This lowest is considered to be the fundamental mode of vibration. A linear relation does appear to be dominant and there is no need for any linear regression procedure to be involved. In the next graph, the frequency is measured at a higher mode of vibration, and the relation does not seem to be as linear as the previous one but, rather a series of flat curves. This is undoubtedly a consequence of a very simple nodal pattern used to represent the structure which inevitably will result in a less accurate prediction of the frequency of the higher modes of vibration.

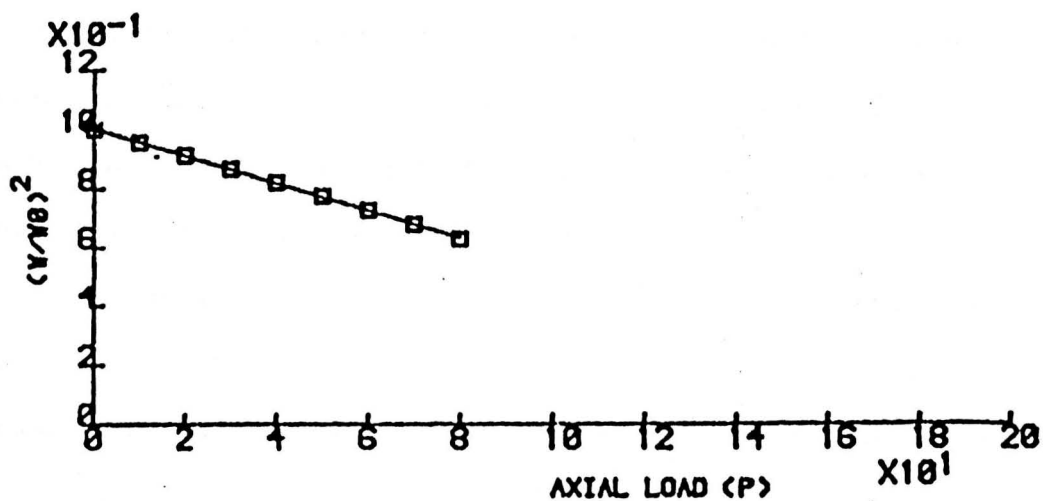
However, it is likely to be best represented by a linear relationship and a linear regression procedure has been used to give the straight line shown in figure-14-.

These aspects have been discussed in section 4.1.2 in more detail. To summarise; our observations suggest that linearity does appear to be the case at the lower modes of vibration since then the modes of buckling and the modes of vibration seem to coincide but, for the higher modes, this linearity begins to deviate due to the factors explained in the previous sections.

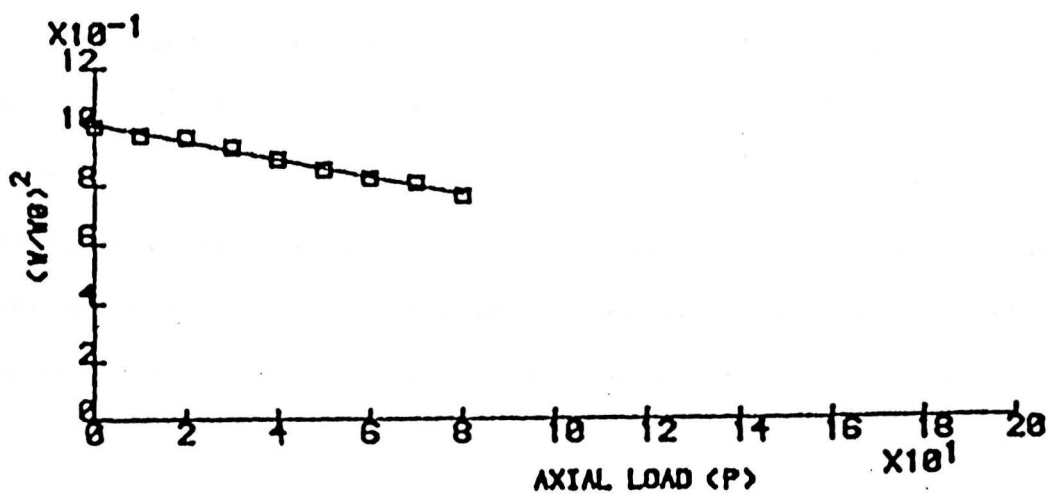
For the higher modes, the analytical analysis seems to rely on the relation between the applied loads and the elements forming the total stiffness matrix; if the relationship is linear then, a linearity between the applied loads and the squared ratio of the frequency will appear otherwise, the contrary is true.

4.2.2

ANALYTICAL GRAPHS OF FREQUENCY-STRESS LEVEL RELATION OF THE AXIALLY LOADED SPACE FRAME STRUCTURE



LOWER FREQUENCY GRAPH



HIGHER FREQUENCY GRAPH

FIGURE NO.14

4.2.3 Comparative Graphs Discussion

The following graphs illustrate the relationship between the applied axial loads and the square of the frequency ratio of the space frame structure as far as the analytical procedure is concerned, the modes of vibration are computed and related graphs are shown in the lower mode (fundamental) and a higher mode (first harmonic) of the vibration frequencies.

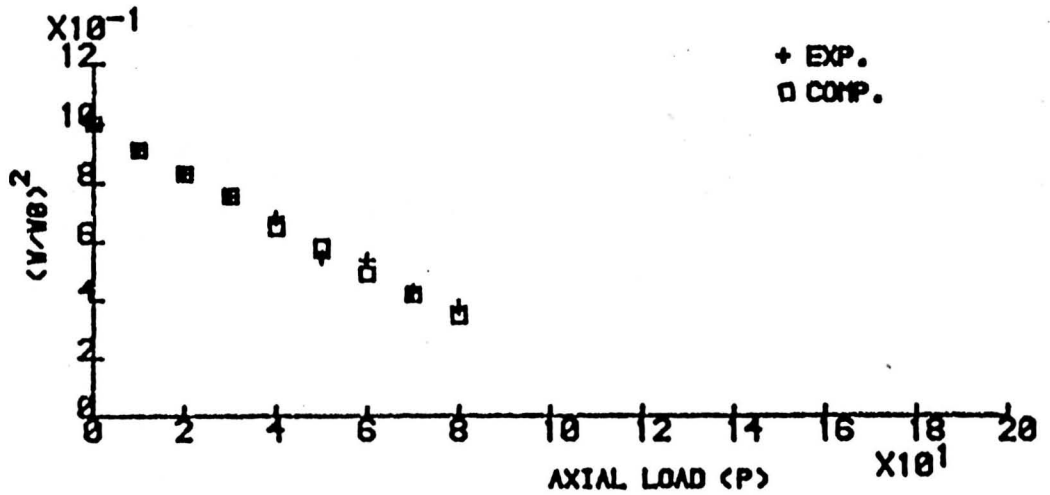
The next four graphs are illustrated to show the good agreement between analytical and experimental analyses; some random experiments were selected for these comparisons at both lower and higher modes of vibration of the space frame structure. At the lower mode of vibration (fundamental mode) experiments 4 and 7 are in good agreement with the computer values, there is a tendency for the experimental values to get slightly higher than the analytical values, but on the overall analysis, the agreement between the two results is very close.

At higher modes (first harmonic), experiments 17 and 20 seem to agree with the computer values, but the tendency for the experimental values to diverge from the analytical values is more clear this time due to the suspected failure in matching between the experimental and the analytical analyses mode shapes at higher frequencies of vibration and at higher applied axial loads.

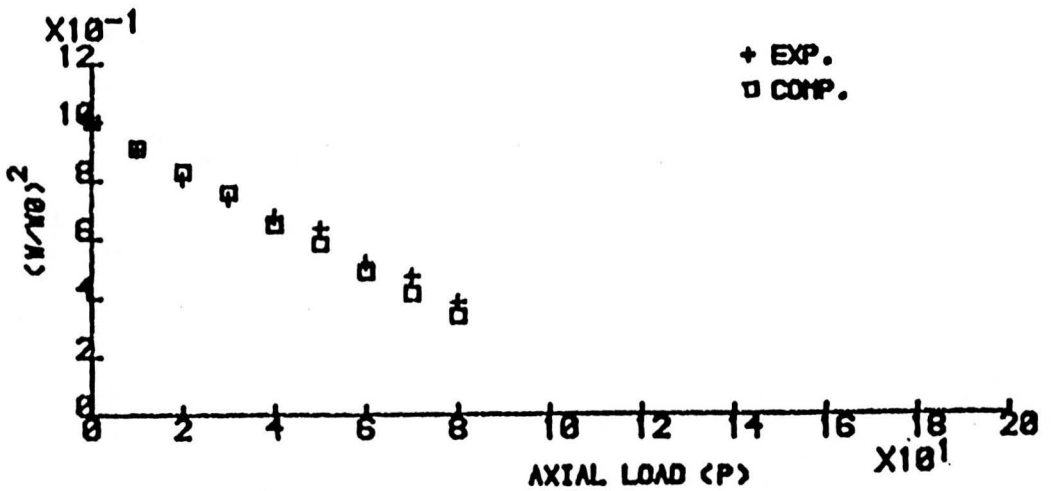
Both situations are illustrated in the following graphs of figure-15- and figure-16- of section 4.2.4.

4.2.4

GRAPHS COMPARING EXPERIMENTAL
VERSUS ANALYTICAL RESULTS FOR AN
AXIALLY LOADED SPACE FRAME STRUCTURE



COMPUTER RESULTS
EXPERIMENT NO.4

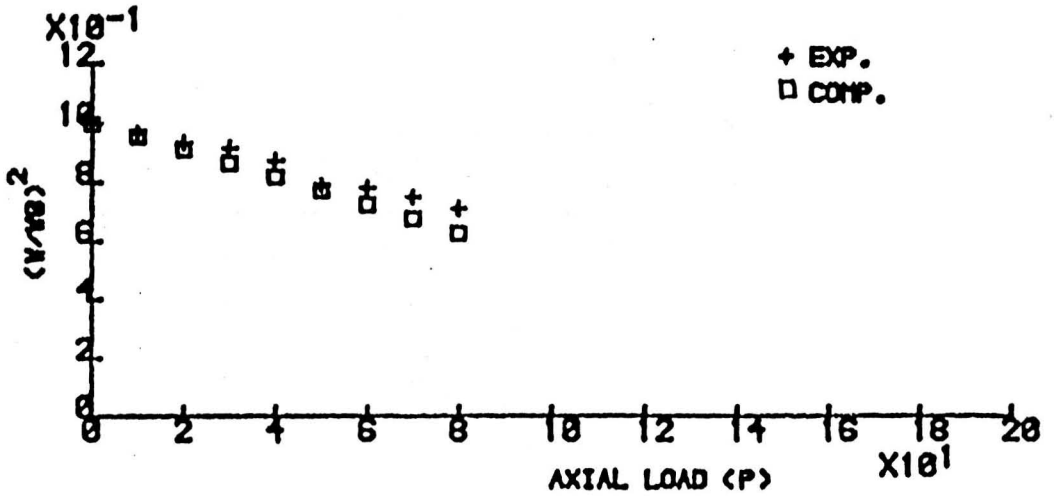


COMPUTER RESULTS
EXPERIMENT NO.7

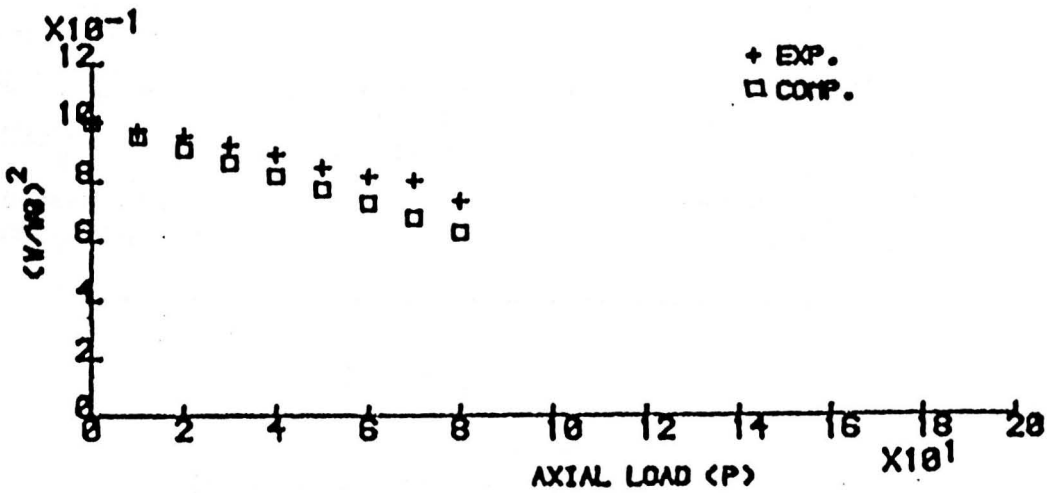
FIGURE NO.15

4.2.4

GRAPHS COMPARING EXPERIMENTAL
VERSUS ANALYTICAL RESULTS FOR AN
AXIALLY LOADED SPACE FRAME STRUCTURE



COMPUTER RESULTS
EXPERIMENT NO.17

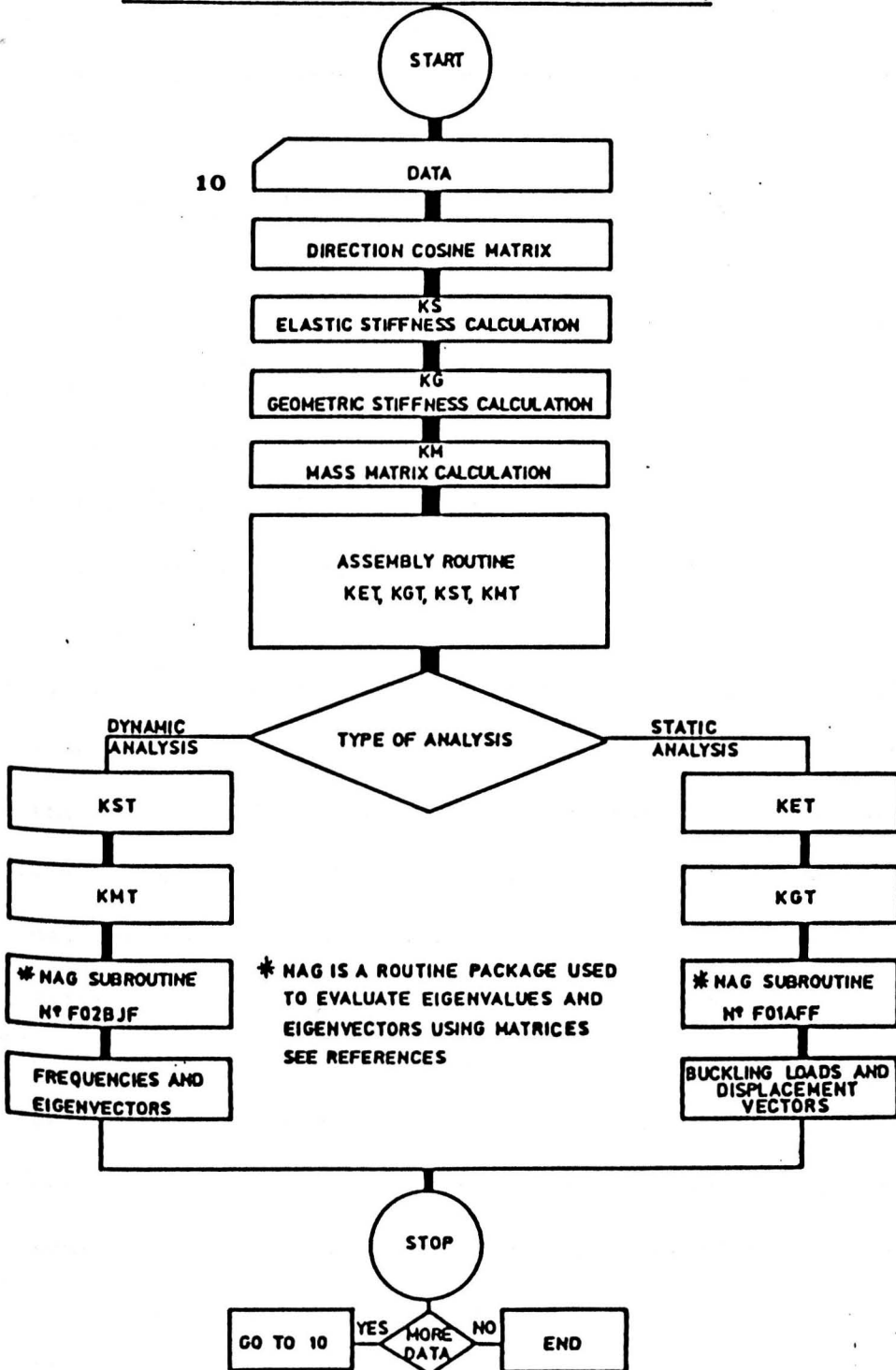


COMPUTER RESULTS
EXPERIMENT NO.20

FIGURE NO.16

4.2.5 Computer Flow Chart

FLOW CHART ON THE USE OF THE F.E.M. PROGRAM TO ANALYSE THE SPACE FRAME STRUCTURES.



4.3 Conclusions and Discussions

To conclude the work on the space frame structure analysed in part I, it can be affirmed that a relationship exists between the axially applied loads and the square ratio of the frequency of the structure vibration, and this relation tends to be linear if the resulting experimental graph points are treated as such; by using a linear regression procedure, (Appendix 2), where some of the scattered points will on the average be aligned with the more linear ones. From these analyses we observe that this linear relationship gives a buckling load close enough (within 10% error) to the theoretical (exact) buckling load.

From the analytical results using the Finite Element Method of analysis, we can confirm that for the lowest possible mode of vibration, the relationship obtained between the applied axial loads and the squared ratio of the frequency is linear but, for the higher mode of vibration case reported in figure-16- when higher values of loads are applied, this linearity tends to diverge due to an irregular change in the values forming the total stiffness matrix, (Elastic Stiffness and Geometric Stiffness combined), which can be explained as the change due to the variation in each value of the Geometric Stiffness caused by the change in the axially applied loads, and this change, is not of a constant factor on the overall spectra of loads applied.

Comparing the experimental and the analytical results shows them to be very close (within 3% difference) for both low and high modes of the frequency of vibration but, for the higher frequency

modes, both experimental and analytical (Finite Element Method) analyses tend towards the nonlinearity due to the difference between the modes of vibration and the modes of buckling of the structure.

Finally, both methods (experimental and theoretical) can produce a linear relationship between the applied loads and the squared ratio of the frequency if certain measures are taken, some of these precautions are summarized as follows:

- 1) The applied loads must be applied axially on each member of the structure, in our analysis this have been secured by introducing a spherical bearing at the point of the bars intersection where the load has been located.
- 2) The loads must be applied statically in order to avoid any unwanted excitations to the system.
- 3) The mass of the applied loads must not be associated in any way with the main structural mass. In our case we introduced a spring system in tension for this purpose.
- 4) The stucture must not be prestressed or prebuckled before the analysis is started.
- 5) Avoid any external excitations as much as possible in order to prevent any extra vibrations added to the introduced vibrations.
- 6) The boundary conditions on the structure should work as designed to avoid any subsidiary constrains on the system.
- 7) Regarding the analytical results, (when F.E.M. is used), the more elements used the more exact the results will be.
- 8) A check on the relation between the Geometric Stiffness and the applied loads is important to understand the true relation between the applied loads and the frequency of excitations.

9) The Mass Matrix used in the analysis was based on the distributed mass assumption which is more efficient than the method of lumped masses which proved to be less accurate in similar analyses.

10) All matrices used should be based on the same assumed deflected shape function, and the small deflection theory should be considered in these analysis.

Finally, an analytical graph is suggested to be used in the design process of a space frame structure under similar conditions, it gives useful information of the structure behavior at an early stage of the design process.

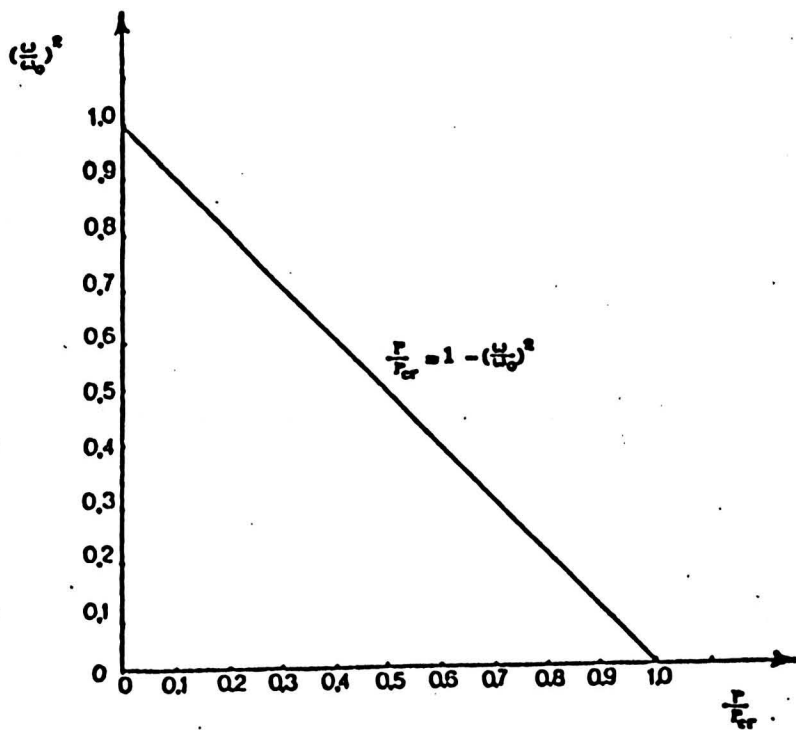


Figure-17-

Suggested analytical graph
for space frame structures

REFERENCES

- 1) ARGYRIS J.H , "On the Analysis of Complex Elastic Structures," Applied Mechanics Reviews, Vol.11, 1958, pp.331-338.
- 2) BARNETT S. and STOREY C., " Matrix Methods in Stability Theory," Thomas Nelson & Sons Ltd., 1970.
- 3) BATHE K.J. and WILSON E.L., "Numerical Methods in Finite Element Analysis," Printise Hall, 1976.
- 4) BISHOP R.E.D. , " The Vibration of Frames," Proc. Inst. Mech. Eng., Vol. 170, 1956, pp. 955-967.
- 5) CHANG C.H., " Vibrations of Frames with Inclined Members," Journal of Sound and Vibration, Vol. 56, No. 2, 1978, pp. 201-214.
- 6) CHU T.C. , "Determination of Buckling Loads by Frequency Measurements," California Institute of Technology, 1949.
- 7) COOK R.D., " Concepts and Applications of Finite Element Analysis," John Wiley & Sons Ltd., 1981.

- 8) GLADWELL G.M.L. , " The Vibration of Frames," Journal of Sound and Vibration, Vol. 1, No. 4, 1964, pp. 402-425.
- 9) GERE J.M. and WEAVER W.Jr., "Matrix Algebra for Engineers," Van Nostrand Co. N.Y., 1965.
- 10) HOFF N.J., NARDO S.K. and ERIKSON B. , "An Experimental Investigation of the Process of Buckling of Columns," Proc. Soc. for Experimental Stress Analysis, Vol.9, 1951, pp.201.
- 11) LURIE H., "Effective End Restraint of Columns by Frequency Measurements," Journal of Aeronautical Sciences, Vol.18, 1951.
- 12) LURIE H. , "Lateral Vibrations as Related to Structural Stability," Journal of Applied Mechanics, Vol.6, 1952, pp.195-204.
- 13) LURIE H. , "A Note on the Buckling of Struts," Journal of Royal Aeronautical Society, Vol.55, 1951, pp.181-184.
- 14) McGUIRE W. and GALLAGHER R.H. , " Matrix Structural Analysis," John Wiley & Sons Ltd., 1979.
- 15) MELOSH R.J. , "Basis for Determination of Matrices for Direct Stiffness Method," Journal of the American Institute of Aeronautics and Astronautics, Vol.1, 1963.

16) PRZEMIENIECKI J.S. , "Generalization of the Unit Displacement Theorem with Applications to Dynamics," Proc.Conf. on Matrix Methods of Structural Analysis, Wright-Patterson Air Force Base, Ohio, 1964.

17) LORD RAYLEIGH , "Theory of Sound," MacMillan and Co., 2nd Edition, London, 1894.

18) SHAKER F.J. , "Effect of Axial Load on Mode Shapes and Frequencies of Beams," NASA TN-8109, 1975.

19) STEINERT G.J. , "Study of Buckling Resistances of Frame Structures by Measuring their Eigenfrequencies," The 6th International Congress of Acoustics, Tokyo-Japan, 1968, pp.G21-G24.

20) STEPHENS B.C. , "Natural Vibration Frequencies of Structural Members as an Indication of End Fixity and Magnitude of Stress," Journal of the Aeronautical Sciences, Vol.4, 1936, pp.54-60.

21) TIMOSHENKO S.P. and GERE J.M. , "Theory of Elastic Stability," McGraw-Hill, 2nd ed., 1961.

22) TIMOSHENKO S.P. and YOUNG D.H. , "Vibration Problems in Engineering," Van Nostrand, 1966.

23) WEAVER W.Jr. and GERE J.M. , " Matrix Analysis of Framed Structures," D. Van Nostrand Company, 1980.

24) WEISBERG S. , " Applied Linear Regression," John Wiley & Sons, 1980.

25) WILLIAMS F.W. , "Stability Functions and Frame Instability- A Fresh Approach," International Journal of Mechanical Sciencies, Vol.23, No.12, 1981, pp.715-722.

PART II

**STABILITY AND VIBRATION OF
ISOTROPIC PLATES AND APPLICATIONS**

CHAPTER 5

BACKGROUND AND LITERATURE REVIEW

5.1 Introduction

External surfaces as well as internal parts of flight vehicles have been found to be susceptible to various types of aeroelastic instabilities, the most noticeable of which is flutter. However, flutter analyses are, to a large extent, dependent on the prediction of vibration characteristics of different structural elements, in particular, plates subjected to inplane loads, under various constraint conditions.

The problem of determining the natural vibration characteristics of isotropic and, more generally, orthotropic rectangular plates, subjected to inplane loads in the presence of different boundary conditions, has been the subject of numerous theoretical investigations.

There have been few experimental investigations due, possibly, to the difficulties arising when attempting to produce specified boundary and loading conditions.

The following chapters of this part deal with the effect of the stress level on the frequency of vibration of a rectangular, isotropic, thin flat plate axially loaded and under various

boundary conditions. Available research is found to have the major portion of it based on theoretical analysis while few experimental investigations have been reported.

Experimental results obtained in this investigation are compared; first against theoretical results, then against analytical results obtained by computer analysis using the method of Finite Elements, and, finally, compared with the results of other investigators when available.

The Finite Element Method, is presented in an easy and a simple method of programing which also provides some saving in computer storage space and time. The assembly routine of the elements is made as simple as possible by arranging that the digital computer does all the work.

The elements used for the Finite Element Method are chosen of a rectangular shape, with four nodes located at the corners. This element shape is appropriate to the rectangular plates under consideration. Other element shapes could be employed for plates of different geometry or if holes or other material discontinuities are present.

5.2 Literature review " Plate Buckling"

The modern need and use of steel and high-strength alloys in the fields of engineering design such as bridges, naval ships, aircraft, and aerospace structures has made elastic instability a problem of great importance.

In recent years practical requirements have led to extensive research and investigation, both theoretical and experimental, in

order to study the conditions governing the stability of plates and shells.

To provide a typical example which can be analysed without undue difficulty, a study of the relation of the axially applied loads to the square of the frequency ratio of a rectangular plate is investigated experimentally and analytically.

The problem of determining the natural vibration characteristics of an isotropic rectangular plate in the absence of inplane loads but with various boundary conditions has been the subject of numerous theoretical investigations, see reference [6]. In fewer instances has the effect of inplane loads been studied. The more general cases of isotropic and orthotropic plates with elastically restrained edges have received even less attention, especially when dealing with the dynamical aspects of the problem.

The most comprehensive treatment of the effect of inplane loading on the vibration of plates with elastically restrained ends is due to Schulman, 1945, who treated the case of an isotropic rectangular plate subjected to inplane forces with elastic restraints along the longitudinal edges, and with simple supports along the lateral edges. The constant inplane loads throughout the plate were assumed to be due to constrained thermal expansion of the plate. The exact natural frequency was derived. However, two assumptions were made, these being:

- 1) that the mode shape remained unaltered with the increase of the load, thus obtaining a linear relationship between frequency squared and load applied (i.e. temperature variation).
- 2) that an energy approach using the Lagrange equation was appropriate.

All the results are available in reference [6], in terms of frequency and temperature graphical relationships.

Orthotropic plates under uniaxial and biaxial direct stresses were analysed first by Wittrick, [44], in 1968, by Williams [40], in 1974, and by both Wittrick and Williams, [41], [42], [45], [46] and [47] from 1969 to 1983.

But in all the available literature, the lack in experimental analysis is very evident.

When studying stability and vibration, exact solutions are not always available, so that experimental verifications of approximate analyses become necessary. Unfortunately, either they tend to be costly or difficult to perform, especially when trying to explore the behaviour of complex structures.

Most of the recent published research work has been concerned primarily with exploring the approximate analytical methods, and attempting closed form solutions by studying various methods.

Among these analytical approximate methods, the Finite Element Method seems to produce very reliable information as long as the assumed boundary conditions (geometric and natural) are satisfied.

5.3 Plate Stability

For the calculation of the critical values of forces applied in the middle plane of a plate at which the flat form of equilibrium becomes unstable and the plate begins to buckle, one could follow the same analysis as that used for compressed bars. There exist many ways to investigate the stability of a thin plate

1) By assuming that from the beginning the plate has some initial curvature or some lateral (out of plane) loading. Then the values of the forces in the middle plane at which deflections tend to grow indefinitely are usually the critical loads. This method of analysis may incorporate nonlinear analysis, in which case it could produce only an approximate value, but, for our analysis, this last statement does not apply due to the linear assumptions used.

2) Assume the plate buckles slightly under the action of forces applied in its middle plane, and then calculate the magnitude of the forces in order to keep the plate in such slightly buckled shape. The differential equation of the deflected surface in this case is known as:

$$W_{xxxx} + 2 W_{xxyy} + W_{yyyy} = (1/D)(N_x W_{xx} + 2 N_{xy} W_{xy} + N_y W_{yy})$$

eq.5.1.

Where N_x , N_y , and N_{xy} are the normal and shear loads.

The simplest case is obtained when N_x , N_y , and N_{xy} must have constant values throughout the plate. In the general case, even though the problem gets more involved since variable coefficients may appear in the above differential equation, the solution concept is likely to be the same.

3) The energy method can be used to investigate the plate buckling and stability. This method is quite useful in the cases where an approximate solution of the above differential equation is needed, or when the plate is reinforced by stiffeners and it is required to produce a good approximation to the buckling load. In such a case, we assume the plate is stressed by loads acting in

its middle plane and undergoes some small lateral bending consistent with the boundary conditions. Such limited bending can be produced without stretching of the middle plane, and we need only to consider the energy due to the bending and the corresponding work done by the forces acting in the middle plane of the plate.

Manelbetsch [25], in 1937, presented his results on the study of the inplane compressed plate, with all edges built in, by using two approximate methods, each of which produced an approximate buckling load, either higher or lower than the exact value reached experimentally, but, earlier than this work, Taylor, in 1933, using the power series method, obtained good results. Then, Faxen extended this method of the power series and obtained the exact solution before Levy [20] in 1942, who presented the exact solution based on the same power series as that used by Faxen.

Weinstein and Trefftz, about 1950, independently have shown that Taylor's solution leads to a lower values of the critical load due to few terms used in the power series.

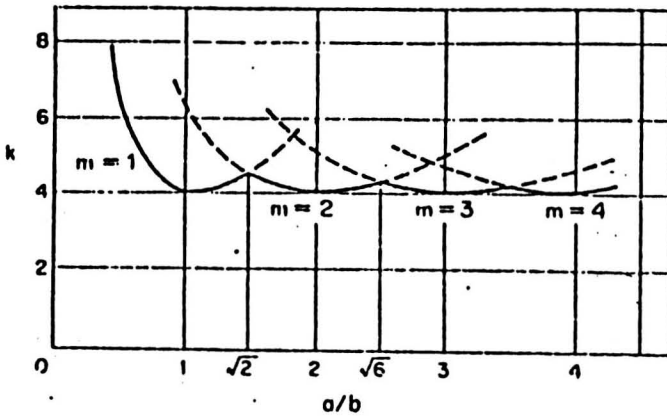
Another approximate method of solution is the energy method first developed by Timoshenko [33]. This method has proved to be efficient in most stability problems with dependable results.

The Ritz method has shown that problems of this type can be solved exactly if infinite series of the properly chosen functions are used.

The values obtained for the buckling load by means of the energy method are of an upper-bound nature, meaning that the structure is put under more constraints than it should have been normally, while the values obtained by fewer series terms are of a

lower-bound nature when compared with the exact solution, due to the fewer constraints used on the analysed structure.

It is reasonable enough to locate the critical load between the Taylor-Trefftz and Timoshenko values at all times as long as the structure is elastic, and obeys the classical theory assumptions.



Buckling stress coefficient k for uniaxially compressed plate.

Ref [33]

Figure -18-

4) The displacement method is a widely used method for Finite Element Analyses (see references [1], [2], [4], [13], [30], [41] and [50]), the same method is followed for the three dimensional frame structures and the isotropic plate analyses by reducing the problem to an eigenvalue problem which is easier to solve by numerical methods.

Relations for the stability study of plates are similar to those reported in the stability study of two or three dimensional frame structures and, when based on the energy considerations, can be explained as:

a) If the work done by these forces is smaller than the strain energy of bending for every possible shape of lateral buckling, that is, $\Delta W < \Delta U$, the flat form of equilibrium of the plate is said to be stable.

b) If the work becomes larger than the strain energy of bending for any shape of lateral deflection, that is, $\Delta W > \Delta U$, the plate is then said to be unstable .

c) Finally, at the instant at which the work done is equal to the strain energy of the system that is, $\Delta W = \Delta U$, the system is neutral and the load then acting is the critical load.

5.4 Calculus of Variations (Applied Cases)

5.4.1 Stability of simply supported plates " Inplane Loads"

It is easily shown that, by the varying the total potential with respect to the lateral deflection for a rectangular plate loaded in its plane, a partial differential equation identical to equation 5.1 in the previous section is developed.

If we, for simplicity, consider the case of uniform axial compression in one direction only applied to a simply supported plate, equation 5.1 will reduce to:

$$D \nabla^4 W + N_x W_{xx} = 0 \quad \text{eq.5.2}$$

Correspondingly, the total potential yields the following equation:

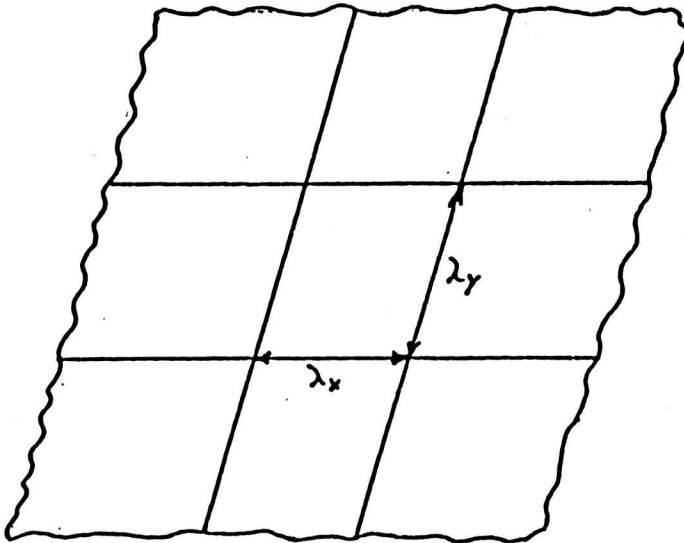
$$U+V = (D/2) \iint [W^2_{xx} + W^2_{yy} + 2W_{xx}W_{yy} - 2(1-\nu)W^2_{xy} - (N_x/2D)W^2_x] dx dy \quad \text{eq.5.3}$$

If we assume the deflected shape according to the boundary conditions as:

$$W = A_{mn} \sin (m\pi x/a) \sin (n\pi y/b) \quad \text{eq.5.4}$$

which satisfies all geometric and natural boundary conditions, a and b being the length and the width of the plate while m and n denote the number of half waves in the x - and y - directions into

which the plate buckles then $\lambda_x = a/m$ and $\lambda_y = b/n$ represent the length and the width of one half-wave in the x- and y- directions, as shown in the following figure.



Half-waves in x and y directions

Figure -19-

Substituting the deflected shape function into the total potential expression in equation 5.3 and integrating gives:

$$U+V = (D/2) \{ [(m\pi/a)^2 + (n\pi/b)^2]^2 - N_x/2 \Lambda_{mn}^2 (m\pi/a)^2 \} ab/4 \quad \text{eq.5.5}$$

then, by taking the variation on the total energy with respect to Λ_{mn} we obtain:

$$N_x = D \pi^2 (\lambda_x^{-2} + \lambda_y^{-2})^2 / \lambda_x^{-2} \quad \text{eq.5.6}$$

It will be noticed that, for this particular case, the same result can be obtained by direct substitution of the assumed deflected shape function into the lateral equilibrium equation. In

other words, the assumed deflected shape function is a solution of the equilibrium equation 5.1.

Hence, the expression for the buckling of the plate out of its original plane can be obtained simply by establishing the values of m and n which render N_x a minimum. Two specific cases reflecting a widely different plate geometries are of practical interest and therefore, they are illustrated by considering a rectangular plate with sides a and b as follows:

Case 1, $a \ll b$,

This case represents a short and wide plate for which the minimum value of N_x is obtained by setting $m = 1$ and minimising N_x with respect to the buckle ratio a/λ_y in the equation:

$$N_x = (D\pi^2/a^2)[1 + (a/\lambda_y)^2]^2 \quad \text{eq.5.7}$$

The minimum value is given, obviously, by setting $a/\lambda_y = 0$, thus;

$$(N_x)_{\text{critical}} = \pi^2 D/a^2 \quad \text{eq.5.8}$$

This result is analogous to Euler buckling load for a slender strut. The plate effect appears in the factor $(1-\nu^2)^{-1}$, by rewriting equation 5.8 in the form;

$$(N_x b)_{\text{cr}} = (\pi^2 E t^3 b)/(12(1-\nu^2)a^2) \quad \text{eq.5.9}$$

by introducing an inertia term I_y , we get:

$$P_{cr} = (\pi^2 EI_y) / (1 - \nu^2) a^2 \quad \text{eq.5.10}$$

Where, $I_y = t^3 b / 12$ as the moment of inertia.

Case 2, $a > b$,

This case represents the other extreme, a narrow strip plate, for which the minimum is obtained by setting $n = 1$ and minimising the equation with respect to a/λ_x . This leads to the following result:

$$N_x = \pi^2 D (1 + \alpha^2)^2 / b^2 \alpha^2 \quad \text{eq.5.11}$$

where, $\alpha = \lambda_x / b$, and then, by taking the variation with respect to α , one gets:

$$2 \alpha (1 + \alpha^2) (\alpha^2 - 1) = 0. \quad \text{eq.5.12}$$

The real root which corresponds to the minimum is $\alpha = 1$ and then:

$$N_x = 4 \pi^2 D / b^2 \quad \text{eq.5.13}$$

The same result is obtained when we deal with a square plate ($a = b$). In fact, as long as m has an integral value, the critical stress ($\sigma_{cr} = N_x / t$) is the smallest stress which can cause the plate to buckle. More generally, for plates with a/b other than integral, the square buckle pattern is precluded and a somewhat

higher critical stress could result. However, the discrepancy diminishes rapidly with the increasing of a/b ratio and becomes negligible at about $a/b \approx 4$.

5.4.2 Stability of the Plate of Boundary Conditions Other

Than All sides Simply Supported (Uniaxial Compression)

a) Plate loaded on the two clamped edges, while the other two are simply supported:

The solution to this case has been obtained by Leissa [19] using the following form for the deflected shape:

$$W = f(x) \sin (\pi y/b) \quad \text{eq.5.14}$$

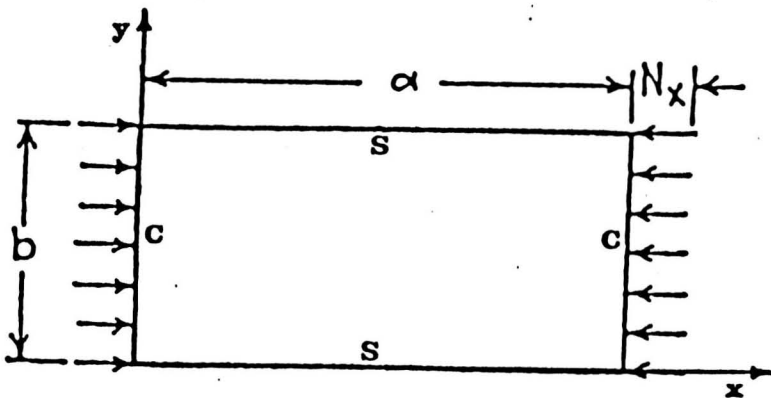


Figure-20-

The assumed equation must satisfy the geometric boundary conditions, i.e., $f(x) = 0$ and $f'(x) = 0$ at $x = 0$ and a .

When we substitute into the total potential energy equation, this leads to:

$$U+V = (Db/4) \int [f''^2 + (\pi/b)^4 f^2 + 2\nu(\pi/b)^2 f' f + 2(1-\nu)(\pi/b)^2 f'^2 - (N_x/2D)f'^2] dx \quad \text{eq.5.15}$$

Applying the variation with respect to f following the variation equation in the form:

$$\delta_f(U + V) = 0 \quad \text{eq.5.16}$$

Equation 5.15 and 5.16 upon integration by parts, taking in consideration the geometric boundary conditions, lead to the following ordinary differential equation:

$$f'''' + A^2 f'' + B^4 f = 0 \quad \text{eq.5.17}$$

where, $A^2 = (N_x/D) - 2(\pi/b)^2$ and $B^4 = (\pi/b)^4$.

By using Laplace Transformations with $F(0) = 0$ and $F'(0) = 0$ as the new boundary conditions at $x = 0$, and then using the Laplace inverse we get:

$$f(x) = [F1(\cos cx - \cos dx) + F2(1/c \sin cx - 1/d \sin dx)] / (d^2 - c^2) \quad \text{eq.5.18}$$

Again, using the boundary conditions at $x = a$ will lead to two simultaneous equations in $F1$ and $F2$, and for these latter to exist, the determinant of the coefficients must vanish, thereby leading to the stability determinant:

$$\begin{vmatrix} (\cos ca - \cos da) & (1/c \sin ca - 1/d \sin da) \\ (-c \sin ca + d \sin da) & (\cos ca - \cos da) \end{vmatrix} = 0$$

Expanding the determinant and simplifying the results through trigonometric identities we get:

$$4 + (K - 4) \cos (c+d)a - K \cos (c-d)a = 0 \quad \text{eq.5.19}$$

where, K is larger than 4 and d and c are always real with:

$$(dc)^2 = 1/2(\pi/b)^2 \{K-2 \pm \sqrt{(K-4)K}\} \quad \text{eq.5.20}$$

$$\text{and, } (ac)^2 = 1/2(\pi a/b)^2 \{K-2 \pm \sqrt{(K-4)K}\} \quad \text{eq.5.21}$$

The buckling equation 5.19 can be solved for the lowest value of K corresponding to a given ratio a/b yielding a buckling coefficient and hence, giving the critical value of axial load N_x .

As an example, for a/b ratio of unity (square plate), the critical value of $K = 6.7432$, which is the same as the exact solution obtained by Timoshenko [33] on the basis of solving the partial differential equation 5.2.

For any value of the ratio a/b , the wave form but, of course, not the amplitude of the buckled plate, can be ascertained from the function $f(x)$. Naturally, as the plate becomes longer, more and more buckles will appear.

When $a/b > 5$ for instance, the solution indicates that $K = 4$, this meaning that the plate is long enough and the effect of the clamped loaded edges becomes negligible.

For $a/b = 1$, where only one wave will appear in each direction one can assume $f(x) = A \sin \pi x/b$ as in equation 5.19, this leads to $K = 6.75$, which is very close indeed to the exact solution.

b) Isotropic plate loaded at two simply supported edges, the other two edges are clamped:

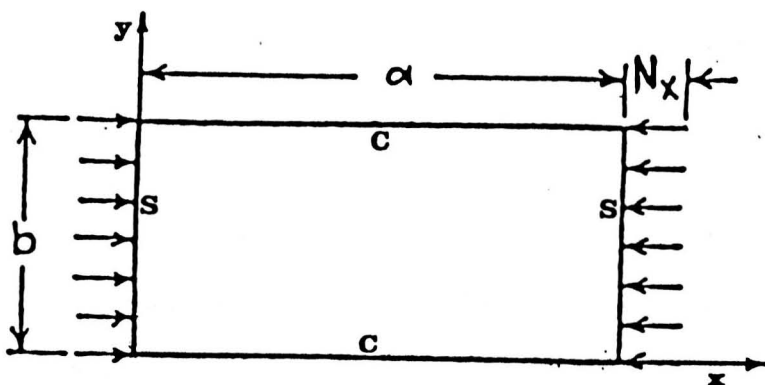


Figure-21-

One can assume the following deflected shape function:

$$W = A_m \sin(\pi x/a)(1 - \cos(2\pi y/b)) \quad \text{eq.5.22}$$

and following the same procedure as in section 5.4.2 (a) leads to:

$$K = \frac{1 + \frac{8}{3} \alpha^2 + \frac{16}{3} \alpha^4}{\alpha^2} \quad \text{eq.5.23}$$

$\alpha = \lambda_x/b$, and λ_x is the buckle half wavelength in x -direction.

By letting $m = a/b\alpha$, for square plate ($a/b = 1$), it gives the following table:

m	K_{xcr}
1	9.0
2	8.0
3	12.3

Table -2-

The approximate critical value for K for a square plate is 8.0 ($K = 8$), while the exact value is $K = 7.69$.

To conclude this discussion, it is important to note that the knowledge of the buckled shape for the previous problems could lead to a precipitate choice for the half wavelength $m = 1$ for both cases, but, as has been shown, the smallest value of the load corresponds to $m = 2$, two half wavelengths between the simple supported edges.

c) Rectangular plates having two opposite sides simply supported, the other two edges may have any type of constraint:

For uniform inplane forces, equation 5.22 still applies for this case when the edges $x = 0$ and $x = a$ are simply supported and the other two edges are open to any constraint as shown, see Figure -22-. A deflection function which satisfies the boundary conditions of zero deflection and bending moment along the edges, in general, is given by:

$$W(x,y) = \sum Y_m(y) \sin(\alpha x) \quad \text{eq.5.24}$$

where $\alpha = m\pi/a$. Using equation 5.24 in equation 5.15, then applying equation 5.16 yields:

$$(Y_m)_{yyyy} - (2\alpha^2 + N_2/D)(Y_m)_{yy} + (\alpha^4 - k^4 + N_1\alpha^2/D)(Y_m) = 0 \quad \text{eq.5.25}$$

where $m = 1, 2, \dots, \infty$.

This differential equation has a general solution of the type:

$$Y_m = A_m \sin v_{my} + B_m \cos v_{my} + C_m \sinh \phi_{my} + D_m \cosh \phi_{my}. \quad \text{eq.5.26}$$

where

$$v_m = \sqrt{\{[(\alpha^2 + N_2/D)^2 - (\alpha^2 - k^4 + N_1\alpha^2/D)] + (\alpha^2 + N_2/2D)\}} \quad \text{eq.5.27}$$

$$\Phi_m = \sqrt{\{[(\alpha^2 + N_2/D)^2 - \sqrt{(\alpha^2 - k^4 + N_1\alpha^2/D)}] - (\alpha^2 + N_2/2D)\}} \quad \text{eq. 5.28}$$

It is seen that equations 5.25 is exactly of the same form as for the case of an isotropic plate investigated in references [6] and [12], the only difference being is the definition of the parameters ν_m and Φ_m .

The standard procedure is to satisfy the boundary conditions along the other two sides $y = 0$ and $y = b$, whatever they may be. This is done by the substitution of equation 5.26 into these conditions. The determinant of the resulting four homogenous equations in A_m , B_m , C_m , and D_m is then set equal to zero for a non trivial solution.

Apparently, the foregoing procedure has not been followed thoroughly in the literature, as will be seen from some numerical results presented here.

The boundary conditions of plates having loads acting on the edges are different than those of the unloaded plate edges because of the component of inplane force which acts normal to the deflected middle surface of the plate. That is, the transverse edge reaction is as explained in reference [19]. By looking at equations 5.27 and 5.28, it can be seen that the parameters ν_m and Φ_m can be of positive, zero, or complex values. The solution of equation 5.26 in the existing literature is based only on the positive solution. No study is known in which an understanding of the character and range of applicability of the other forms of the solution has been accomplished. It appears that very little effort has been made to obtain the other possible solutions of the problem.

Further study of this subject, considering all possible values of the parameters of the above equations, would be useful to understand them and to see their practical applicability on the stability of structures.

5.5 Literature Review " Plate Vibration "

The natural frequency of a rectangular plate with either clamped or simply supported edges is readily available. However, the fact of the existence of a relation between this natural frequency and the level of the stresses in the plate could in some situations be very important. Lurie [24] 1952, showed how the fundamental frequency is easily determined as a function of the rectangular plate buckling factor K. This had been achieved simply by assuming a sine function in a selected direction (i.e. x-direction) so that the buckling differential equation takes the form:

$$\frac{d^4 f}{dX^4} - \frac{2 m^2 \pi^2}{a^2} \frac{d^2 f}{dX^2} + \left(\frac{m^4 \pi^4}{a^4} - \frac{N_x m^2 \pi^2}{D a^2} \right) f = 0 \quad \text{eq.5.29}$$

where N_x is the only applied load.

In a rather similar way, the corresponding vibration equation could have the following form:

$$\frac{d^4 f}{dX^4} - \frac{2 m^2 \pi^2}{a^2} \frac{d^2 f}{dX^2} + \left(\frac{m^4 \pi^4}{a^4} - \frac{\rho \omega^2}{D} \right) f = 0 \quad \text{eq.5.30}$$

where ρ is the mass per unit area.

By applying the boundary conditions to the general solution the

critical buckling coefficient K is found in the following equations:

$$N_x = K \frac{\pi^2 D}{b^2} \quad \text{eq.5.31}$$

$$\omega^2 = \frac{m^2 \pi^4 D}{\mu} \frac{K}{(ab)^2} \quad \text{eq.5.32}$$

Equation 5.32 will provide the natural frequency, this is done by the use of either NACA reports or Timoshenko Theory [33] in order to obtain the value for K .

According to Lurie [24], the vibration problem does differ in one aspect from that of buckling, that is to say; the fundamental frequency always corresponds to $m = 1$. Hence, the last equation becomes:

$$\omega^2 = \frac{\pi^4 D}{\mu} \frac{K}{(ab)^2} \quad \text{eq.5.33}$$

This may not correspond to the lowest value of K for a given aspect ratio of the plate (a/b), where a and b are the dimensions of the plate, whereas in the case of buckling m is always chosen to give the lowest value of the coefficient K .

Regarding the plate vibration, D. Young [49] in 1950, selected the Ritz method for a rectangular plate analysis to produce an upper-bound solution, this is to say that Young's natural frequencies are higher than those of the exact solutions for the same plate under the same conditions. The method seems to work but very lengthy calculations need to be performed and there are preferred boundary conditions.

The Rayleigh-Ritz method was applied by S. Durvasula et al [8] in 1967, and an analogy between the vibration problem and buckling under uniform compressive loads was obtained by simply evaluating the corresponding natural frequency from the exact solution.

This method is purely theoretical and in the case of our study there will be a parallel to it experimentally as well as theoretically.

The Rayleigh-Ritz and Galerkin methods were compared [8] to confirm that the Rayleigh-Ritz method is consistently better than the Galerkin method. However, the tendency is for both methods to converge towards the exact solution as the energy parameter is varied. Each method will approach the exact solution from a particular direction, one (Rayleigh-Ritz) is an upper-bound while the other (Galerkin) is a lower_bound.

Vibrations of clamped plates have been investigated by Laura [16] 1974, using simple polynomials and the Galerkin method to determine the response of a thin, elastic rectangular plate clamped along the boundaries and subjected to sinusoidal excitations. This work could be applied to different categories of plates and to different applied loads. Laura's work [16] showed a good agreement between approximate and exact values under certain conditions.

Correlation between orthotropic and isotropic plate assemblies was studied by W.H Wittrick and Williams [47] 1974, subjecting the plate to uni-axial and bi-axial stresses for different end conditions.

This work achieved a relation between the buckling coefficient K and the side ratio C as shown in the following equation:

$$K = \frac{b^2 N_x}{a^2 \sqrt{D_1 D_2}} + C \left(1 - \frac{D_{12}}{\sqrt{D_1 D_2}} \right) \quad \text{eq.5.34}$$

where $C = 2.4$ for the case of ends simply supported and sides clamped, and $C = 2.46$ for the case of all edges clamped, see ref.[44].

5.6 Vibration of Rectangular Plates

5.6.1 Orthotropic Considerations

The differential equation of motion of a plate is expressed in general as follows:

$$\begin{aligned} D_x W_{,xxxx} + 2D_{xy} W_{,xxyy} + D_y W_{,yyyy} + \rho W_{,tt} \\ = N_x W_{,xx} + 2N_{xy} W_{,xy} + N_y W_{,yy} \end{aligned} \quad \text{eq.5.35}$$

where, D_x , D_{xy} , and D_y are the constants of the rectangular orthotropy, and ρ is the mass per unit area.

There are few published results, Leissa [19], gives a solution for the plate vibration when both inplane forces and orthotropy are present. The inplane forces N_x , N_{xy} and N_y are assumed to be functions of only the spatial coordinates x, y (or R, θ in the case of polar coordinates). That is, they do not depend either upon time or upon the transverse (out of plane) deflection W . Further assumptions:

- 1) The vibration is assumed to be free.
- 2) The equations of motion are assumed to remain linear.

The inplane forces which are not depending on W could be realised in one of the following ways:

- 1) The boundary conditions are with no fixity in the plane of the plate.
- 2) The deflection is sufficiently small relative to the initial tension or compression in the plate so that the inplane forces are not significantly effected.

Here, the plate equation is solved considering the general case in which there is orthotropy, inplane loading and vibrations, assuming the small deflection theory to hold for the analysis.

To solve this equation, we introduce an approximation such as:

$$W(x,y,t) = A(x/a) B(y/b) e^{i\omega t} \quad \text{eq.5.36}$$

where, ω is the natural frequency, $A(x/a)$ and $B(y/b)$ are the mode shapes that satisfy the boundary conditions of the sides parallel to the x - and the y - axes respectively and which have to be determined.

Only for the special case of two opposite edges simply supported is an exact solution known. For all other cases an approximate solutions will suffice. Using approximate methods such as Galerkin's which reduce equation 5.35 to the following ordinary fourth order differential equation:

$$X''''(\xi) - 2\pi^2 \underline{A} X''(\xi) - \pi^4 \underline{B} X(\xi) = 0 \quad \text{eq.5.37}$$

where $\xi = x/a,$

$$\underline{A} = f(D_x, D_y, D_{xy}, y/b, N_x), \quad \text{eq.5.38a}$$

and $\underline{B} = f(D_x, D_y, D_{xy}, W, N_y, y/b) \quad \text{eq.5.38b}$

One way of solving the above equation is to assume [16]:

$$X(\xi) = X_a + X_b \quad \text{eq.5.39}$$

Where X_a and X_b in the above equation are the roots of the characteristic equation. More details of the solution of this problem are reported in reference [19].

5.6.2 Isotropic Considerations

It is emphasised that the inplane forces are generally found first by solving the plane elasticity problem for the known boundary values of N_x, N_{xy}, N_y . If these quantities are constant around the boundary, it is generally accepted that they are constant throughout the plate as well. After some necessary simplifications, the assumptions of isotropy will reduce equation 5.29 to the following equation of motion:

$$D\nabla^4 W + \rho W_{,tt} - N \nabla^2 W = 0 \quad \text{eq.5.40}$$

where ρ is the mass per unit area.

Assuming sinusoidal response ($W = W \sin \omega t$), the above equation becomes:

$$D\nabla^4 W - \rho\omega^2 W - N\nabla^2 W = 0 \quad \text{eq.5.41}$$

where, $W = W(x,y)$. Equation 5.41 can be factorised in the following relation:

$$(\nabla^2 + \alpha^2) (\nabla^2 - \beta^2) W = 0 \quad \text{eq.5.42}$$

where, $\alpha^2 = (N/2D) [\sqrt{(1+4\rho\omega^2 D/N^2)} - 1]$ eq.5.42.1

$$\beta^2 = (N/2D) [\sqrt{(1+4\rho\omega^2 D/N^2)} + 1] \quad \text{eq.5.42.2}$$

$$\beta^2 - \alpha^2 = N/D \quad \text{eq.5.42.3}$$

and, $\alpha^2 \beta^2 = \rho\omega^2/D$ eq.5.42.4

Results were found in the literature for all the 21 possible combinations of the boundary conditions for isotropic rectangular plates, with or without the presence of inplane forces. As will be shown later, published results exist for only a few cases where inplane forces are present.

To illustrate the extreme cases, equation 5.41 could be again rewritten as:

$$D(\nabla^4 W - k^4 W) = N_1 W_{,xx} + N_2 W_{,yy} \quad \text{eq.5.43}$$

where, $N_1 = N_x$, $N_2 = N_y$, $N_{xy} = 0$, and $k^4 = \rho\omega^2/D$, when more than one inplane loads are present. In this equation:

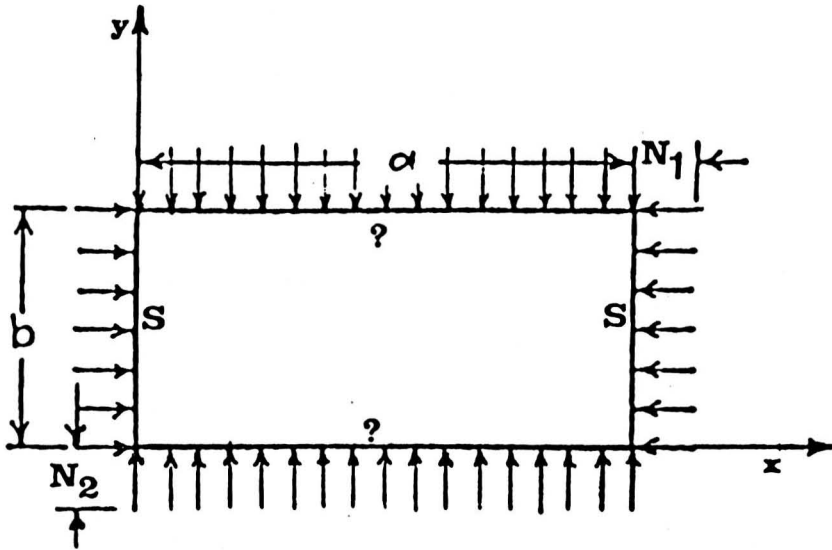


Figure-22-

Case a) Rectangular plates having all sides simply supported:

$$\text{Using } W(x,y) = \sum A_{mn} \sin m\pi x/a \sin n\pi y/b, \quad \text{eq.5.44}$$

which, clearly satisfies the boundary conditions of the plate in the above figure, Leissa[16] has shown that using equation 5.14 in equation 5.13, will yield the following frequency equation:

$$\rho\omega^2 = D[(m\pi/a)^2 + (n\pi/b)^2]^2 + N_1(m\pi/a)^2 + N_2(n\pi/b)^2 \quad \text{eq.5.45}$$

1) If $N_1 = N_2 = 0$,

$$\rho\omega^2 = D[(m\pi/a)^2 + (n\pi/b)^2]^2 \quad \text{eq.5.46}$$

which is the solution to the unloaded plate.

2) As either N_1 or N_2 or a combination of them, becomes large and negative, (level of the compression), the frequency tends to reduce towards the zero value. the loading at zero frequency will be the critical buckling loading. This parallels the behavior of the space frame structure experimentally covered in detail in part I of this thesis. For example, with $N_2 = 0$, the critical value given by the equation is:

$$N_{1cr} = -(D\pi^2/a^2)[m + n(na^2/mb^2)]^2 \quad \text{eq.5.47}$$

3) If both N_1 and N_2 are compressive, it is seen from equation 5.45, that the fundamental modes of vibration do not necessarily occur when $m = 1$ and $n = 1$ but depend upon N_1 , N_2 and the ratio. This is shown clearly in Herrmenn's analysis [11] which states that the fundamental frequency for the critical load will always occur when $n = 1$, but not necessarily when $m = 1$ when $a/b > 1$, meaning that the length of the plate is a factor in the selection of the mode of vibrational displacements.

Lurie[21] and [24], was considered one of the earliest scientists to conduct experimental tests on plates in vibration, but his reported nonlinear curves relating the square of the frequency to the inplane applied loads increased the necessity for more investigation in the theory and in the related experiments in order to verify the correctness of his findings.

The results obtained in part I differed from those found and Predicted by experimentalists in the past. This suggests that

more experimental tests on other types of structure are to be desired. The isotropic plate problem is investigated theoretically and experimentally following the same line of assumptions.

CHAPTER 6

THE FINITE ELEMENT METHOD

6.1 Review

The Finite Element Method has been and will be mostly studied and used to produce solutions as close as possible to the exact ones; these solutions can be more or less accurate depending on many factors, some of which are controllable such as the selection of the shape functions, and the selection of the number of elements and their shape and size, others are not easily controlled such as the software speed, and the storage limits.

Many authors have used this method to solve very complicated problems which are not easily tackled by simpler means, some of these solutions were tested and proved to be reliable, while others are not.

A historical review of this method of analysis is valuable to emphasise that it has a long established and a very reliable ancient mathematical background. In the seventeenth century Newton (1643-1723) introduced the calculus of variation which forms the core for this present method, Euler (1707-1783), and D'Alembert (1717-1783) have treated the variational principle from an integral point of view, as D'Alembert defined that in the "Traite'" in 1743, see reference [43].

When we deal with structures, nonlinearities could arise either from the geometry of the problem or from the material properties. These nonlinearities make it difficult to use ordinary linear analysis, so it was a necessity to introduce other methods see [1], [4], and [50], to overcome this problem, the only price paid was in the accuracy of results obtained, which to a certain extent could be accepted.

To follow this argument in more detail one could refer to historical papers which cover all aspects of Finite Element Methods, see reference [43] for more details. Most recently Argyris [2] underlined the great achievement in using matrices in the field of structural analysis by reducing the stability and vibration problems to a simple eigenvalue problem. This work, when introduced and applied by Argyris himself, produced great advantages to the analyst and to the digital machines as well. Gere and Weaver [9], produced a similar treatment of the problem using the matrix analysis as the basis of the method of informing the computer regarding the problem to be solved. In their books [9] and [37] they introduced and used special codes such as NASTRAN to solve for the stress analysis of elastic or plastic materials.

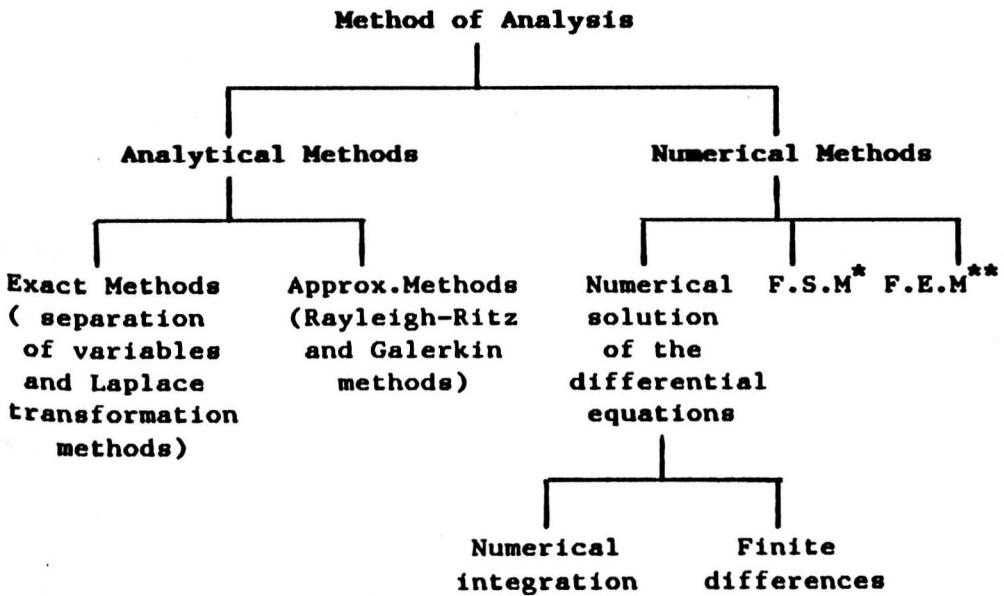
On the theoretical background, we are not to forget the advances achieved by Timoshenko and Gere [33], as they produced a reliable reference on stability analysis of structures. This reference is used as a guideline for this research work, especially during its first stages in order to develop an approach based on a sound and a well accepted theory.

The essential similarity of buckling and vibration analyses by the Finite Element Method is well established.

The wide range of use of the Finite Element Method is seen in its many successful engineering and science applications, see reference [50] for further details.

6.2 Comparison between the F.E.M. and other Analytical Methods

The following scheme is made available to show the position of all the various methods and their classifications depending on historical origins, see reference [4].



* F.S.M. is the abbreviation of the Finite Strip method and,

** F.E.M. is the abbreviation of the Finite Element Method.

6.3 General Steps towards the F.E.M. Programs

The solution of the general continuum problem by the Finite Element Method always follows an orderly step by step process. The following steps are followed in constructing the computer program needed for the analytical solution of the dynamic problem:

Step 1). Discretisation of the structure:

A definite number of the structural elements is obtained by subdividing the whole structure into small elements. The element number, type, size and their arrangement has to be decided in this phase.

Step 2). Selection of a proper interpolation:

or displacement function:

This usually takes the form of a polynomials, the choice being made to give a reasonable accuracy of the solution to the problem.

Step 3). Derivation of element stiffness matrices:

From step 2, the stiffness matrices are computed either from equilibrium considerations or by using a suitable variational principle.

Step 4). Assembly of the matrices:

This is done by adding the element matrices according to the position of each element node and the constraint conditions around

it. The assembled matrices are often called global or total matrices.

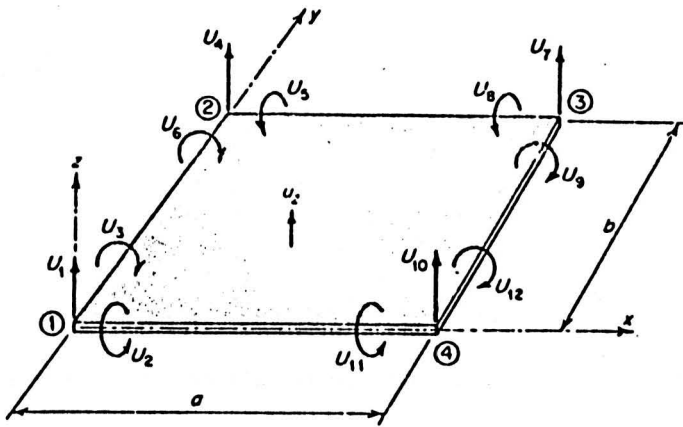
Step 5). Solving for the unknowns:

Either by direct methods or by using available subroutines designed to handle the size of the problem; the NAG subroutines were used for this research work.

6.4 Finite Elements and Rectangular Plates

Observing the selection of element type, one finds that the geometry of the structure dictates to a certain extent the shape of element to be chosen. In a very general way the triangular element is the common selection for almost any problem including thin plates. Sometimes a combination of triangular and rectangular elements is used; in other situations only rectangular elements might be preferred. Our case of analysing the isotropic rectangular plates does not contain any geometric irregularities (such as irregular shapes, the presence of holes, or discontinuities), so, accordingly, the rectangular element was chosen to represent the plates under investigation. Of the various sequences used to number the element nodes, to represent linear displacements or rotations, some are seen to be advantageous than others. We selected Przemieniecki's [29] numbering system due to the proven versatility of this numbering of similar problems in the digital machines.

The following figure shows the set up of the element axes and numbering sequence which is used in this analysis.



Rectangular plate element with
node displacements in bending

Figure-23-

By selecting the plate element as in figure 23 ensures at least an approximate continuity of the slopes . The element nodal displacement vector can be represented by:

$$u_e = \{ W_1, \theta_{x1}, \theta_{y1}, W_2, \theta_{x2}, \theta_{y2}, W_3, \theta_{x3}, \theta_{y3}, W_4, \theta_{x4}, \theta_{y4} \} \quad \text{eq.6.1}$$

The following polynomial expression is used, see reference [50], to represent the out of plane displacement of the element:

$$W_e = a_1 + a_2x + a_3y + a_4x^2 + a_5xy + a_6y^2 + a_7x^3 + a_8x^2y + a_9xy^2 + a_{10}y^3 + a_{11}x^3y + a_{12}xy^3.$$

. eq.6.2

Introducing the nodal coordinates into equation 6.2 and assuming $\theta_x \triangleq W_{,y}$, and $\theta_y \triangleq W_{,x}$, then one can obtain:

$$\{ u \}_e = [C] \{ a \} \quad \text{eq.6.3}$$

where [C], is dependent upon the nodal coordinates, this equation can be written in the following form:

$$\{ a \} = [C]^{-1} \{ u \}_e \quad \text{eq.6.4}$$

to provide the unknown values of { a }.

The elemental displacement function is dependent on {u}_e:

$$W_e = [P] \{ u \}_e = [L] [C]^{-1} \{ u \}_e \quad \text{eq.6.5}$$

where [P], is often referred to as the shape function, and matrix [L] has the form

$$[L] = [1, x, y, x^2, xy, y^2, x^3, x^2y, xy^2, y^3, x^3y, xy^3] \quad \text{eq.6.6}$$

Once, the elemental displacement function {W}_e is obtained, we could generalise the strain-displacement, and the stress-strain relations as:

$$\{ \epsilon \}_e = [H] \{ u \}_e \quad \text{eq.6.7}$$

where [H] is the curvature matrix obtained by differentiating equation 6.5 and using the:

$$\{ \sigma \}_e = [E^*] \{ \epsilon \}_e \quad \text{eq.6.8}$$

Here the stresses and the strains are generalised, and $\{\sigma\}_e$ is a row of stresses.

$$\text{where } \{\epsilon\}_e = \{ W_{,xx} \quad 2 W_{,xy} \quad W_{,yy} \} \quad \text{eq.6.9}$$

$$\text{and } [E^*] = [E/(1-\nu^2)] \begin{vmatrix} 1 & \nu & 0 \\ \nu & 1 & 0 \\ 0 & 0 & (1-\nu)/2 \end{vmatrix} \quad \text{eq.6.10}$$

The elastic rigidity matrix for an isotropic plate is derived as:

$$[D] = t^3/12 [E^*] \quad \text{eq.6.11}$$

All the above manipulations are very useful for the calculation of the stiffness matrices for the elements, as for the elastic stiffness for instance, one could compute only:

$$\{\epsilon\} = [B] \{u\} \quad \text{eq.6.12}$$

$$\{\sigma\} = [D] [B] \{u\} \quad \text{eq.6.13}$$

$$F = \iint \epsilon^T D B u \, dx dy \quad \text{eq.6.14}$$

$$F = \iint [B]^T [D] [B] u \, dx dy \quad \text{eq.6.15}$$

$$F = K u \quad \text{eq.6.16}$$

$$[K]_e = \iint [B]^T [D] [B] dx dy \quad \text{eq.6.17}$$

where $[B] = [H] [C]^{-1}$, see reference [46].

Introducing the element nodal force vector $\{Q\}_e$, then the element equilibrium equation is given by:

$$[K]_e \{u\}_e = \{Q\}_e \quad \text{eq.6.18}$$

and, when treating the global structure equilibrium is represented by:

$$[K] \{u\} = \{Q\} \quad \text{eq.6.19}$$

where $[K]$ is the total (elastic and geometric, see Appendix 5 for their full development) stiffness matrix, $\{Q\}$ is the total force vector, and $\{u\}$ is the displacement vector.

Hence, the general analytical procedure for solving the plate (or shell) problem by the Finite Element Method (see references [4], [28], [29], [30], [46] and [50]) which involve the following steps:

- 1) Determine the elastic stiffness matrix, the geometric stiffness matrix, the mass matrix, and load vector for the element shape selected.
- 2) Assemble the matrices in the order of numbering chosen when selecting the element geometry and coordinates.

3) If the dynamic problem is to be solved, the mass matrix must be assembled and introduced in the analysis, otherwise elastic and geometric stiffnesses are sufficient for the buckling analysis alone.

4) For stability analysis (buckling) use the equation of the type:

$$[K_e] \{u\} + \lambda [K_g] \{u\} = 0 \quad \text{eq.6.20}$$

Where K_e and K_g denote the elastic stiffness matrix and the geometric stiffness matrix respectively.

5) For dynamic analysis (vibration) one follows:

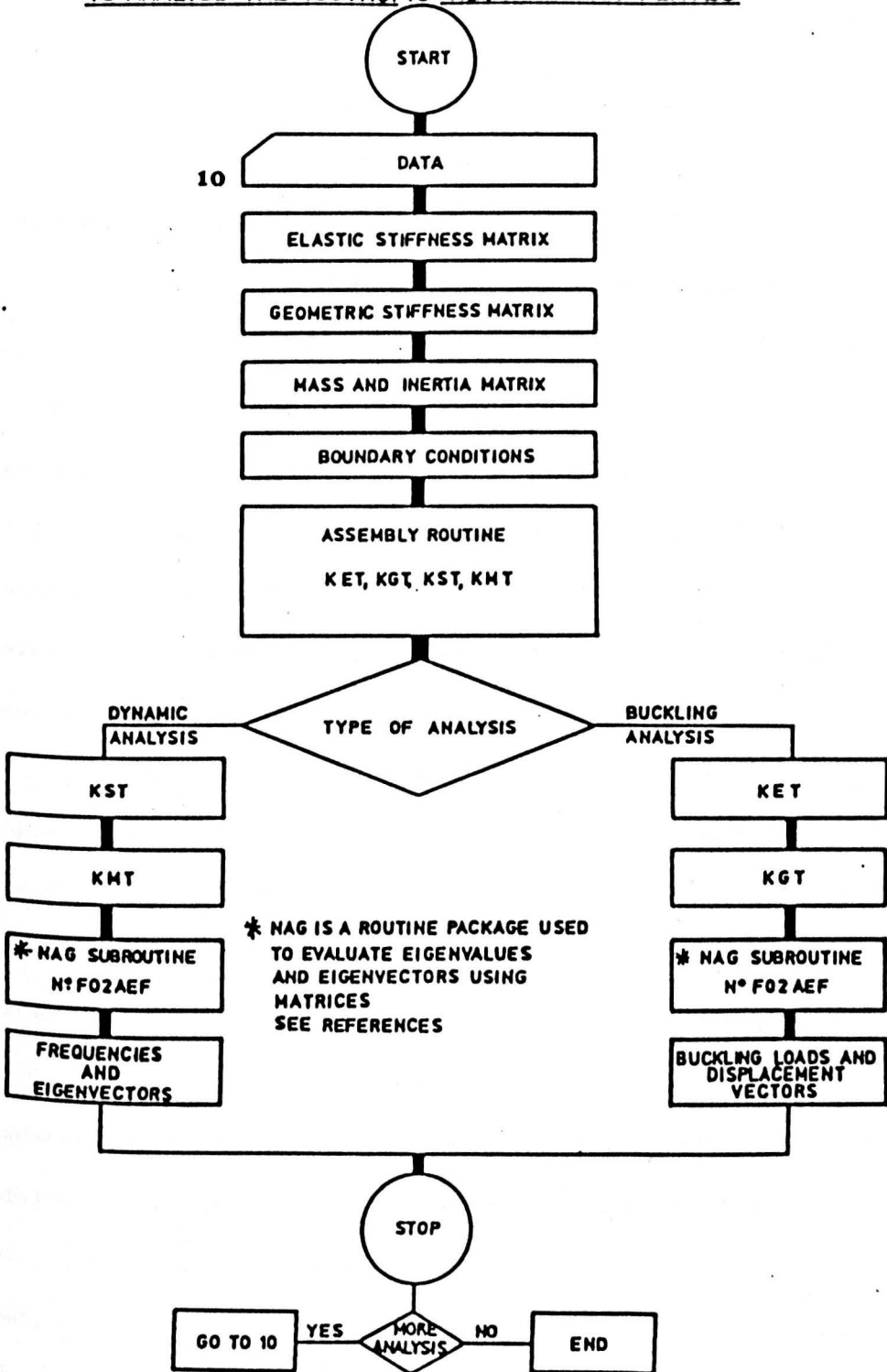
$$[K] \{u\} + \lambda [K_m] \{u\} = 0 \quad \text{eq.6.21}$$

where, K is the total (elastic and geometric) stiffness matrix (elastic and geometric), K_m is the mass matrix (consistent mass matrix) excluding the inertia effects.

The concept of calculating the stiffness matrices will be illustrated, and typical elastic stiffness, geometric stiffness, and mass matrices will be produced to introduce the theory behind obtaining and using these matrices. Some difference in the matrices was found in the literature due to the different assumptions on shape functions and whether or not the compatibility equations were truly satisfied. These differences could lead one to obtain different results when measurements are not taken carefully and assumptions are not followed correctly.

6.4.1 Finite element flow chart of the plate

FLOW CHART ON THE USE OF THE F.E.M. PROGRAM TO ANALYSE THE ISOTROPIC RECTANGULAR PLATES



CHAPTER 7

CONCEPT OF MATRIX METHODS IN PLATE ANALYSES

7.1 General theory

The matrix methods of structural analysis, developed specifically for the use of digital computers, have become now universally accepted in the fields of structures and design. These methods provide the means for a rapid and accurate stress and deflection analysis of simple and complex structures subjected to static and/or dynamic loads. The matrix methods can be used very effectively in stability analysis as well as in vibration analysis as explained earlier in part I.

In the conventional stability analysis two possible approaches are normally used: either the differential equations describing the equilibrium in the deflected state of the structure are formulated and the lowest eigenvalue representing the buckling load condition is found for given boundary conditions, or alternatively, if the differential equations are too complex to prescribe (i.e. nonlinear equations), approximate deflection shapes are used in the strain energy expression for large deflections which are subsequently minimised with respect to the unknown amplitudes, leading to the stability determinant whose lowest root represents the instability condition.

When designing a wing, fuselage, or any other structure, the use of the conventional method is extremely difficult therefore, we should rely on the matrix method approach for the stability and vibration analysis.

The matrix methods of determining buckling loads have recently received considerable attention, and a large number of papers have appeared. Both displacement and force methods have been used for the stability analysis (the difference between the force and the displacement methods was illustrated in part I of this manuscript) based on the concept of discrete element idealisation as will be illustrated later in this chapter.

When the total stiffness or resultant stiffness matrix is mentioned, it is meant that this matrix is obtained by summing algebraically the elastic stiffness matrix and the geometric stiffness matrix for the given element, for which the total matrix is an initial state dependent (sensitive to applied loads and change in geometry).

The basic concept of geometrical stiffness was first used by Turner (see Leissa [19] and Melosh [27]) for the analysis of structures idealised into pin_jointed bars and triangular plates carrying membrane stresses. The method studied was essentially based on the strain energy formulation for large deflection analysis. Similar approaches have been used by several other authors for the analysis of structures made up of bars and beams see Pian [28], triangular plates [29] and [30], rectangular plates [26], and shell structures [35] where a set of displacement functions was assumed.

7.2 Displacement Functions

A deflection function that ensures the deflection and the slope compatibility was first introduced by Dawe [7] in 1967.

One of the displacement functions used by Dawe was introduced to calculate the stiffness properties of the rectangular plate in bending in the following form:

$$u_z = \underline{a} u \tag{eq.7.1}$$

where, $u = \{ u_1, u_2, \dots, u_{12} \}$ eq.7.2

or, $u = \{ w_1, \theta_{x1}, \theta_{y1}, \dots, w_4, \theta_{x4}, \theta_{y4} \}$ eq.7.3

where, u is the displacement vector, w_i are the deflections in the z - direction, and θ_{xi} and θ_{yi} are the rotations of the nodes.

The value of \underline{a} is put in a matrix of the form:

$$\underline{a}^T = \begin{bmatrix} (1+2\xi)(1-\xi)^2(1+2n)(1-n)^2 \\ (1+2\xi)(1-\xi)^2n(1-n)^2b \\ -\xi(1-\xi)^2(1+2n)(1-n)^2a \\ (1+2\xi)(1-\xi)^2(3-2n)n^2 \\ -(1+2\xi)(1-\xi)^2(1-n)n^2b \\ -\xi(1-\xi)^2(3-2n)n^2a \\ (3-2\xi)\xi^2(3-2n)n^2 \\ -(3-2\xi)\xi^2(1-n)n^2b \\ (1-\xi)\xi^2(3-2n)n^2a \\ (3-2\xi)\xi^2(1+2n)(1-n)^2 \\ (3-2\xi)\xi^2n(1-n)^2b \\ (1-\xi)\xi^2(1+2n)(1-n)^2a \end{bmatrix} \tag{eq.7.4}$$

Equation 7.4 is used to determine elements of the total strain matrix \underline{b} (as will be shown later in equation 7.13), the general forms of which are given in the equations which relate strains to displacements, as will be illustrated next.

7.3 Stiffness Determination Based on the Assumed Displacements

The nonlinear total strain_displacement equations for elastic continua are:

$$\epsilon_{xx} = u_{,x} + 1/2(u^2_{,x} + v^2_{,x} + w^2_{,x}) \quad \text{eq.7.5}$$

$$\epsilon_{yy} = v_{,y} + 1/2(u^2_{,y} + v^2_{,y} + w^2_{,y}) \quad \text{eq.7.6}$$

$$\epsilon_{zz} = w_{,z} + 1/2(u^2_{,z} + v^2_{,z} + w^2_{,z}) \quad \text{eq.7.7}$$

$$\epsilon_{xy} = v_{,x} + u_{,y} + u_{,x}u_{,y} + v_{,x}v_{,y} + w_{,x}w_{,y} \quad \text{eq.7.8}$$

$$\epsilon_{yz} = w_{,y} + v_{,z} + u_{,y}u_{,z} + v_{,y}v_{,z} + w_{,y}w_{,z} \quad \text{eq.7.9}$$

$$\epsilon_{zx} = u_{,z} + w_{,x} + u_{,z}u_{,x} + v_{,z}v_{,x} + w_{,z}w_{,x} \quad \text{eq.7.10}$$

where u , v and w are the three displacements in the x -, y - and z -directions.

The total strain vector is:

$$\epsilon = \{ \epsilon_{xx}, \epsilon_{yy}, \epsilon_{zz}, \epsilon_{xy}, \epsilon_{yz}, \epsilon_{zx} \} \quad \text{eq.7.11}$$

the total strain vector can be divided into linear and nonlinear terms:

$$\epsilon = \epsilon_L + \epsilon_{NL} \quad \text{eq.7.12}$$

Following the work of Leissa [19], we assume \underline{b} to represent a matrix of linear strains ϵ_L due to unit displacement u , while $\Sigma \underline{b}_{i1}$ and $\Sigma \underline{b}_{i2}$ will represent the column matrix of the nonlinear strains:

$$\epsilon_L = \underline{b} u \quad \text{eq.7.13}$$

$$\epsilon_{NL} = \Sigma \underline{b}_{i1} u * \underline{b}_{i2} u \quad \text{eq.7.14}$$

where $i = x, y, z$.

Any thermal stresses (strains) associated with the mechanical stresses (strains) could be added to the elastic strains in the form:

$$e = \epsilon + \epsilon_T \quad \text{eq.7.15}$$

where $\epsilon = \epsilon_L + \epsilon_{NL}$ as shown in equation 7.12.

Since the structure is elastic, Hooke's Law relates the stresses, σ , and strains, e , in the following form:

$$\sigma = E \epsilon + E_T \alpha T \quad \text{eq.7.16}$$

where E and E_T are the matrices of elastic constants, α is the coefficient of thermal expansion, and T is the temperature difference to which the structure is subjected.

The strain energy expression can now be easily evaluated from the integral:

$$U = 1/2 \int \epsilon^T \sigma \, dv \quad \text{eq.7.17}$$

Simply, by substituting the values in equations 7.5 to 7.10 into the above equation 7.17, assuming the nonlinear product terms to be very small compared with the single nonlinear strain terms, and separating linear and nonlinear stresses by two distinct matrices, an expression for the strain energy equation is obtained as:

$$U = 1/2 \int (u^T \underline{b}^T E \underline{b} u + 2u^T \underline{b}^T E_T \alpha T + \epsilon_T^T E \epsilon_T + 2 \sum \sigma^T (\underline{b}_{i1} u) * (\underline{b}_{i2} u)) \, dv \quad \text{eq.7.18}$$

It is emphasised that σ is considered constant when differentiating with respect to the displacement u , so by using equations 7.5 to 7.15 terms into 7.18 and using the integrals defining the elastic and the geometric matrices as will be shown later, we obtain:

$$P = (K_e + K_g) u + P_T \quad \text{eq.7.19}$$

where K_e , is the elastic stiffness matrix, simply obtained by evaluating the integral:

$$K_e = \int \underline{b}^T E \underline{b} \, dv \quad \text{eq.7.20}$$

and K_g , the geometric stiffness (initial state dependent) matrix, is similarly obtained from:

$$K_g = \sigma \int \Sigma (\underline{b}_{i1}^T \underline{b}_{i2} + \underline{b}_{i2}^T \underline{b}_{i1}) dv \quad \text{eq.7.21}$$

and finally P_T , the thermal force matrix, when needed is given by:

$$P_T = \int \underline{b}^T u_T \alpha T dv \quad \text{eq.7.22}$$

It should be noted here that, for vibration analysis it is suitable to compute the total stiffness matrix $K = K_e + K_g$ instead of dealing with each matrix separately, this results in economic advantages in the computer applications.

Equation 7.18 can be simplified by writing $\underline{b}_1 = \{ \underline{b}_{x1} \ \underline{b}_{y1} \ \underline{b}_{z1} \}$ and $\underline{b}_2 = \{ \underline{b}_{x2} \ \underline{b}_{y2} \ \underline{b}_{z2} \}$ which replace the summation sign in order to simplify the integration.

$$K_g = \sigma \int (\underline{b}_1^T \underline{b}_2 + \underline{b}_2^T \underline{b}_1) dv \quad \text{eq.7.23}$$

Equation 7.23 allows for a systematic investigation of the effect of higher order terms in the strain_displacement relationships.

Clearly, the above equation is independent of the choice of the coordinate system to be used for the analyses, this is an advantage of the method which may be applied even in the analysis of axisymmetrical shell structures.

Other names have been used in the past to identify K_g , such as the Incremental Stiffness Matrix, the Initial Stress Matrix, and the Coefficient Matrix, but recently the term "Geometric Stiffness Matrix" has become the most used due to the fact that it is really the result of a small change in the geometry of the structure.

In the following sections, the above geometric matrix is evaluated for the plate element chosen for our analysis, followed by the other sections to evaluate the elastic stiffness matrix and the consistent mass matrix, all the above matrices were made for an assumed compatible displacement and consistent masses (for full details on these matrices see related references).

7.3.1 Geometric Stiffness Matrix

All terms must be multiplied by $\lambda = (N_{x0}b/1260 a)$ where, a and b are the plate length and width:

552												
66b	12b ²											
-42a	0	56a ²										
204	39b	21a	552									
-39b	9b ²	0	-66b	12b ²								Symmetric
-21a	0	28a ²	-42a	0	56a ²							
-204	39b	21a	-552	66b	42a	552						
39b	9b ²	0	66b	12b ²	0	-66b	12b ²					
-21a	0	7a ²	-42a	0	-14a ²	42a	0	56a ²				
-552	66b	42a	-204	39b	21a	204	-39b	21a	552			
-66b	12b ²	0	-39b	9b ²	0	39b	-9b ²	0	66b	12b ²		
-42a	0	14a ²	-21a	0	-7a ²	21a	0	28a ²	42a	0	56a ²	

Reference Przemieniecki [29]

$$F = [20\beta^2 + 4(1 - \nu)]a^2$$

$$G = 30(\beta^2 - 2\gamma^2) - 3(14 - 4\nu)$$

$$H = -[30\gamma^2 + 3(1 - \nu)]b$$

$$I = [-15\beta^2 + 3(1 + 4\nu)]a$$

$$L = [10\gamma^2 - (1 - \nu)]b^2$$

$$M = 0 \text{ (zero)}$$

$$N = [30\beta^2 + 3(1 - \nu)]a$$

$$P = [10\beta^2 - (1 - \nu)]a^2$$

$$Q = [5\gamma^2 + (1 - \nu)]b^2$$

$$R = [10\beta^2 - 4(1 - \nu)]a^2$$

$$S = [10\gamma^2 - 4(1 - \nu)]b^2$$

$$T = [5\beta^2 + (1 - \nu)]a^2$$

$$V = 30(\beta^2 + \gamma^2) + 3(14 - 4\nu)$$

$$W = [-15\gamma^2 + 3(1 - \nu)]b$$

$$X = [15\beta^2 - 3(1 - \nu)]a$$

$$Y = -30(2\beta^2 - \gamma^2) - 3(14 - 4\nu)$$

$$Z = [-15\gamma^2 + 3(1 + 4\nu)]b$$

$$\beta = (a/b)^2$$

$$\gamma = 1/\beta.$$

7.3.3 Other Geometric and Elastic Stiffness developments

An alternative analysis based on total potential energy variation, was given in Kapur and Hartz [13], which obtained elastic and geometric stiffnesses by starting from the potential energy due to in-plane stress in a rectangular plate element:

$$V = t/2 \iint (\sigma_x w^2_{,x} + \sigma_y w^2_{,y} + 2\tau_{xy} w_{,x} w_{,y}) dx dy \quad \text{eq.7.24}$$

where t is the plate thickness, and the strain energy equation is given by:

$$U = 1/2 \iint \mathbf{M}^T \mathbf{x} dx dy \quad \text{eq.7.25}$$

where σ_x , σ_y , and τ_{xy} are normal and shear stresses, w is the displacement function, \mathbf{M} is the column matrix of moments per unit length, and \mathbf{x} denotes the curvature and twist vector at any position in the plate. By adding equations 7.24 and 7.25, using simplifying terms, we end up with the total energy equation:

$$\mathbf{E} = \mathbf{U} + \mathbf{V} \quad \text{eq.7.26}$$

or,
$$\mathbf{E} = 1/2 \underline{\mathbf{b}}^T (\mathbf{K}_e + \mathbf{K}_g) \underline{\mathbf{b}} \quad \text{eq.7.27}$$

where $\underline{\mathbf{b}}$ is the strain matrix. For full development of the elastic, geometric stiffness matrices see Appendix 5.

7.4 Mass matrix determination

From the computational point of view, it could be easier to compute the equivalent mass matrix for the unassembled element, using local coordinates to start with, then making use of the transformation rules to obtain the total mass for the structure as a whole.

The element mass matrix for instance (see references [14], [26], [28], and [30]) is given by:

$$m = \int \rho \underline{a}^T \underline{a} dv \quad \text{eq.7.28}$$

where ρ is the material density (mass per unit volume), and \underline{a} is the factor matrix of all nodal displacements in the local coordinate axes shown in equation 7.4. When the integration is accomplished, then, by using the direction cosine matrix of transformation [D.C.M], we will obtain the global mass m for all the structure from the local system. In other words:

$$u_{\text{global}} = [\text{D.C.M}] u_{\text{local}} \quad \text{eq.7.29}$$

where [D.C.M] is an $n \times n$ matrix, where n is the total number of degrees of freedom for the element, and u is a matrix representing displacements.

For the case of our analysis where a rectangular plate is used, there are two different approaches for the displacement

distributions; in the first the displacement is incompatible, meaning that the displacement of adjacent plate elements are compatible in translation, but not so for the rotations at the common edges at the nodes; in the second both translations and rotations are compatible.

For the plate in our analysis the selection is for the second approach in order to achieve more precise results.

Having obtained \underline{a}^T as shown in equation 7.4, then by substituting in equation 7.28 we will get the following mass matrix for a compatible displacement.

$$m_{31} = -3,432a$$

$$m_{32} = -484ab$$

$$m_{33} = 624a^2$$

$$m_{41} = 8,424$$

$$m_{42} = 2,028b$$

$$m_{43} = -1,188a$$

$$m_{52} = -468b^2$$

$$m_{53} = 286ab$$

$$m_{73} = -702a$$

$$m_{75} = -1,188b$$

$$m_{76} = -2,028a$$

$$m_{82} = -162b^2$$

$$m_{83} = 169ab$$

$$m_{85} = 216b^2$$

$$m_{93} = -162a^2$$

$$m_{96} = -468a^2$$

To be noted again that a and b are length and width of the plate element.

CHAPTER 8

EXPERIMENTS AND EQUIPMENT USED

8.1 Introduction

During the years 1983-1986, experiments were conducted in the Department of Aeronautics and Fluid-Mechanics at Glasgow University as part of research into the relation between the stress level in a structure and the resonant frequency under forced vibration.

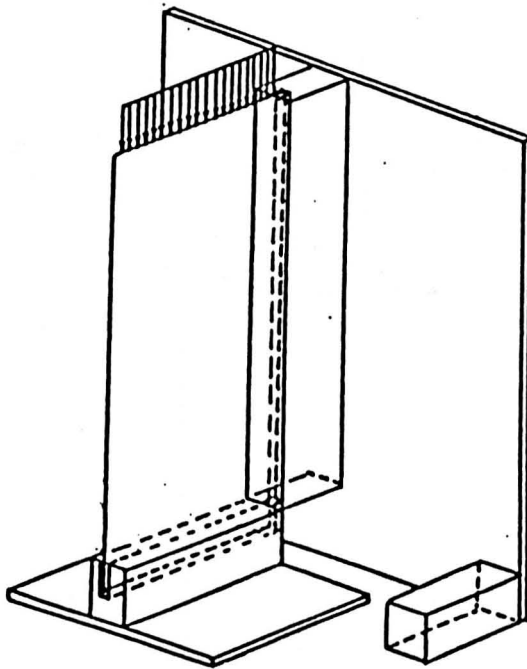
In part I of this thesis, the work on a three-dimensional frame structure was described and discussed.

In this chapter, we will turn our attention to a more complicated problem, namely, the plate problem, and the tests performed on isotropic, thin, flat plates. Results and concluding remarks will follow in chapter 9. Here the design criteria, the equipment used, the method employed, and an extension to the three-dimensional thin walled structure will be discussed.

8.2 Plate Models

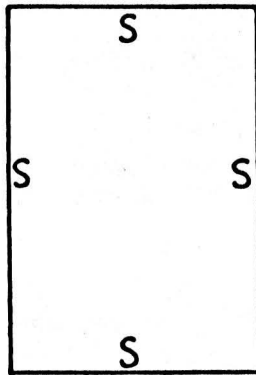
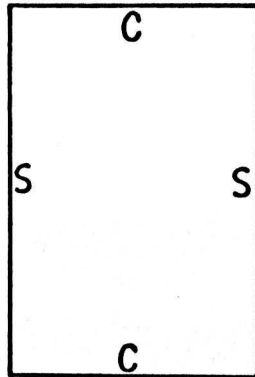
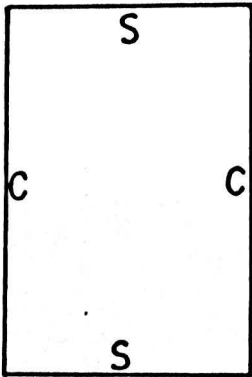
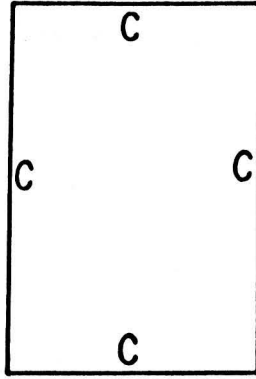
A set of three isotropic flat steel plates were made available. These were pieces of precision ground gauge plate and were supplied by the manufacturer to dimensions 45x5x0.08 cm, 45x15x0.08 cm and 45x15x0.16 cm.

These plates were mounted in a special test rig with edge members of a designed U- and V-section so that both clamped and simply supported boundary conditions could be simulated, as shown in the following pictures and sketches.



Pictures of the edge members

Figure-24-



Sketches of the plates with
different boundary conditions

Figure-25-

The plates were subjected to uni-axial, inplane loading only for simplicity in testing and computer analysis. The figure below shows the load direction employed.

By applying a continuous uniform pressure along the upper edge of the plate, and holding the plate in the manner shown in the pictures below, the plate was ready to be tested experimentally. The material properties were taken to be:

$E = 2.09 \times 10^{11} \text{ N/m}^2$, $\rho = 7.8 \times 10^6 \text{ Kg/m}^3$, and $\nu = 0.3$, as the Young's modulus, material density, and Poisson's ratio respectively.

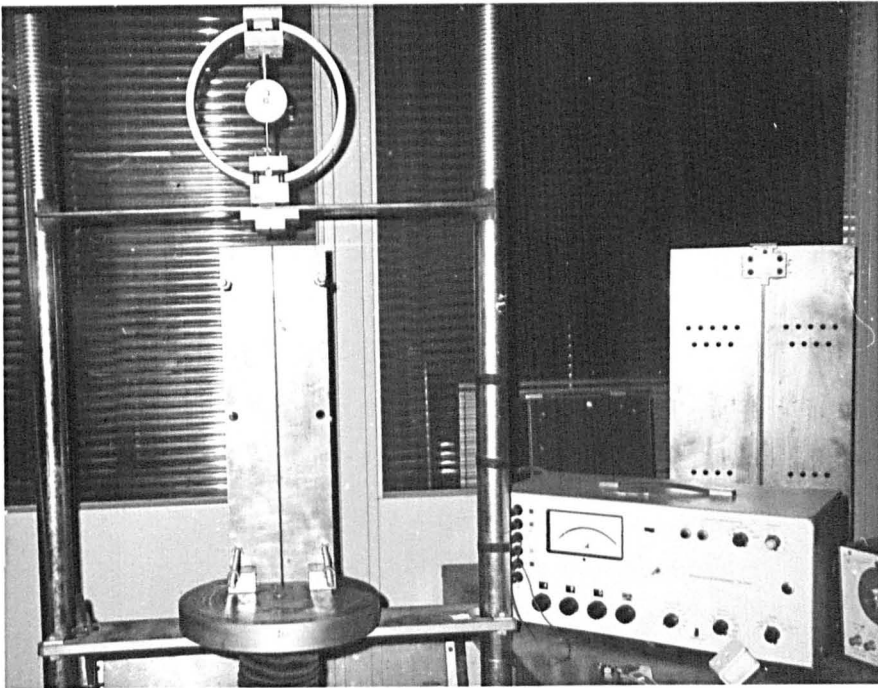


Plate set up for testing

Figure-26-

8.3 Equipment Used for the Experiment

Apart from the plate itself and the test rig, the equipment was essentially the same as used earlier for testing the three-dimensional frame structure.

The test rig was mounted between the plattens of a small screw loading type of testing machine, surface mounted strain gauges were employed to check the uniformity of the stress level in the loaded plate. Each plate was checked for flatness.

Pictures of the equipments used for the plate test are shown below:

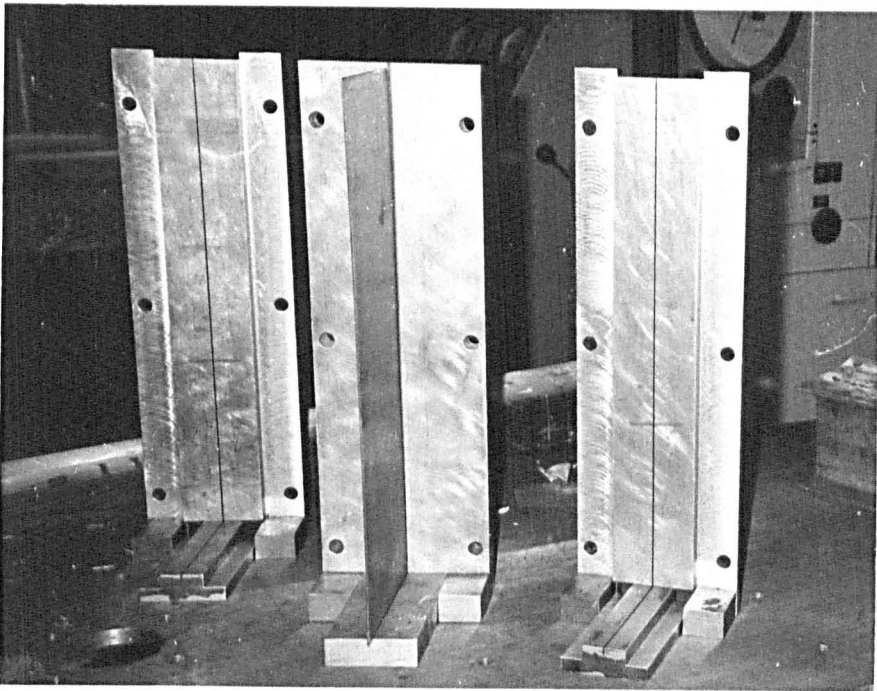


Plate sideways containers

Figure-27-

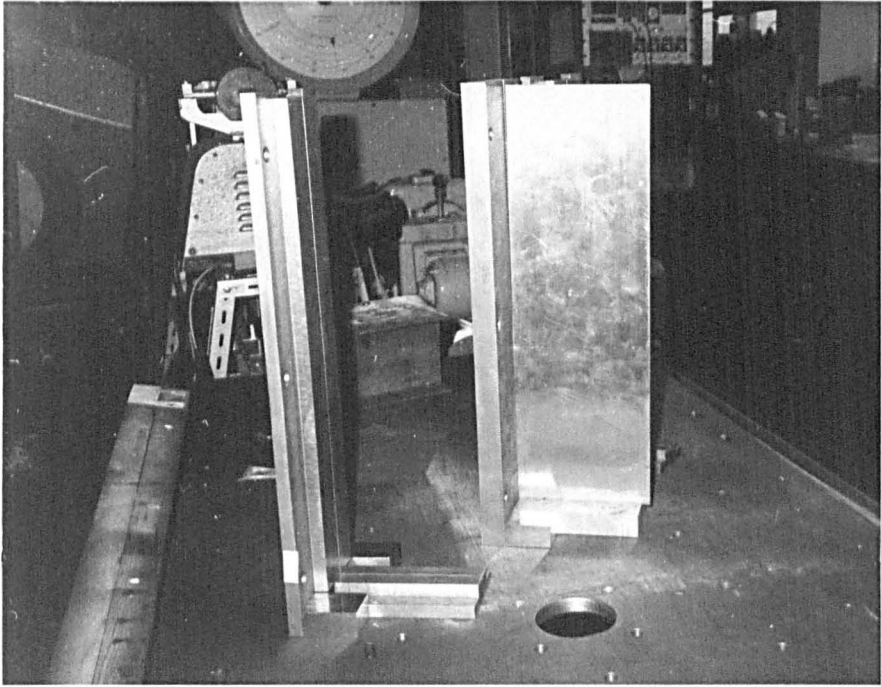


Plate set up

Figure-28-



Phillips Multimeter

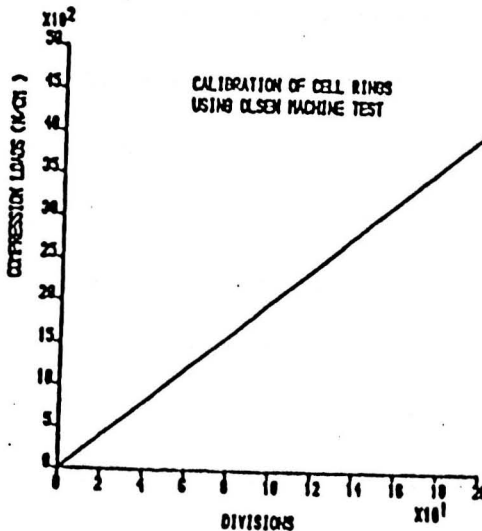
Figure-29-

8.4 Experimental Procedure

The general procedure was as follows: The plate was sinusoidally excited by applying a varying lateral force produced by the small electromagnetic exciter which was driven by the signal generator. The response was picked up by the accelerometer, amplified and transmitted to the Narrow Band Spectrum Analyser which gave the frequencies and amplitudes of the harmonics in the signal.

The signal generator frequency was varied until the resonant condition was obtained, which was identified by observing the amplitude of the dominant harmonic. The accelerometer position was varied on the plate surface in order to identify the position of any nodal points.

The load, measured by the one ring-type load cell, was increased in small increments and at each level of loading the frequency and the amplitude of the dominant harmonic was observed and recorded. The calibration chart for the load cells is shown below:



Load-Gauge chart

Figure-30-

The load was applied statically and the increments in loading followed the same treatment in order to neglect the inertia effects which would be present if the loads were applied in any other way.

A check on the frequency of excitation was provided by the Phillips frequency meter, this being particularly useful at the lowest and highest frequencies used.

8.5 Some Important Observations

The early experiments showed the existence of a set of harmonics. It was noted that the frequency of the harmonic of greatest amplitude did not coincide with the excitation frequency in the response at resonance. It suggested the possibility of the existence of a mode shape difference between the buckling modes and the vibration modes. If all the analysis were based on the different modes of buckling and vibration a nonlinear relationship between the applied loads and the square of the frequency ratio is the most acceptable answer but, when both modes of buckling and vibration were very close to each other, an almost linear relationship appeared to exist between the applied axial (inplane) loads and the square of the frequency ratio.

It was noted also that when there is a drop in the excitation frequency values (lower modes of vibration) the amplitude of the response harmonics show a noticeable increase, this increase is in linear relation with the plate out of plane deflection under the applied loads. The applied loads were kept at less than 60% of the expected buckling load, this margin allows for more testing of the

same plate to get more information and to save the time consumed in replacing a permanently deformed plate.

Laboratory induced noise coming from other machines in the department was avoided as far as possible by running most of the experiments in the evening when most of the machines are at rest.

Regarding the strip type of plates, the boundary conditions were slightly different, as shown in figure -32-. One side of the plate is left free, while the other three edges were clamped. The test rig for this condition differed from that used for the other two plates.

8.6 Extended use of the experimental set up

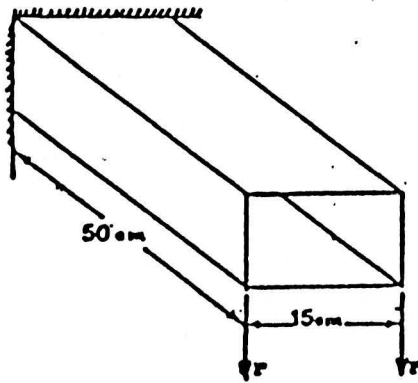
Final experiments were conducted on a Three-dimensional thin walled structure. The monocoque beam shown below was designed and tested using a procedure similar to that previously employed for the isotropic plates but with some difference in the loading direction.

Bending loads instead of axial loads were applied, and the data collected were only for the lower plate of the monocoque structure, where this specific plate was subjected to a varying axial compression. The stress condition for this plate differs from that of the other components of the beam, and, of course, from that of the earlier tested plates.

The mass producing the bending load was supported by a spring in order to separate the mass of the system from the mass of the load. These loads were increased, and variation was detected in both frequency and amplitude of the vibration.

This experiment was made as an application of what had been done earlier on single plates, to show that for even more complicated structures, the relation between the stress level and the ratio of the frequency squared is overall linear, as verified earlier for the space frames and the plates.

The computer programme made for the monocoque structure was not intended for the whole structure but considered only the lower, compression plate. The boundary conditions assumed for the plate were clamped at the root and along the two axial edges which are connected to the vertical webs and free at the loaded end. The number of elements used for the analysis (F.E.M.) was 15 of size 9×3 cm, so that there were three spanwise rows of six nodes each.



Monocoque structure

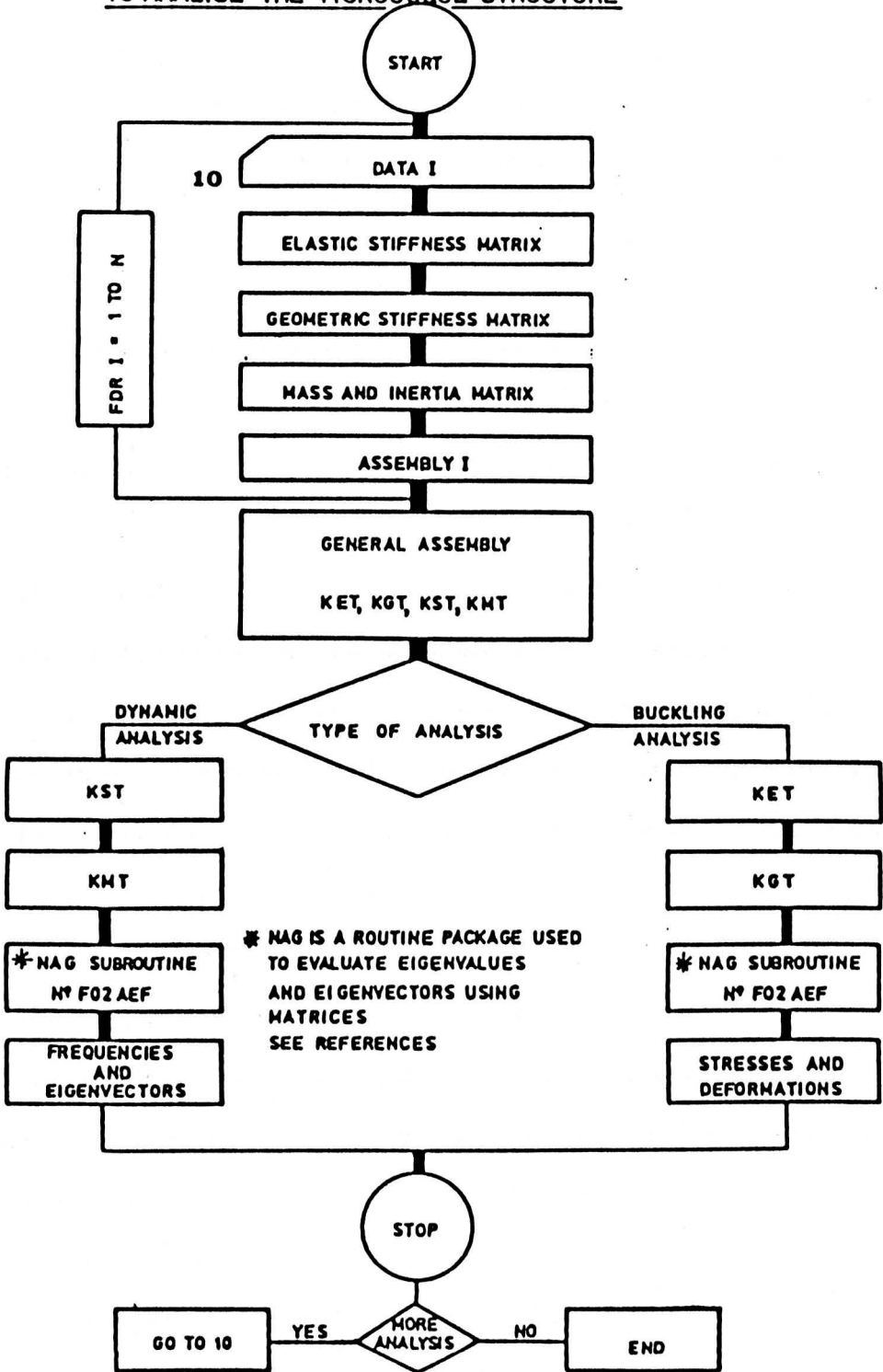
Figure-31-

In the above structure, for the computer set up, the inplane loads for the elements of the lower plate were increased by a constant increment from the loaded end to the root to account for the stress increase so that each element carries an end load corresponding to the engineering theory of bending value at its midpoint.

For this reason, the geometric stiffness matrix was increased progressively so that the assembly procedure was modified slightly to allow for this increase, as shown in the following flow chart.

8.6.1 Flow chart used for the monocoque structure

FLOW CHART ON THE USE OF THE FEM PROGRAM TO ANALYSE THE MONOCOQUE STRUCTURE



CHAPTER 9

CORRELATION BETWEEN EXPERIMENTAL AND THEORETICAL ANALYSIS

From the results obtained by testing the steel plate strip of 45 x 5 x 0.08 cm. a graph illustrating the stress-frequency relationship has been produced. With only a few points, it was possible to trace a linear relation between the axial applied loads and the square of the frequency ratio with respect to the resonant frequency of the unloaded plate vibration.

It is worthy to mention, that there is no apparent change in mode shape in vibration or in buckling for this type of plate. The value deducted for the critical stress is very close (within 5%) to the theoretical and exact value.

It should be noted that when increasing of the excitation frequency value occurs (double or triple of that of the first mode) the linearity can still persist, but with a higher value of the critical load obtained, but these values could easily be reduced to the exact one when divided by a factor, two or three, depending on how much the frequency of excitation mode was raised.

The reason to substantiate this phenomenon is based on the fact that if the mode shape of vibration of the plate is doubled

or tripled, it will coincide with the second or the third mode of the buckling load forming a linear relationship between the applied loads and the square ratio of the frequency of vibration. If the factor raising the order of the mode shape is known exactly, by using it in the related graphs will lead to the buckling load determination at the $(\omega/\omega_0)^2 = 0$ but, this is not likely to occur in the theoretical analysis unless special equations are introduced to involve the mode order factor.

The following figure shows the plate strip used for the first experimental tests, the boundary conditions are C-C-C-F, which differ from those for the other plates used later.

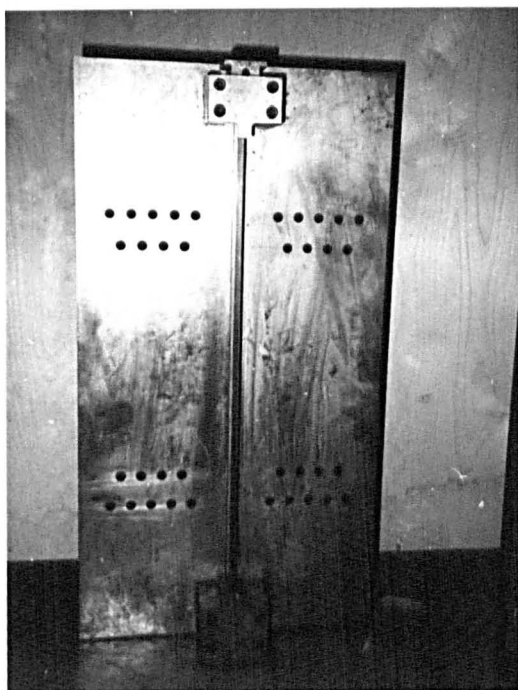


Plate strip

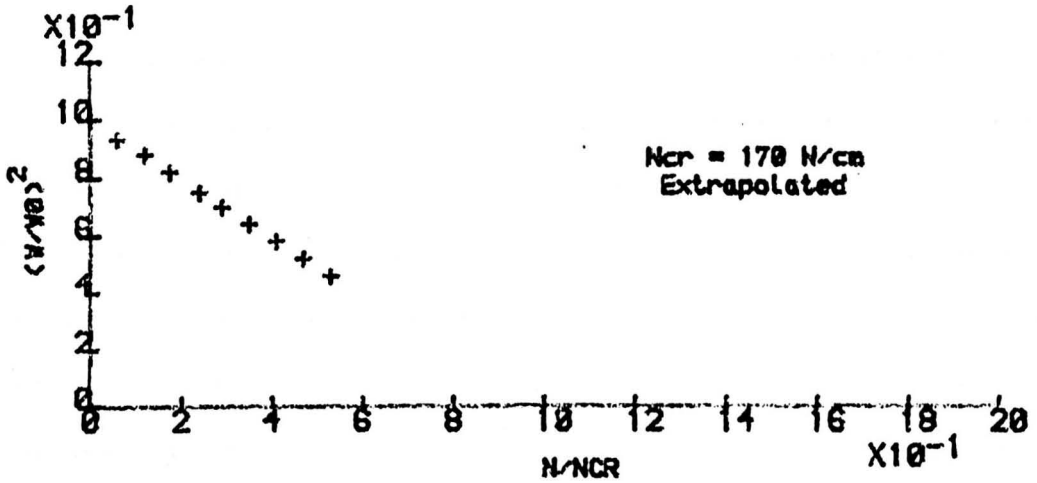
Figure-32-

The following graph, figure-33-, which relates the square ratio of the frequency to the applied axial loads is based on the data obtained experimentally.

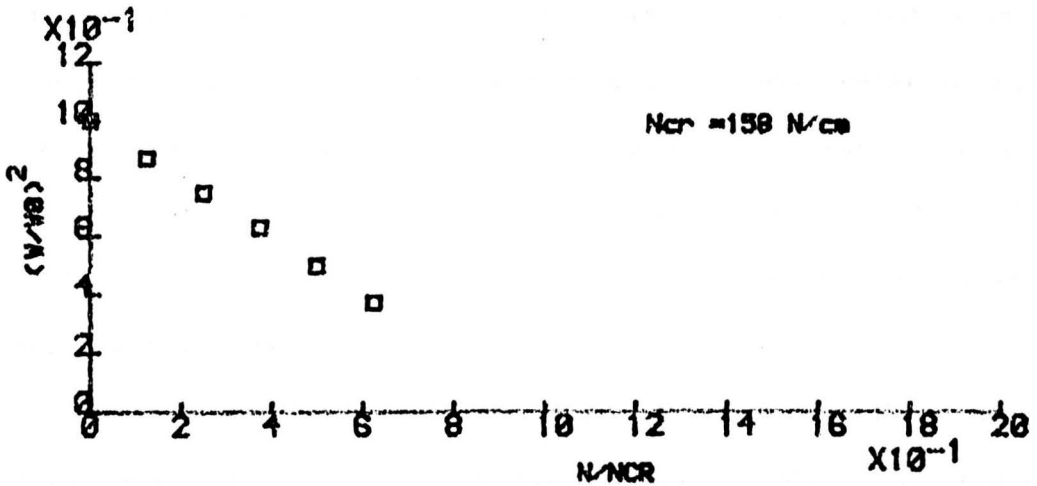
By extending the straight line joining the experimental points to the point of zero frequency ratio ($(\omega/\omega_0)^2 = 0$), one can detect the buckling load value. This result of the experimental buckling load of 850 Newtons falls within 5% lower than the exact buckling load of 875 Newtons, which is an acceptable error. The numerical results produce as close result (790 Newtons) as the experiments predict.

In the following page, the experimental and the analytical graphs, figure -33-, are shown for the strip plate analysis:

GRAPHS OF THE
 FREQUENCY-STRESS LEVEL RELATION IN A
 MIXED BOUNDARY (CCCF) STRIP



EXPERIMENT RESULTS



COMPUTER RESULTS
 VIA F.E.M.

FIGURE NO.33

All plates were located in their respective holders, which simulate the desired boundary conditions as has been shown in earlier sketches. The loads were statically applied and increased while the frequency of the plate vibrations are applied, recorded and their respective amplitudes noted.

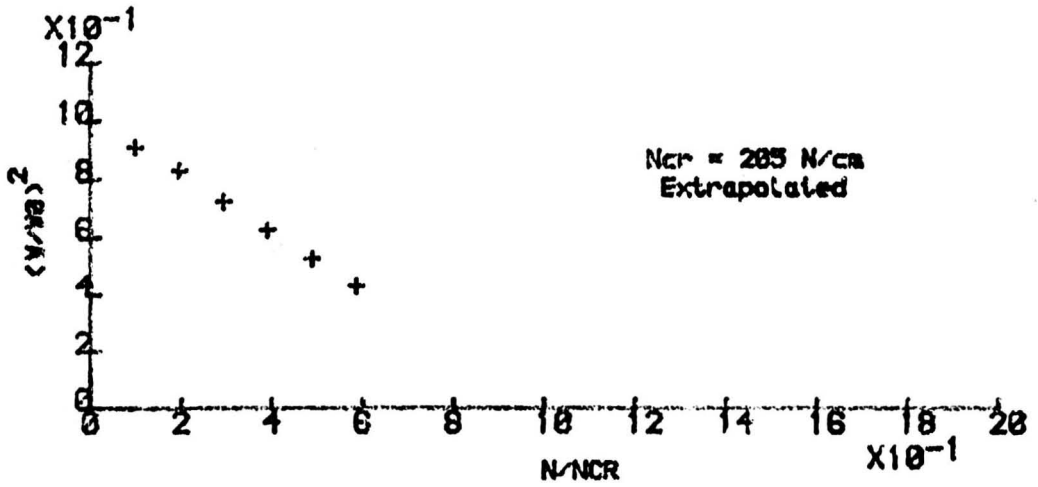
The exciter and the accelerometer were carefully moved from one end of the plate to the other to search for any possible nodes to account for a new mode shape in the structure.

For lower modes of vibrations, no more than the first mode shape is detected experimentally, but as has been discussed earlier, a change in the mode shape was apparent at a certain set of loads producing a change in the slope of the relation between the applied loads and the squared ratio of the frequencies of vibration.

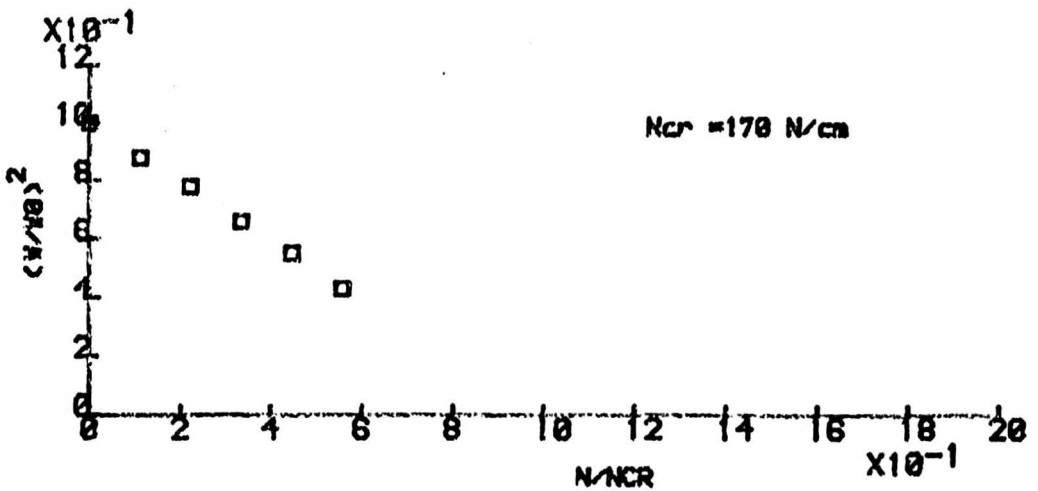
It is useful to underline the importance of the role of the mode shape changes after certain load increments, this, in fact, produces a change in the overall linearity behaviour in the theoretical results (via Finite Element Method), but when this phenomenon has been carefully studied, a linear relation results for each set of loads (individual linearity) between the applied stresses and the square of the frequency ratio, and the final critical load is within only 5 - 6 % in error when compared with the exact values.

The following graphs, figures -34- to -37-, show the experimental and the computer results for the plates of ($a/b = 3$), subjected to selected boundary conditions made available for the experimental and the theoretical analysis.

GRAPHS OF THE
 FREQUENCY-STRESS LEVEL RELATION IN A
 SIMPLY SUPPORTED THIN PLATE



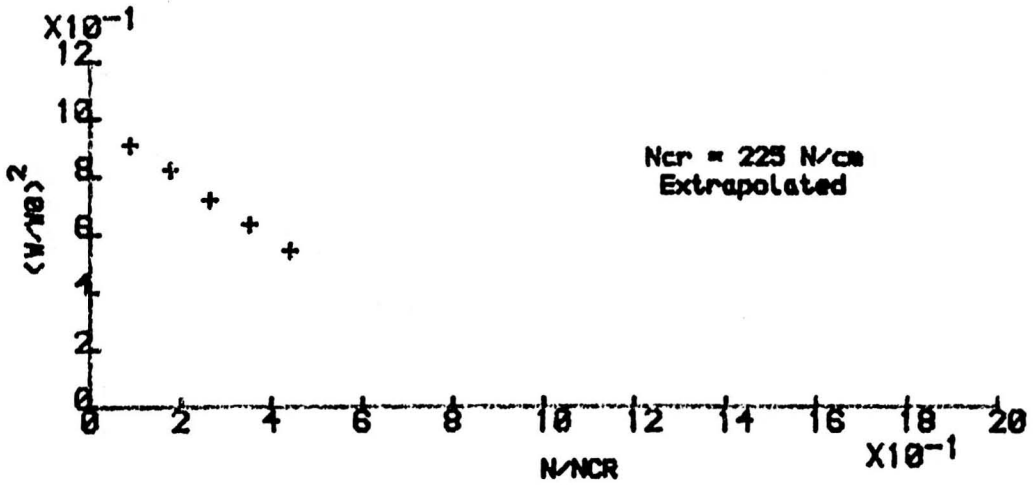
EXPERIMENT RESULTS



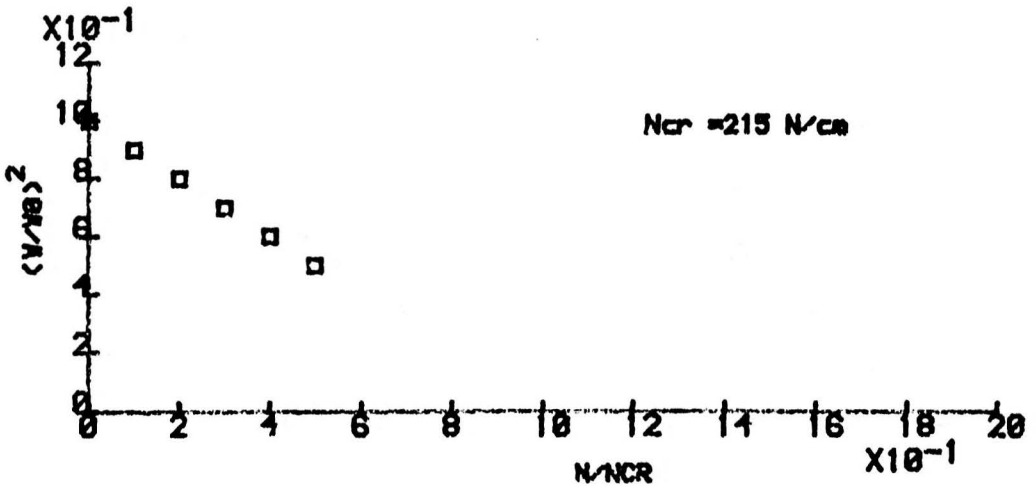
COMPUTER RESULTS
 VIA F.E.M.

FIGURE NO.34

GRAPHS OF THE
 FREQUENCY-STRESS LEVEL RELATION IN A
 MIXED BOUNDARY (SSCC) PLATE



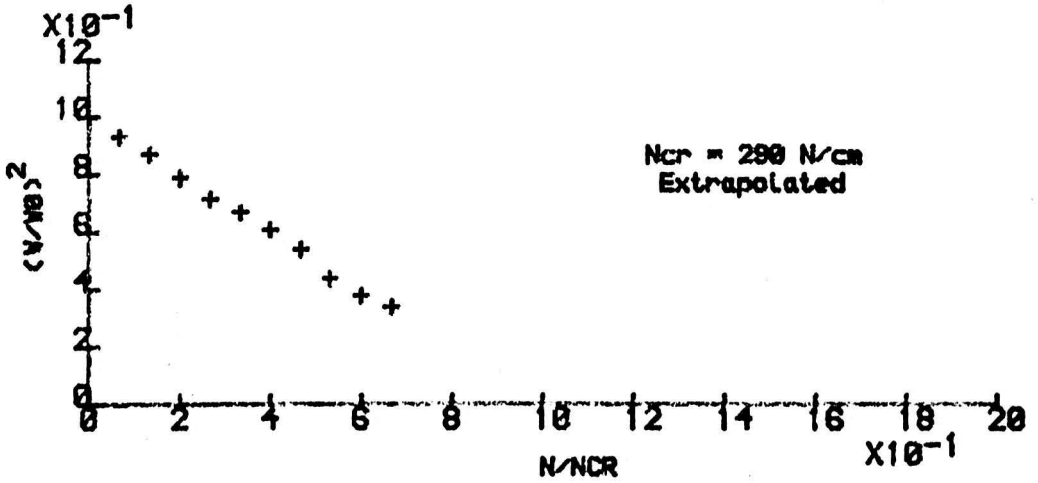
EXPERIMENT RESULTS



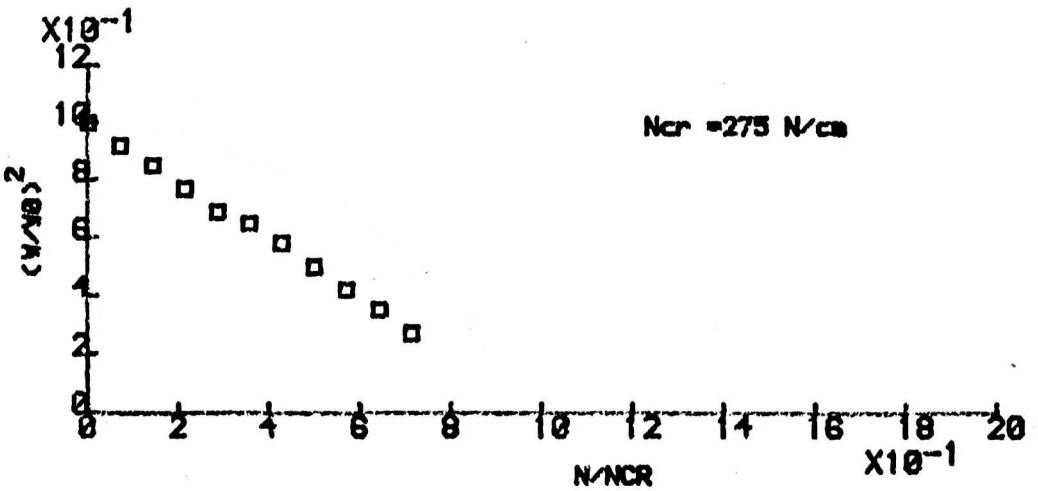
COMPUTER RESULTS
 VIA F.E.M.

FIGURE NO.35

GRAPHS OF THE
 FREQUENCY-STRESS LEVEL RELATION IN A
 MIXED BOUNDARY (CCSS) PLATE



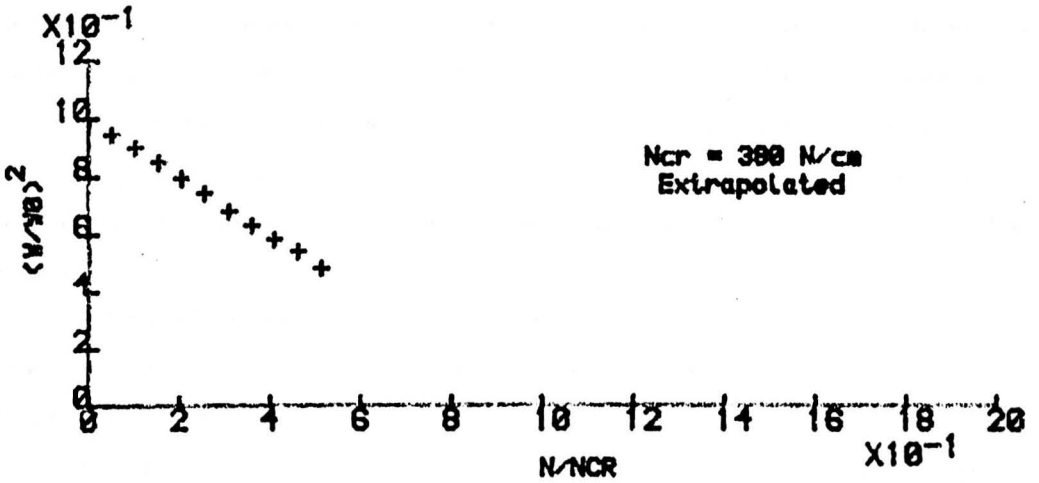
EXPERIMENT RESULTS



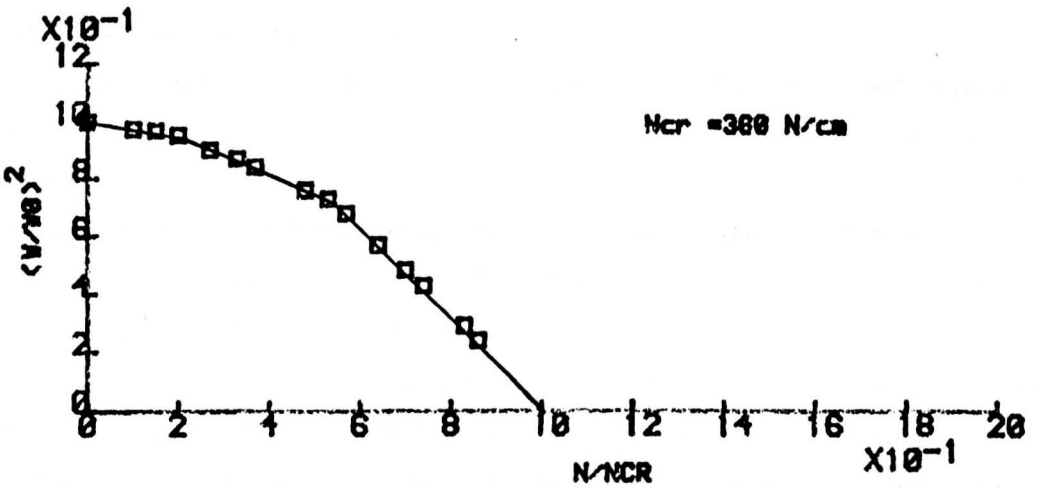
COMPUTER RESULTS
 VIA F.E.M.

FIGURE NO.36

GRAPHS OF THE
 FREQUENCY-STRESS LEVEL RELATION IN A
 FULLY CLAMPED THIN PLATE



EXPERIMENT RESULTS



COMPUTER RESULTS
 VIA F.E.M.

FIGURE NO.37

For the fully clamped plate, considering the analytical results in particular, as shown in the previous graph, figure-37-, the change in the total stiffness matrix (Elastic and Geometric) due to the increase in the applied loads produces a change in the vibrational mode shapes in the plate, if these changes in the mode shape are amplified it leads to a local linear relationship between the vibrational and the buckling mode shapes, which is a necessary condition to ensure a linear relation between the applied loads and the square ratio of the frequency of vibration, but when the two modes are different, a nonlinear relationship is shown in the graph for the overall analysis of the fully clamped plate.

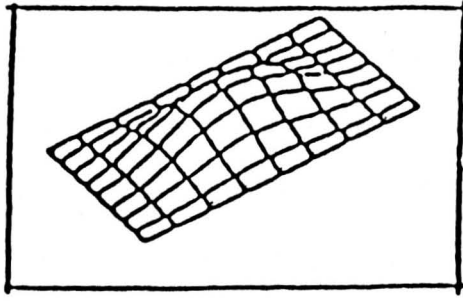
This phenomenon neither appeared in literature, nor was it encountered in the present experimental analysis for this set of boundary conditions.

The general linear relation, therefore, is slightly disturbed for the case of the fully clamped plate, this is due to the change in the buckling mode shape as will be shown in figure-38-.

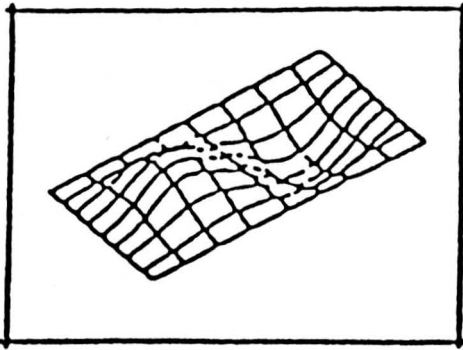
Although this situation occurred only analytically (F.E.M.), a linear relationship is suggested, based on the experimental analysis. The piecewise linearity is due to the approximation procedure in the computational analysis of this investigation and the handling of the boundary condition and the assumptions relative to the approximate methods.

The buckling mode shapes for the fully clamped plate are illustrated in figure -38-. They are produced from the computer data obtained from the F.E.M. output data of the node displacements corresponding to the eigenvalues. These buckling modes give an indication of the plate behaviour under the applied inplane loads when forced to vibrate.

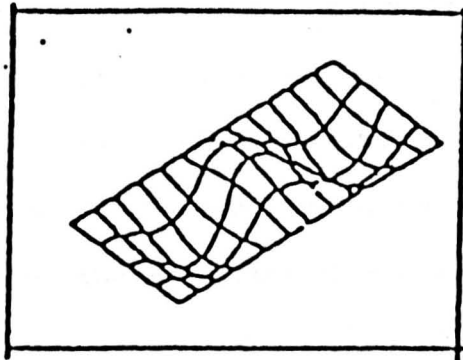
In fig-37-, the computer analysis show a piecewise linear relation between the square ratio of the frequency and the applied loads. This is due to the (piecewise) similarity between the buckling and the vibration mode shapes. If this necessary relation between the mode shapes is not accomodated, a nonlinear relation between the frequency and the applied loads will be the outcome of the analysis, see Appendix 4 (figures A4.9 and A4.10).



1st Buckling mode($N_{cr}=360$ N/cm)



2nd Buckling mode($N_{cr}=700$ N/cm)



3rd Buckling mode($N_{cr}=1060$ N/cm)

Buckling modes of the clamped plate

Figure-38-

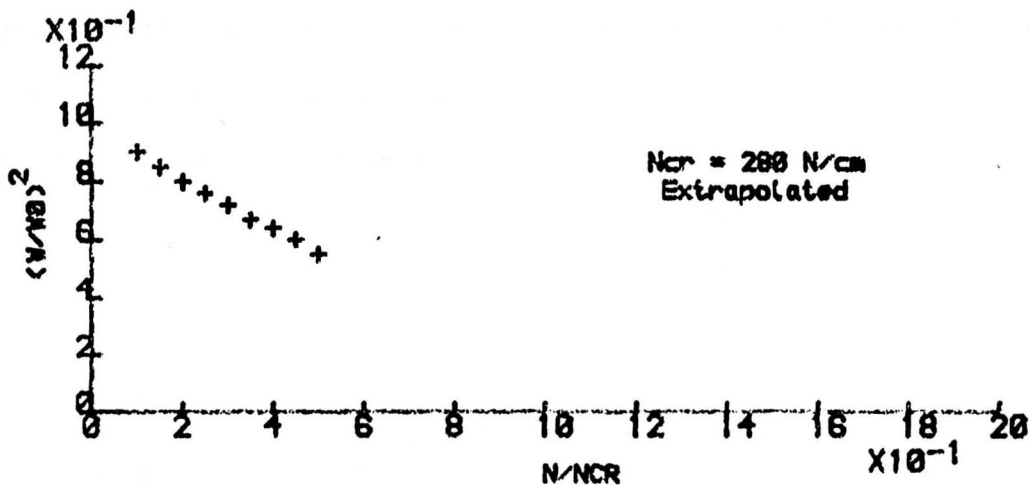
Figure-39- shows the experimental and the analytical results for the monocoque beam structure. Both graphs show a linear relationship between the squared ratio of the frequency of vibration and the applied inplane loads.

In the case of the thicker plate analysis, a higher buckling load value is obtained, see ref.[19]. It is important to state that, for this plate, the tendency towards nonlinearity becomes more evident. This phenomenon is due only to the change in the mode of vibration as the load is increased. Each mode of vibration corresponds to a particular mode of buckling and, consequently, of the slope of the $(\omega/\omega_0)^2$ against the load curve. In other words, only the mode shape is controlling the nonlinearity for these elastic, isotropics, flat plates.

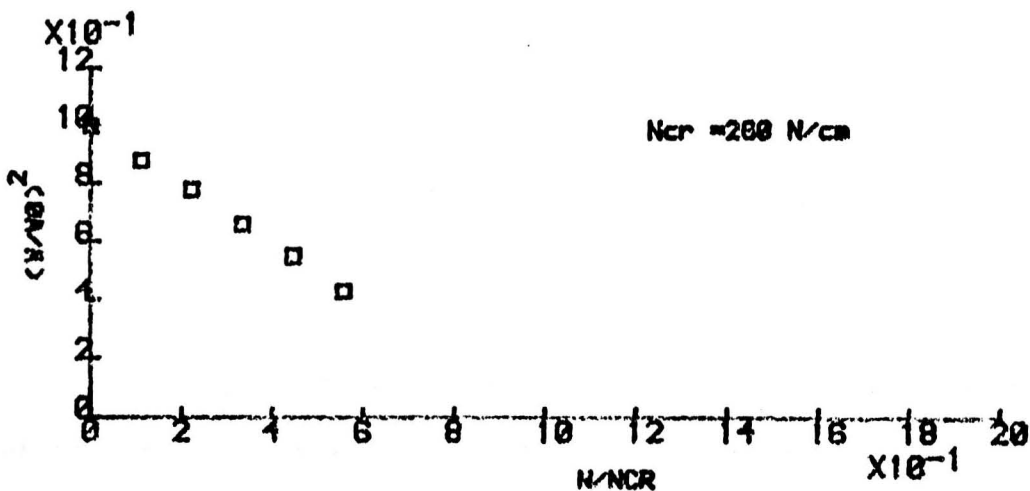
Loads applied, in all the previous experiments on the plates and on the monocoque beam structure, were kept under 60% of the expected critical load ,see figure-39-, in order to allow the experiments to be repeated before any permanent deformation occurs of the structure's geometry due to buckling or postbuckling.

Finally, graphical results from other sources (see Appendix 4) are reported for comparison, this information is included to show how important this study is for the structural safety. Taking an overall view, the experimental and analytic results show that the linear relationship between the applied loads and the square ratio of the frequency are predominant in most of the cases considered.

GRAPHS OF THE
 FREQUENCY-STRESS LEVEL RELATION IN A
 MONOCOQUE FIXED END BOX BEAM STRUCTURE



EXPERIMENT RESULTS



COMPUTER RESULTS
 VIA F.E.M.

FIGURE NO.39

With regard to the Finite Element Method computer analysis, the plate is divided into different element meshes, some of the elements are of the same aspect ratio of the plate dimensions of $a/b = 3$ while others have an aspect ratio of unity ($a/b = 1$). The elements of $a/b = 3$ were chosen, they produce more reasonable results due to their having the same aspect ratio as the whole plate. The more elements used to divide the structure the closer we get to the exact results.

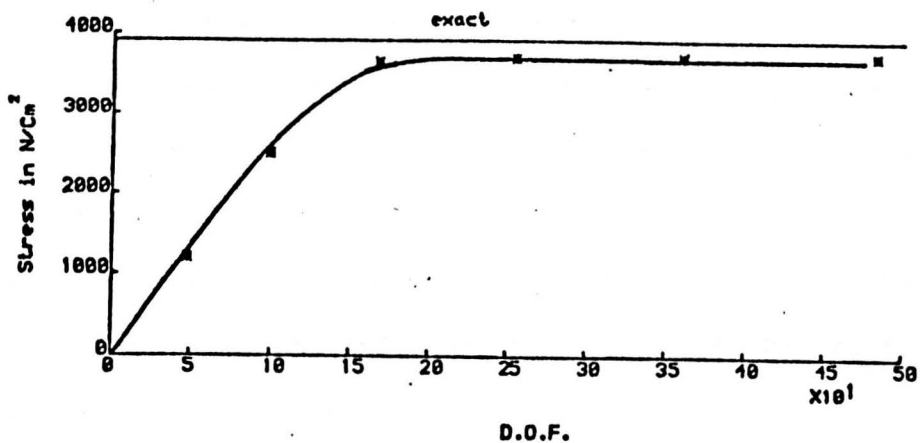


Figure-40-

Approach to the exact results

Comparing the computer results with the experimental results, after careful consideration, we can say that they are similarly linear, the only departures from linearity appearing in the computer results for the clamped plate are possibly explained as follows:

The computer graphical results are linear for each range of loads, and this phenomenon will continue until a final characteristic mode is reached by the structure, most of the analytical points agree very well with the experimental values when the modes of the two approaches are similar. The departure from linearity, when it occurs, and as shown in some analytical results, is due to the sudden change in the vibration mode shape which occurs at certain loads, which mathematically speaking, is due to the change in the form of the geometric stiffness matrix and hence of the total stiffness matrix resulting in a change of the mode of the structural vibration.

This nonlinearity was most noticeable in the fully clamped plate, for the mixed boundary condition plates it was less evident and for the fully simply supported plate this phenomenon was almost absent. This suggests that the boundary conditions the plate is subjected to influence the effect of the applied load in the plane of the plate.

As a final remark on this subject, one is very much inclined to affirm that linearity dominates the relationship between the applied loads and the square of the frequency ratio of the structures if careful consideration is given to the representation of the boundary condition.

The following graph, figure-41-, shows a summary comparison between experimental, analytical and exact results obtained earlier in this investigation.

Three distinct lines are shown for each case of the plate boundary conditions, the upper set of lines represent the fully clamped plate and the lower set represent the fully simply

supported plate, in between these two sets the plates with mixed boundary conditions are located. For each case, the upper line represents the exact solution, the middle line represents the experimental results, and the lower line represents the approximate analytical (F.E.M.) results.

The stiffness of the plate is seen to decrease in the analytical analysis while it is in its higher values for the experiment and the exact analysis. This summary graph shows how close all three sets of analyses are.

Finally, it is to be noted that in the simply supported plate (SSSS) exact line and the mixed plate (SSCC) analytical line are very close, they are represented on the graph only with one line, see figure-41-.

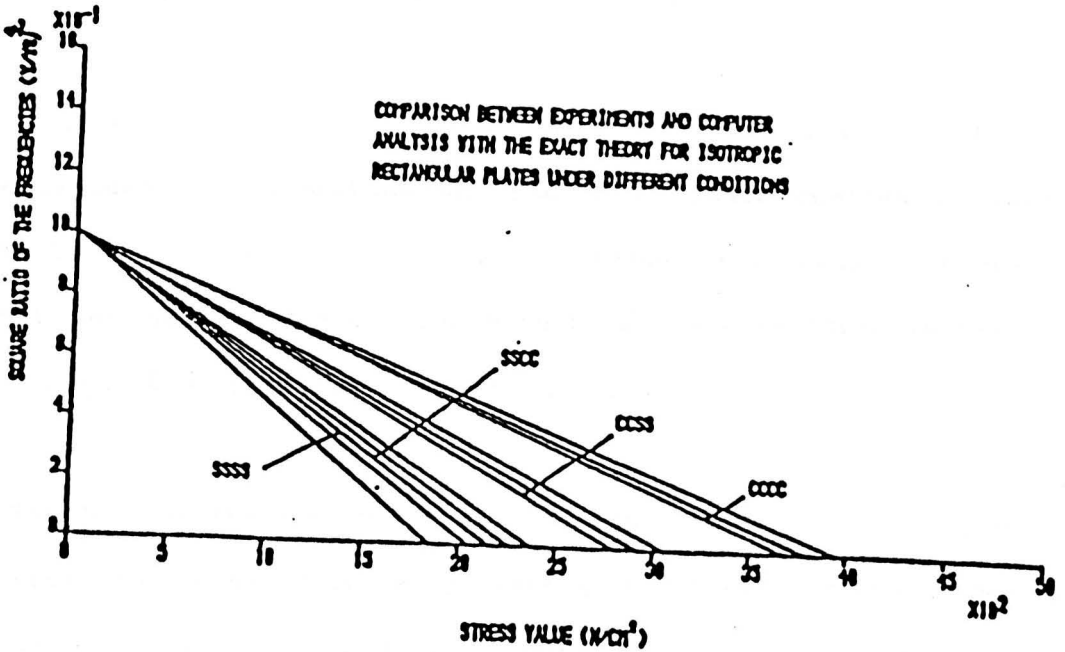


Figure-41-

CHAPTER 10

CONCLUSIONS AND FUTURE PROSPECTS

Conclusions

As a result of the previous discussion of this research topic both the theoretical and the experimental investigation outcome are summarized in the following conclusions:

1) A linear relationship does exist between the square ratio of the frequency of vibration and the axial loads applied to some selected types of three dimensional frame structures if certain conditions were satisfied, the conditions were explored in detail in chapter 4 of part I of this manuscript.

2) The load at the zero value of the square ratio of the frequency of vibration obtained by extrapolating in the given graphs gives a close estimation of the buckling load (within 6% of the exact buckling load).

3) The geometric stiffness matrix is initial state dependent, and this explains the relation between the applied loads and the effective stiffness matrix of the structure (total stiffness

matrix); the geometric stiffness alone leads the relationship between the applied loads and the square ratio of the frequency to to be linear if the elastic and the geometric matrices are similar, ie., the ratio between any pair of elements in one matrix is the same as that between a similarly located pair in the other.

4) When the analysed structure was of a plate strip (the ratio of $a/b \gg 3$), where a and b are the plate dimensions, a linear relationship was clearly shown between the square ratio of the frequency of vibration and the applied uniaxial loads.

5) It is shown in figure-37-, for the fully clamped plate analysed, that a piecewise linear relationship exists between the applied inplane loads and the square ratio of the frequency of vibration. This is due to a progressive change in the mode of vibration and, consequently, to the corresponding buckling mode. This linearity, if not studied carefully (as seems to have been the case in some early investigations, see Appendix 4), could lead to erroneous conclusions.

For all other boundary conditions the overall linearity is seen to be more likely to occur due to the similarity in the mode shapes of buckling and vibration.

6) The Finite Element Method is a reliable method of analysis, provided that the results obtained are checked carefully, this method and other similar numerical methods are used when exact solutions are not available or when experimental analysis could not be easily accomplished.

7) In the thicker plate ($t = 0.16 \text{ cm}$) when tested, higher modes of buckling and vibrations (2nd and 3rd modes) are in a better agreement, and a linear relationship is obtained between the applied loads and the square ratio of the frequency of vibration for both analytical and experimental analysis. This could be expected, since the out-of-plane geometrical imperfections will have less effect on the uniformity of the in-plane stresses than was so in the case of the thinner plate analysed earlier.

8) For the thin plate ($t = 0.08 \text{ cm}$), the nonlinearity between the applied loads and the square ratio of the frequency could be caused by either prestresses in the plate, out-of-plane imperfections as explained above, or non-coincidence of the mode shapes of vibration and the buckling, as has been illustrated by the analytical graphs shown in the text.

9) Good agreement between theory and experiment has been shown in the previous discussion and the related graphs were shown in the previous chapters of this manuscript to illustrate this agreement.

10) Experimental verifications are very important when exact or approximate results fail to exist, as has been verified in the literature survey throughout this investigation, so the experiments were done in order to obtain results for practical problems.

11) The experimental set up gave a variety of boundary conditions which could be used when analysing the structure. For the

rectangular plate this facility is advantageous by providing more applications in both mechanical and aeronautical areas of research investigations.

12) The exact solutions (when found) lie above both the experimental and the analytical (F.E.M.) solutions. The more constraints are on the structure in the first case (exact) and cause the absolute value of the frequency to arise. For the analytical (F.E.M.) case these constraints are less, to reduce the size of the matrices to be used in the analysis, consequently, the absolute value of the frequency is less. Finally, the constraints used for the experiment cause the frequency to be in between the above two cases, see chapter 9, figure-41-, which illustrates this relation for a plate at different boundary conditions.

13) The application of this method of analysis on a more complex structure is possible experimentally as well as analytically, only a slight modification is needed to use the analytical method. This is essentially in the assembly procedures. The existing experimental design rig could be used for various types of structures and could be modified to meet other requirements.

14) Some of the commercially available computer packages such as PAFEC, FLASH2 could not apply easily to the dynamic part of the analysis due to their poor handling of the stiffness matrix of the structure. The static analysis, when using these packages, gave similar results to those obtained by the Finite Element Method programme made especially to solve the static as well as the

dynamic cases. The stiffness matrix formulation in the above packages fails to include the geometric stiffness sensitivity to the applied external loads.

The mass matrix in the above packages also does not account for all the inertia effects in the vibrating structure.

15) A suggested graph relating the applied loads to the square ratio of the frequency of vibration for rectangular isotropic plates of $a/b = 3$ is introduced as a practical and theoretical solution, this graph can help the designer at the early stages of the design process on these or similar structures subjected to a uniform axial load and forced to vibrate at the same time.

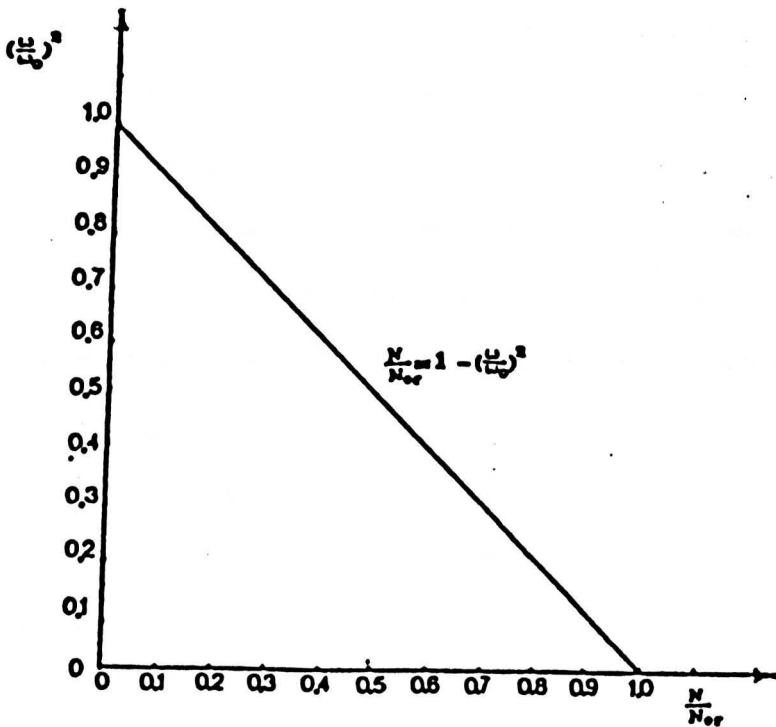


Figure-42-

Future Prospects

Further development of this method analytically and experimentally could lead to study more complex structures such as shells, stiffened plates. Some work could be done even on composite material and structures subjected to different types of loads in order to verify the relation between the vibration frequency in the structure and the applied loads in order to avoid all destructive testing methods and to give to the engineer a good design criteria.

More computer analysis is needed to study the aspects of nonlinearities observed earlier but, from an experimental point of view, similar structures could be well tested on simple rigs and most available equipment.

This method could be applied in booms, antennas, and space platforms proposed for future space applications due to their structural similarities to the three dimensional structure tested in this investigation.

All this and any other future related studies will be beneficial for both academic and industrial areas of research and development.

REFERENCES

- 1) ANDERSON R.G., IRONS B.M, and ZIENKIEWICZ O.C., "Vibration and Stability of Plates Using Finite Elements," International Journal of Solids and Structures, Vol.4, 1968, pp.1031-1055.
- 2) ARGYRIS J.H., "Recent Advances in Matrix Methods of Structural Analysis," Progress in Aeronautical Sciences, Vol.4, 1964.
- 3) BASSILY S.F. and DICKINSON S.M. , "Buckling and Vibration of In-Plane Loaded Plates Treated by Unified Ritz Approach," Journal of Sound and Vibration, Vol.59, No.1, 1978, pp.1-14.
- 4) BATHE K.J. and WILSON E.L., "Numerical Methods in Finite Element Analyses," Printise-Hall, 1976.
- 5) CARMICHAEL T.E. , "The Vibration of a Rectangular Plate with Edges Elastically Restrained Against Rotation," Quart. Journal of Mechanics and Applied Mathematics, Vol.12, Part 1, 1959, pp.29-42.
- 6) COURANT R., "Variational Methods for the Solution of Problem of Equilibrium and Vibration," Bulletin of American Mathematical Society, Vol.49, 1939, pp.1-23.

- 7) DAWE D.J. , "On Assumed Displacements for the Rectangular Plates Bending Elements," Royal Aeronautical Society, Vol.71, 1967, pp.722-724.
- 8) DURVASULA S. and SPRINIVASAN S. , "Vibration and Buckling of Orthotropic Rectangular Plates," Journal of Acoustic Society of India, Vol.19, No.3, 1967.
- 9) GERE J.M. and WEAVER W.Jr, "Matrix Algebra for Engineers," Van Nostrand Company, N.Y., 1965.
- 10) HEARMON R.F.S., "The Frequency of Vibration of Rectangular Isotropic Plates," Journal of Applied Mechanics, Trans. ASME., Vol.74, 1952.
- 11) HERRMANN G., "Dynamic Stability of Structures," Proceedings of the International Conference, 1965. (Edited by George herrmann)
- 12) JUBB J.E.M., PHILLIPS I.G. and BECKER H., "Interpolation of Structural Stability, Stiffness, Residual Stress and Natural Frequency," Journal of Sound and Vibration, Vol.39, 1975, pp.121-134.
- 13) KAPUR K.K., and HARZ B.J., "Stability of Plates Using the Finite Element Method," Journal of Engineering Mechanics Division, A. S. C. E., Vol.92, No.EM2, 1966.

- 14) KAPUR K.K. , "Prediction of Plate Vibration Using Consistent Mass Matrix," American Journal of Aeronautics and Astronautics, Vol.4, 1966, pp.565-566.
- 15) KIELB R.E. and HAN L.S. , "Vibration and Buckling of Rectangular Plates Under In-Plane Hydrostatic Loading," Journal of Sound and Vibration, Vol.70, No.4, 1980, pp.543-555.
- 16) LAURA P.A.A. and ROMANELLI E. , "Vibrations of Rectangular Plates Elasticity Restrained Against Rotation along edges and Subjected to a Bi-Axial State of Stress," Journal of Sound and Vibration, Vol.37, 1974, PP.367-377.
- 17) LEE Y.C. and REISMANN H. , "Dynamics of Rectangular Plates," International Journal of Engineering Sciences, Vol.7, 1969, pp.93-113.
- 18) LEISSA A.W. , "The Free Vibration of Rectangular Plates," Journal of Sound and Vibration, Vol.31, 1973, pp.237.
- 19) LEISSA A.W. "Vibration of Plates", NASA SP-160, 1969.
- 20) LEVY S. , "Buckling of Rectangular Plates with Built-in Edges," Journal of Applied Mechanics, Vol.9, 1942, pp.171-174.
- 21) LURIE H. , "Effective End Restraint of Columns by Frequency Measurements," Journal of Aeronautical Sciences, Vol.18, 1951, pp.566-567.

- 22) LURIE H., "A Note on the Buckling of Struts," Journal of the Royal Aeronautical Society, Vol.55, 1951, pp.181-184.
- 23) LURIE H., "Vibrations of Rectangular Plates," Journal of Aeronautical Sciences, Vol.18, 1951, pp.137-140.
- 24) LURIE H., "Lateral Vibrations Related to Structural Stability," Journal of Applied Mechanics, Vol.19, No.2, 1952, pp.195-204.
- 25) MANELBETSCH J.L. , "Buckling of Compressed Rectangular Plates With Built-In Edges," Journal of Applied Mechanics, ASME, Vol.59, 1937.
- 26) MELOSH R.J., "Basis for Derivation of Matrices for the Direct Stiffness Method," Journal of the American Institute of Aeronautics and Astronautics, Vol.1, 1963.
- 27) MELOSH R.J., "A Stiffness Matrix for the Analysis of Thin Plates in Bending," Journal of Aero. Sciences, Vol.28, No.64, 1961, pp.34-42.
- 28) PIAN T.H., "Derivation of Element Stiffness Matrices," Journal American Institute of Aeronautics and Astronautics, Vol.2, 1964, pp.576-577.
- 29) PRZEMIENIECKI J.S., "Theory of Matrix Structural Analysis," McGraw Hill, 1968.

- 30) PRZEMIENIECKI J.S., "Equivalent Mass Matrecies for Rectangular Plates in Bending," Journal of American Institute of Aeronautics and Astronautics, Vol.4, 1966, pp.949,500.
- 31) LORD RAYLEIGH , "Theory of Sound," MacMillan and Co., London, Second Edition, Vol.1, 1894.
- 32) TIMOSHENKO S.P , "Vibration Problems in Engineering," D.Van Nostrand Co., New York, 1928.
- 33) TIMOSHENKO S.P. and GERE J.M. , "Theory of Elastic Stability," McGraw-Hill Company Ltd., 1978.
- 34) TIMOSHENKO S.P., and KRIEGER S.W., "Theory of Plates and Shells," McGraw-Hill Co., 2nd Ed., 1959.
- 35) UGURAL A.C., " Stresses in Plates and Shells," McGraw-Hill Co., 1981.
- 36) WARBURTON G.B., "The Vibration of Rectangular Plates," Proc. Inst. Mech.Eng., London, Vol.168, 1954, pp.371.
- 37) WEAVER W.Jr, "Computer Programs for Structural Analysis," Van Nostrand Co., 1967.
- 38) WEEKS G.E. and SHIDELER J.L. , "Effect of Edge Loadings on the Vibration of Rectangular Plates with Various Boundary Conditions," NASA TN D-2815, 1965.

39) WHITE R.G. and TEH C.E., "Dynamic Behavior of Isotropic Plates Under Combined Acoustic Excitation and Static Inplane Compression" Journal of Sound and Vibration, Vol.75(4), 1981, pp.527-547.

40) WILLIAMS F.W., "Natural Frequencies of Repetitive Structures," Quarterly Journal of Mechanics and Applied Mathematics, Vol.24, 1971, pp.285-310.

41) WILLIAMS F.W, and WITTRICK W.H., "Computational Procedures for Matrix Analysis of the Stability and Vibration of Thin Flat Walled Structures in Compression," International Journal of Mechanical Sciences, Vol.11, 1969, pp.979.

42) WILLIAMS F.W. and WITTRICK W.H , "Exact Buckling and Frequency Calculation Surveyed," Journal of Structural Engineers, Vol.109, No.1, 1983, pp.169-187.

43) WILLIAMSON F.Jr , "A Historic Note on Finite Element Method," International Journal of Numerical Methods in Engineering, Vol.15, 1980, pp.930-935.

44) WITTRICK W.H., "Correlation Between some Stability Problems for Orthotropic and Isotropic Plates under Bi-Axial and Uni-Axial Direct Stress," The Aeronautical Quarterly, Vol.4, 1952, pp.83-92

45) WITTRICK W.H., "General Sinusoidal Stiffness Matrices for Buckling and Vibration Analysis of Thin Flat Walled Structures," International Journal of Mech. Sci., Vol.10, 1968, pp.949.

46) WITTRICK W.H. and WILLIAMS F.W., "A General Algorithm for Computing Natural Frequencies of Elastic Structures," Quarterly Journal of Mechanics and Applied Mathematics, Vol.24., 1971, pp.263-284.

47) WITTRICK W.H. and WILLIAMS F.W., "An Algorithm for Computing Critical Buckling Loads of Elastic Structures," Journal of Structural Mechanics, Vol.1, 1973.

48) WITTRICK W.H. and WILLIAMS F.W., "Buckling and Vibration of Anisotropic or Isotropic Plate Assemblies Under Combined Loading," Int. Journal Mech. Sci., Vol.16, 1974, pp.209-239.

49) YOUNG D.H. , "Vibration of Rectangular Plates by Ritz Method," Journal of Applied Mechanics, Vol.17, 1950, pp.448-453.

50) ZIENKIEWIEZ O.C., "The Finite Element Method," McGraw-Hill Company U.K. Ltd., 1977.

APPENDICES

APPENDIX 1

**Mathematical Model used
for the Space Frame Analysis**

APPENDIX 1

MATHEMATICAL MODEL

A. Mathematical Model

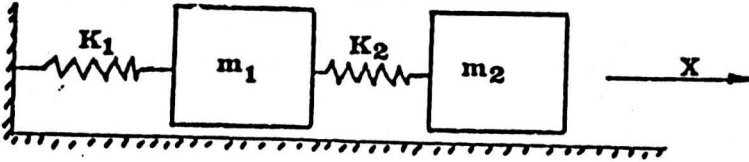
To start analysing any engineering problem, a simple mathematical model must be constructed, two phases are essential to emphasise in this regard:

Phase 1) The construction of a very simple dynamic system with the minimum possible number of degrees of freedom, the simplest among which the analysis is satisfied is the Spring-Mass (two degree of freedom) system, when one of the springs represents the elastic stiffness of the structure represented by the mass block m_1 , the other spring represents the external spring supporting the external loads applied to the system and represented by the block m_2 , as shown in figure A1-1. Out of the first phase of analysis we achieve:

- i) A preliminary estimate of the external spring stiffness to be designed to support the external loads keeping the effect of the mass of this external load to a minimum.
- ii) An estimate of the natural frequency of the system, by solving the two coupled system of equations, where the frequencies are defined as the square root of the stiffness K to mass m ratio, the two coupled equations are:

$$m_1 \frac{d^2 X_1}{dt^2} + (K_1 + K_2) X_1 - K_2 X_2 = 0 \quad \text{eq.A1.1}$$

$$m_2 \frac{d^2 X_2}{dt^2} + K_2 X_2 - K_2 X_1 = 0 \quad \text{eq.A1.2}$$



Mathematical Model

Figure A1-1

Phase 2) In this phase the structure is divided into a finite number of small elements, connected together through nodes, this second phase is based on the concept of the energy method, this mathematical procedure being considered a better approach to obtain results close to the exact solution.

This analysis can not be handled easily without the involvement of the digital computers. The computer results will be compared with the experimental results to see how close the approximation is. The Finite Element Method was detailed in chapters 3 and 6 of this manuscript both from the theoretical background and the techniques involved to set it in the computer programme, Computer flow charts were shown earlier to illustrate the methodology of the programming procedure .

B. Frequency Estimation

Before analysing and solving the coupled equations shown earlier in this Appendix.

To evaluate the stiffness of the main space frame structure we considered only the vertical displacement δ neglecting the effects of the other displacement component.

By considering one bar as shown in figure A1-2, the axial load applied to it is only a fraction of the total load applied externally to the structure.

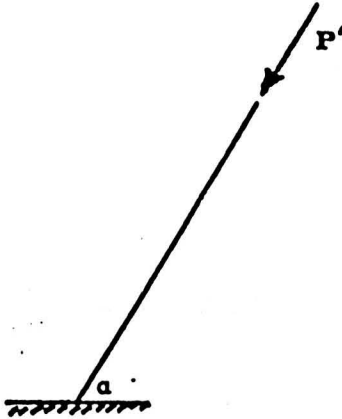


Figure A1-2

From the small deflection theory, see ref. [11] in part I, it was found that:

$$\epsilon = \delta \cos \alpha / L \quad \text{eq.A1.3}$$

$$\sigma = E\epsilon \quad \text{eq.A1.4}$$

$$\text{and } P' = \sigma A \quad \text{eq.A1.5}$$

where A , E , σ , and P' are the cross sectional area of the bar, the

elastic modulus, the stress, and the applied axial load inclined from the vertical at an angle α .

$$P' = (\delta E A/L) \cos \alpha \quad \text{eq.A1.6}$$

For this case, $\alpha = 30^\circ$ and then the value of P' is:

$$P' = \sqrt{3} E A \delta / 2L \quad \text{eq.A1.7}$$

For all bars of the structure, the total load will be:

$$P_{\text{tot}} = 3 E A \delta / L \quad \text{eq.A1.8}$$

The elastic stiffness value is estimated as:

$$K = 3 E A / L \quad \text{eq.A1.9}$$

Solving equations A1.1, and A1.2 simultaneously gives:

$$\omega^2 = ((K_1 + K_2)/2m_1) + (K_2/2m_2) \pm \sqrt{0.25 (\gamma - \beta)} \quad \text{eq.A1.10}$$

$$\text{where, } \gamma = [(K_1 + K_2)/m_1 + K_2/m_2]^2 \quad \text{eq.A1.11}$$

$$\text{and, } \beta = K_1 K_2 / m_1 m_2 \quad \text{eq.A1.12}$$

where K_1 is the structural stiffness, while K_2 is the spring stiffness, m_1 and m_2 represent the respective masses of the frame structure and the applied load respectively.

APPENDIX 2
Summary of the
Linear Regression Procedure

APPENDIX 2

LINEAR REGRESSION PROCEDURE

The linear regression method is well known, see NAG Library Manual (section G-02-), but for the purpose of the following discussion is to illustrate the theory behind the linear regression procedure involving all dependent and independent variables x and y . For the actual analysis of the space frame results, x represents the applied loads and y represents the square of the frequency ratio (u/u_0).

This computer oriented procedure is based on fitting a straight line of the form:

$$y = a + bx \qquad \text{eq.A2.1}$$

When using all points (x_i, y_i) the above equation becomes:

$$y = a + bx_i + e_i \qquad \text{eq.A2.2}$$

where e_i is the expected error in the estimation.

The computer routine calculates the regression coefficients b and the regression constant a by minimising the error presented in the form $\sum e_i$, the mean values of x and y can be calculated as:

$$x = \Sigma x_i / N \quad \text{eq.A2.3}$$

and,
$$y = \Sigma y_i / N \quad \text{eq.A2.4}$$

where N is the number of points considered.

The standard deviation is calculated as follows:

$$S_x = \sqrt{((1/(N-1)) \Sigma (x_i - x)^2)} \quad \text{eq.A2.5}$$

$$S_y = \sqrt{((1/(N-1)) \Sigma (y_i - y)^2)} \quad \text{eq.A2.6}$$

The regression coefficient b , and the regression constant a , can be calculated as follows:

$$b = \frac{\Sigma (x_i - x) (y_i - y)}{\Sigma (x_i - x)^2} \quad \text{eq.A2.7}$$

$$a = y_i - bx_i \quad \text{eq.A2.8}$$

Assuming the squares attributed to the regression (SQR), by evaluating the squares of the deviation (SQD) and the squares of the total sum (SQT) and then subtracting them from each other as shown below:

$$SQT = \Sigma (y_i - y)^2 \quad \text{eq.A2.9}$$

$$SQD = \Sigma (y_i - a - bx_i)^2 \quad \text{eq.A2.10}$$

$$SQR = SQT - SQD \quad \text{eq.A2.11}$$

Dividing the last two equations by the degree of freedom number which is for the space frame under investigation is:

$$DFD = N - 2 = 7 \quad \text{eq.A2.12}$$

and the degree of restraint is given by:

$$DFR = 1 \quad \text{eq.A2.13}$$

The mean squares of regression and deviation are obtained as:

$$MSR = SQR/DFR \quad \text{eq.A2.14}$$

$$MSD = SQD/DFD \quad \text{eq.A2.15}$$

Finally, to calculate the standard error S_e of the regression coefficient b and that of the regression constant a one uses the following equation:

$$S_e(b) = \sqrt{\frac{MSD}{\sum (x_i - \bar{x})^2}} \quad \text{eq.A2.16}$$

$$S_e(a) = \sqrt{MSD \left(\frac{1}{N} + \frac{\bar{x}^2}{\sum (x_i - \bar{x})^2} \right)} \quad \text{eq.A2.17}$$

In the following page, a simple programme on the linear regression procedure is shown to demonstrate the efficiency of this procedure when used to select the best fit linear relation among any spread points obtained experimentally or otherwise.

Linear regression sample computer programme

```

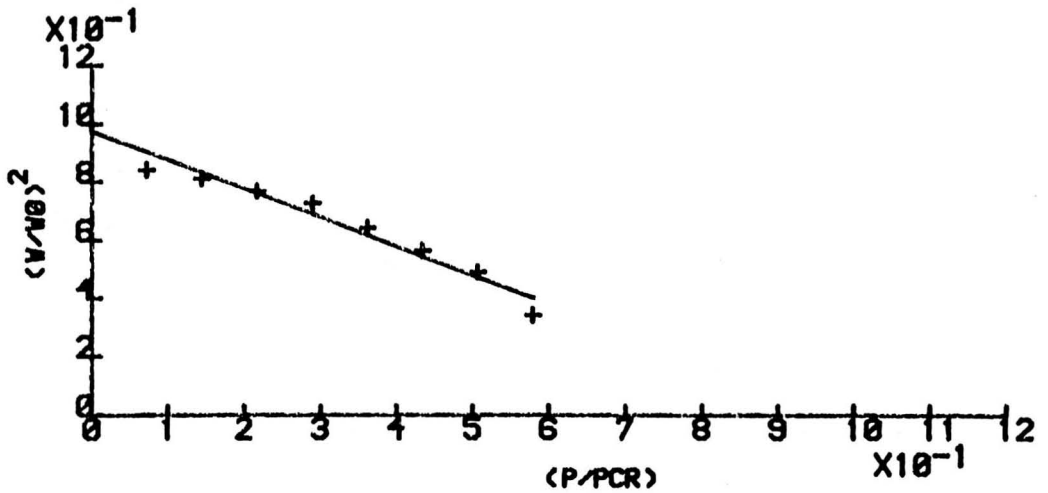
1 C ===== THIS PROGRAM PROVIDES A LINEAR REGRESSION=====
2 C ===== TO CONNECT EXPERIMENTAL DATA OBTAINED TO =====
3 C ===== FORM THE BEST FIT LINE BETWEEN THE POINTS =====
4     DIMENSION X(120),Y(110),RESULT(21)
5 C     READING THE EXPERIMENTAL DATA
6     READ(5,*)N
7     READ(5,*)(X(I),Y(I),I=1,N)
8 C     CALL SYSTEM TO DRAW THE GRAPH
9 C     SYSTEMS AVAILABLE ARE: ADM3AG,HP747,MAIN FRAME.
10 C    DRAWING THE AXIS AND LABLING THEM.
11     CALL AXIPOS(1,60.,60.,120.,1)
12     CALL AXIPOS(1,60.,60.,110.,2)
13     CALL AXISCA(1,10,0.,120.,1)
14     CALL AXISCA(1,10,0.,1.1,2)
15     CALL AXIDRA(1,1,1)
16     CALL AXIDRA(-1,-1,2)
17     CALL GRASYM(X,Y,N,4,0)
18     CALL GRAMOV(65.,-0.1)
19     CALL CHASIZ(2.,2.)
20     CALL CHAHOL('LOAD(LBS)*. ')
21     CALL GRAMOV(40.,-0.2)
22     CALL CHAHOL('FIGURE NO.*. ')
23     CALL GRAMOV(-26.,1.0)
24     CALL CHAHOL('(W/WN)*. ')
25     CALL MOVBY2(0.,3.)
26     CALL CHASIZ(1.5,1.5)
27     CALL CHAHOL('2*. ')
28     CALL CHASIZ(2.,2.)
29     CALL GRAMOV(70.,-.85)
30     CALL GRALIN(119.,-.85)
31     CALL GRALIN(119.,1.1)
32     CALL GRALIN(70.,1.1)
33     CALL GRALIN(70.,-.85)
34     CALL GRAMOV(75.,1.05)
35     CALL CHAHOL('EXPERIMENT NO. *. ')
36     CALL GRAMOV(72.,1.)
37     CALL CHAHOL('EXCITER,T,BAR NO.*. ')
38     CALL GRAMOV(72.,.95)
39     CALL CHAHOL('ACCELER',R,BAR NO.*. ')
40     CALL GRAMOV(80.,.90)
41     CALL CHAHOL('R=RADIAL, T=TAN"L*. ')
42 C    USE OF THE LINEAR REGRESSION PROCEDURE
43 C    STARTS HERE, USING THE NAG SUBROUTINES.
44     IFAIL=0
45     CALL G02CAF(N,X,Y,RESULT,IFAIL)
46     YW1=RESULT(7)+RESULT(6)*X(1)
47     CALL GRAMOV(X(1),YW1)
48     YW2=RESULT(7)+RESULT(6)*X(N)
49     CALL GRALIN(X(N),YW2)
50     CALL DEVEND
51     STOP
52     END

```

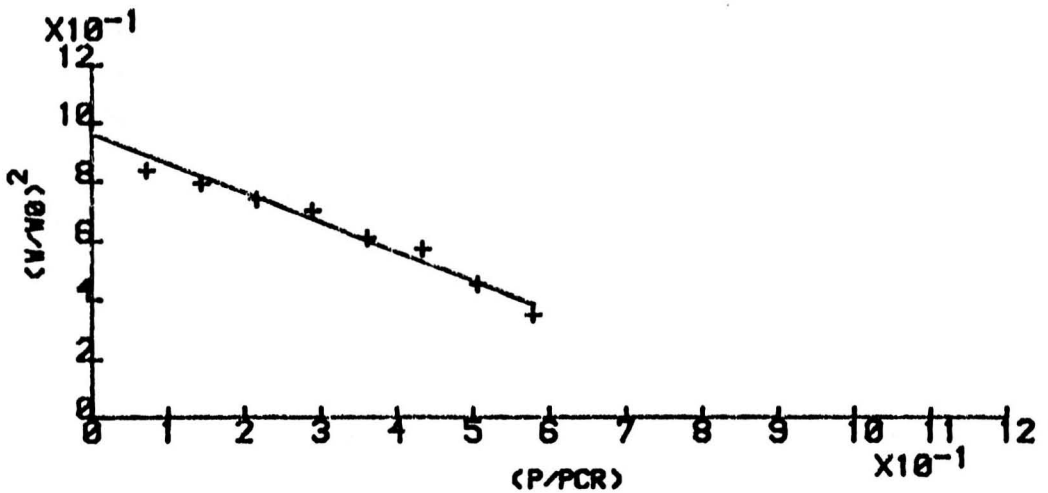
APPENDIX 3

Space Frame Experimental Graphs

EXPERIMENTAL GRAPHS OF
FREQUENCY-STRESS LEVEL RELATION OF THE
AXIALLY LOADED SPACE FRAME STRUCTURE



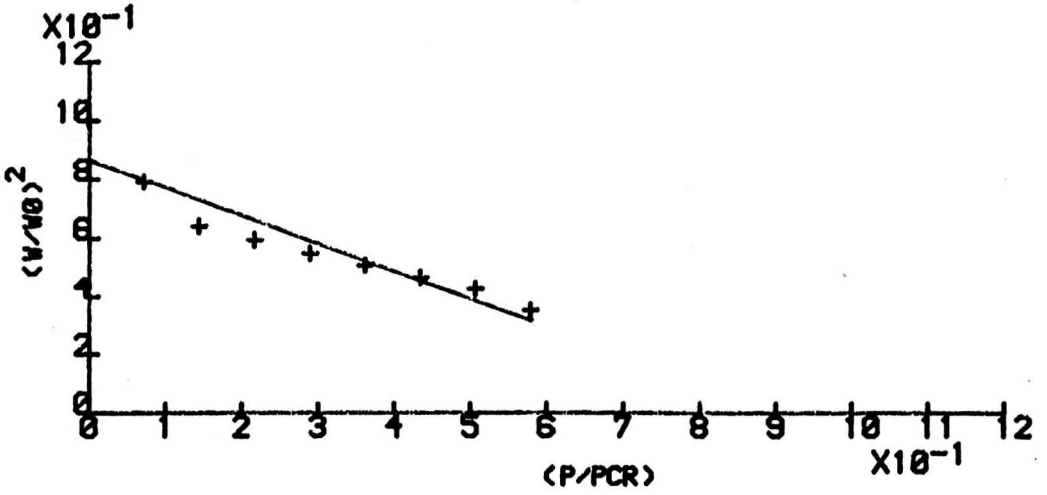
EXPERIMENT NO.1



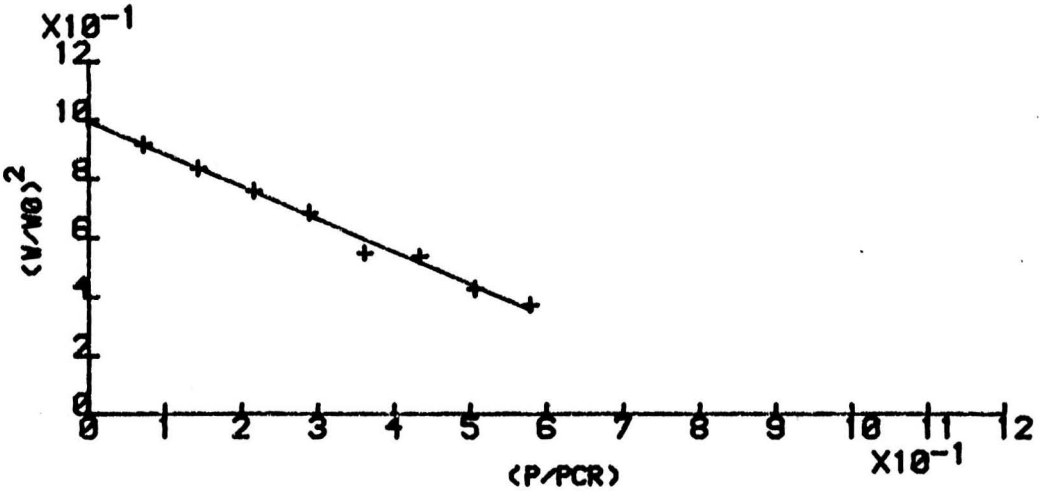
EXPERIMENT NO.2

FIGURE NO. A3-1

EXPERIMENTAL GRAPHS OF
 FREQUENCY-STRESS LEVEL RELATION OF THE
 AXIALLY LOADED SPACE FRAME STRUCTURE



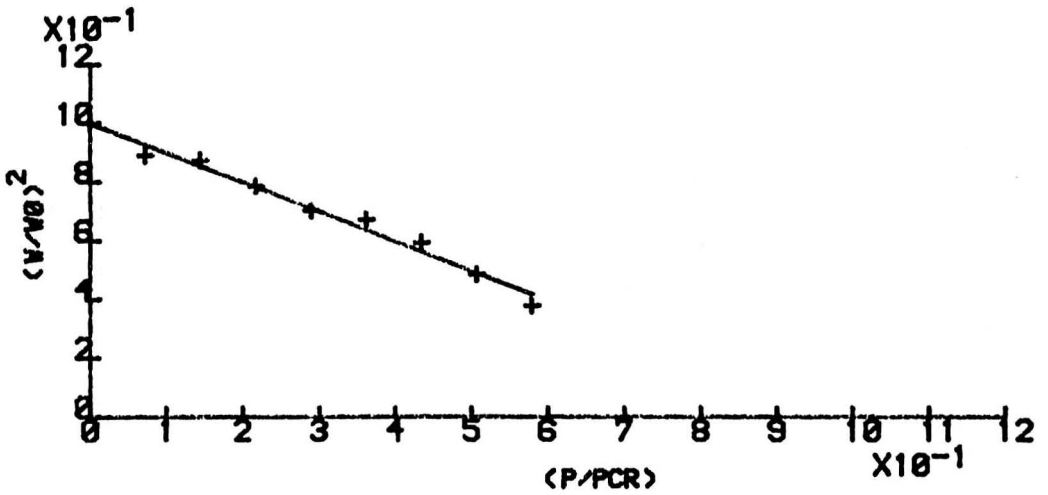
EXPERIMENT NO.3



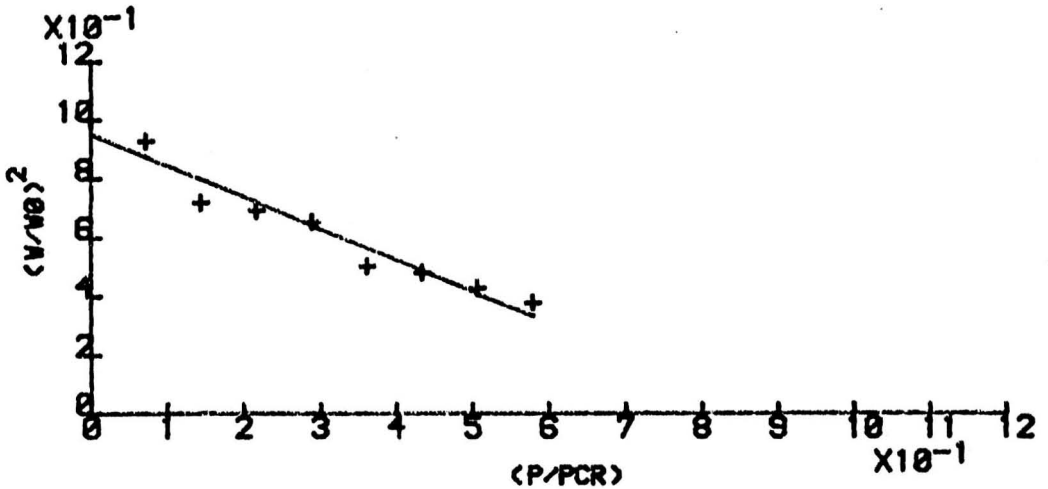
EXPERIMENT NO.4

FIGURE NO. A3-2

EXPERIMENTAL GRAPHS OF
 FREQUENCY-STRESS LEVEL RELATION OF THE
 AXIALLY LOADED SPACE FRAME STRUCTURE



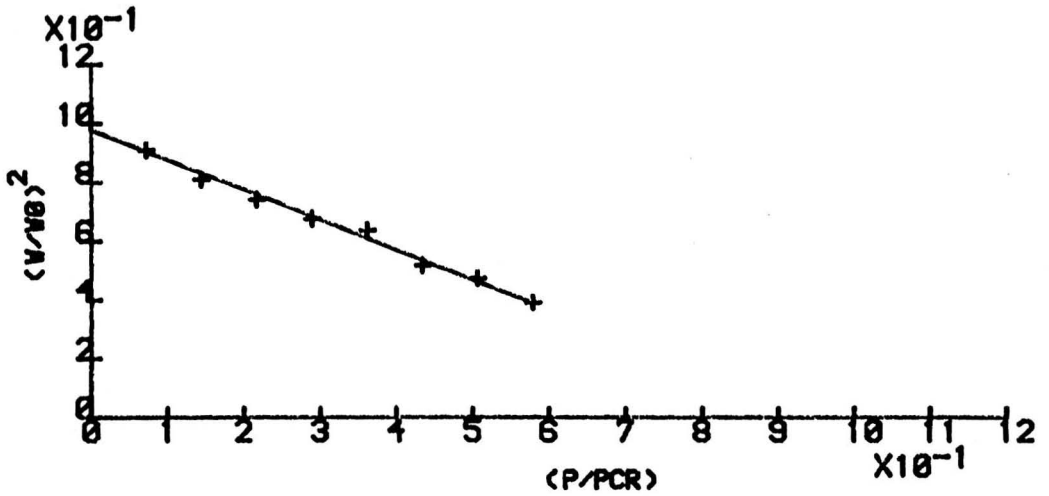
EXPERIMENT NO.5



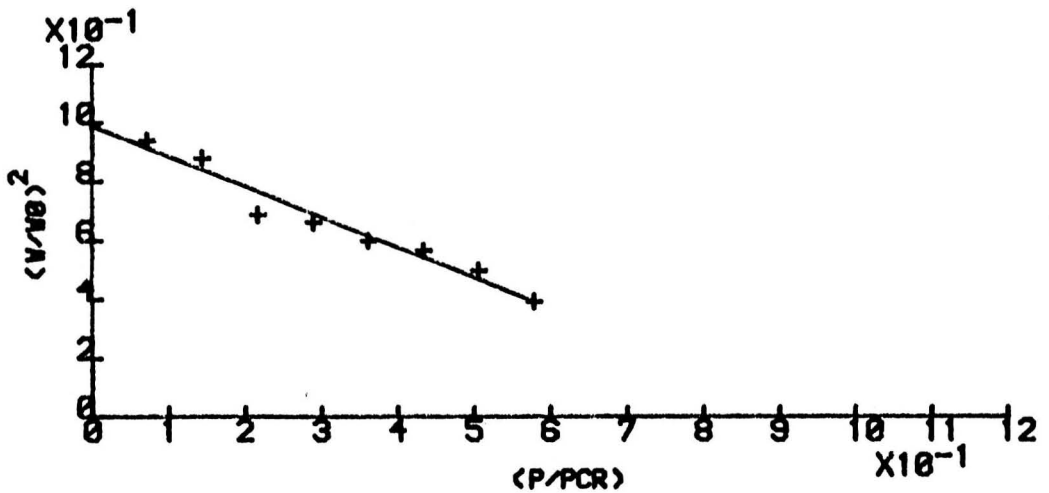
EXPERIMENT NO.6

FIGURE NO. A3-3

EXPERIMENTAL GRAPHS OF
 FREQUENCY-STRESS LEVEL RELATION OF THE
 AXIALLY LOADED SPACE FRAME STRUCTURE



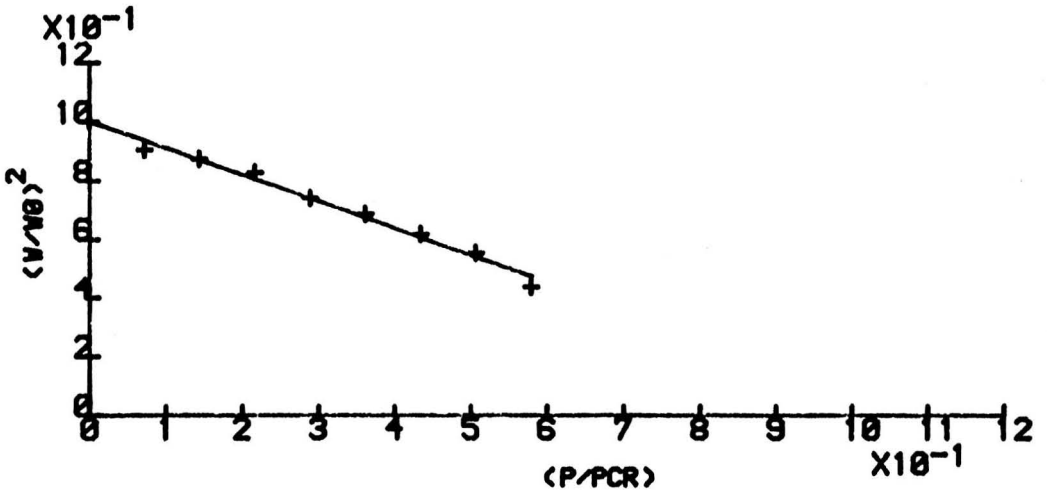
EXPERIMENT NO.7



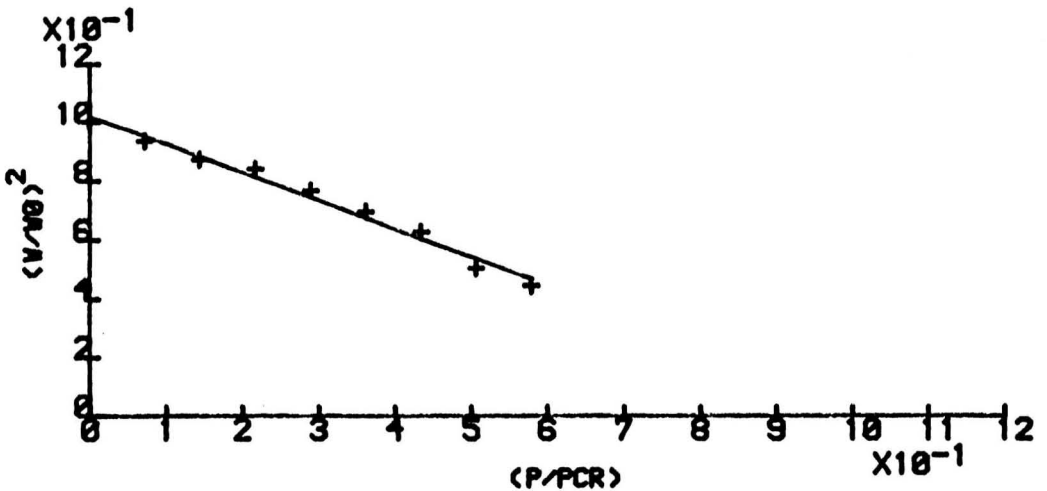
EXPERIMENT NO.8

FIGURE NO. A3-4

EXPERIMENTAL GRAPHS OF
 FREQUENCY-STRESS LEVEL RELATION OF THE
 AXIALLY LOADED SPACE FRAME STRUCTURE



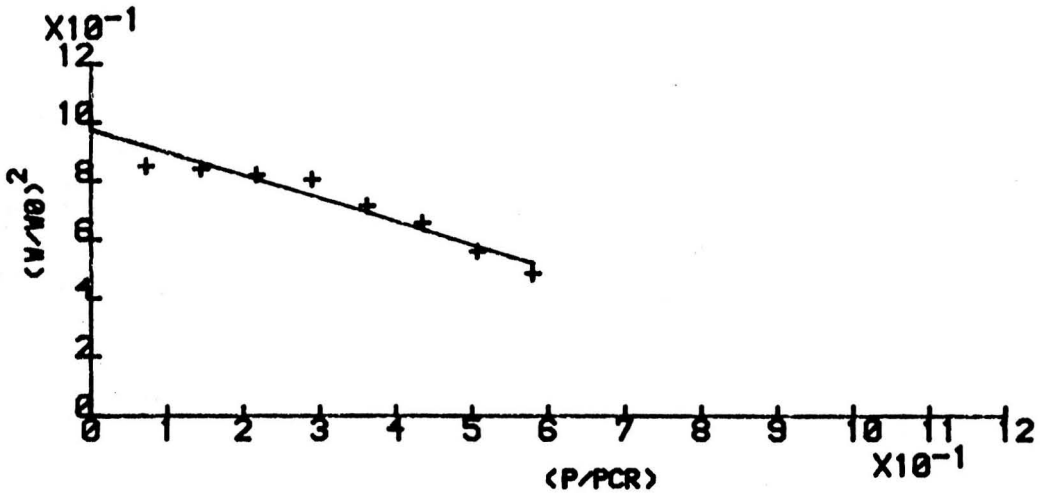
EXPERIMENT NO.9



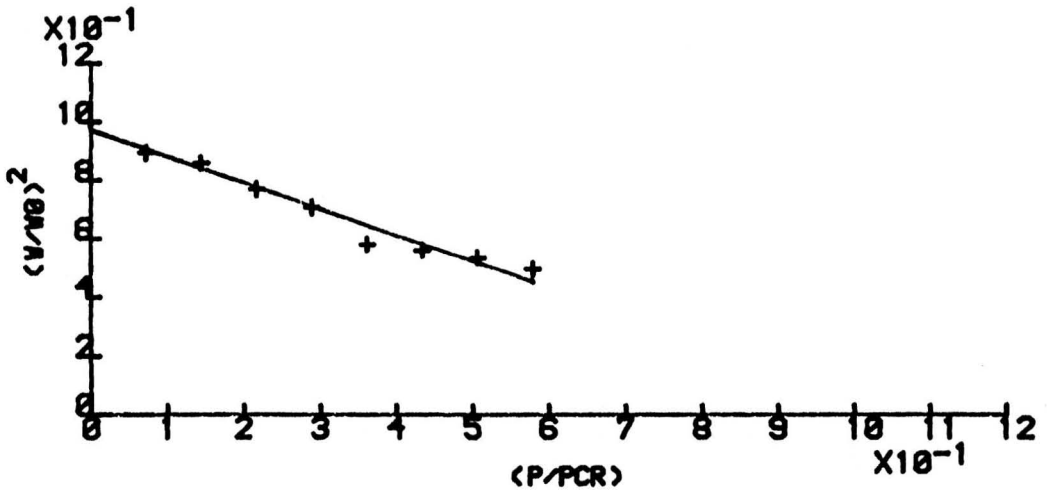
EXPERIMENT NO.10

FIGURE NO. A3-5

EXPERIMENTAL GRAPHS OF
 FREQUENCY-STRESS LEVEL RELATION OF THE
 AXIALLY LOADED SPACE FRAME STRUCTURE



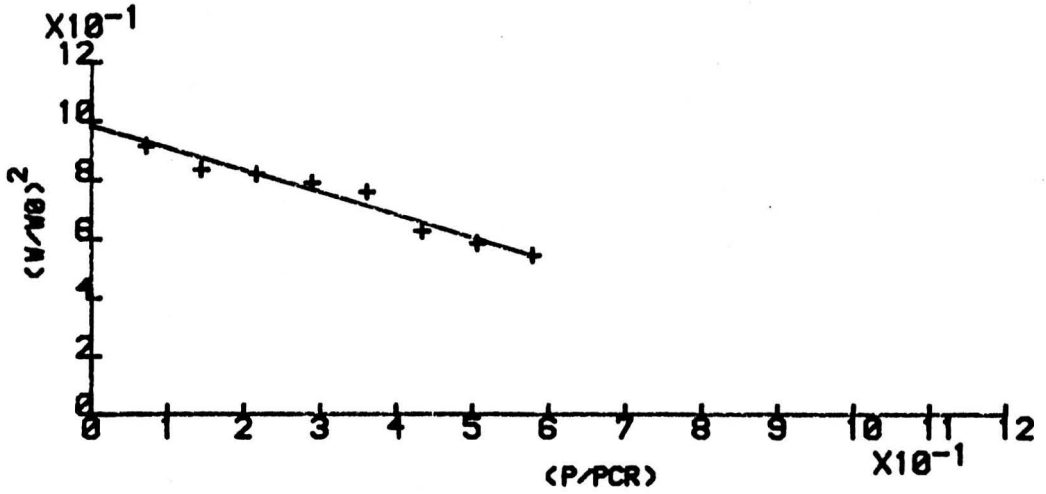
EXPERIMENT NO.11



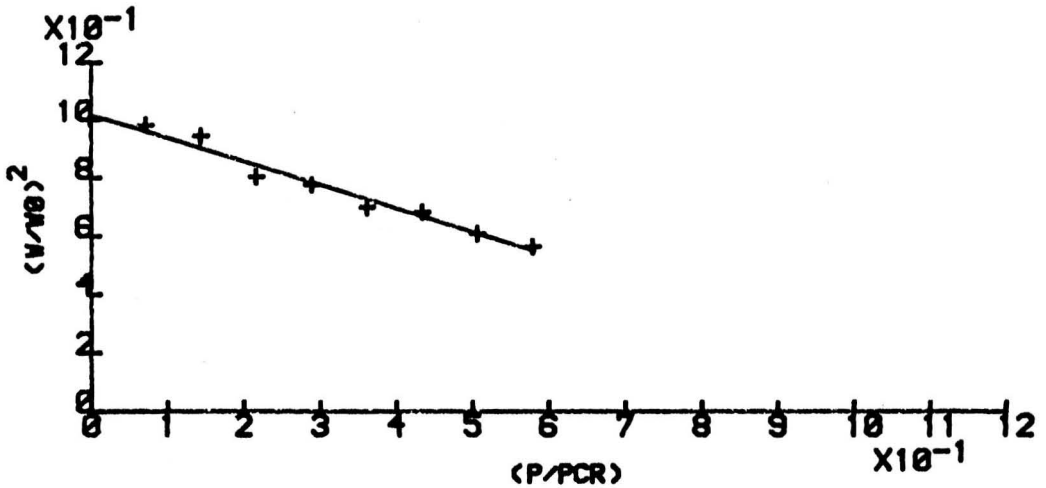
EXPERIMENT NO.12

FIGURE NO. A3-6

EXPERIMENTAL GRAPHS OF
 FREQUENCY-STRESS LEVEL RELATION OF THE
 AXIALLY LOADED SPACE FRAME STRUCTURE



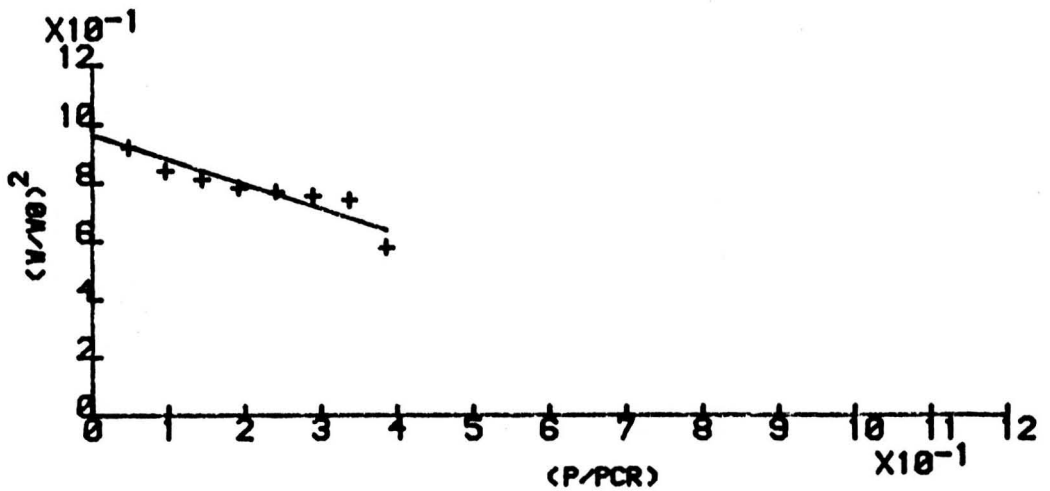
EXPERIMENT NO.13



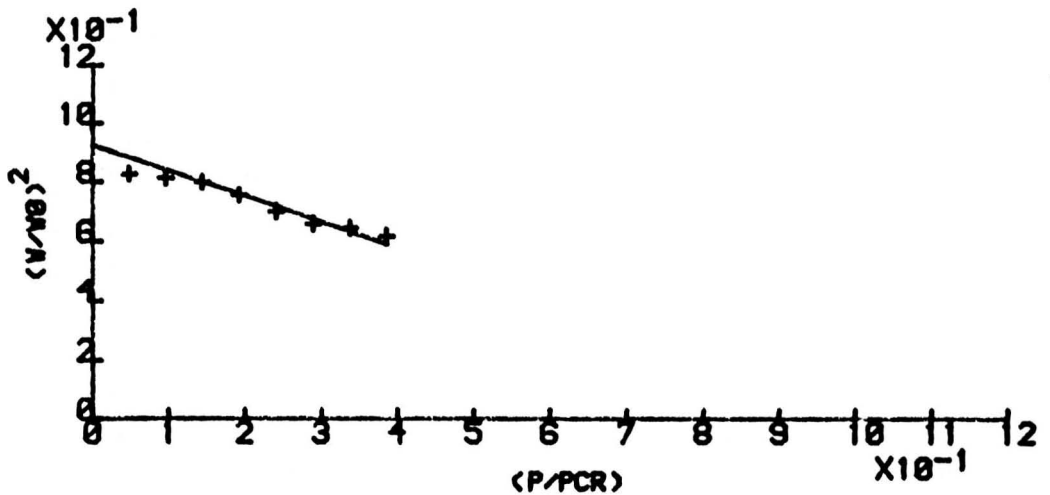
EXPERIMENT NO.14

FIGURE NO. A3-7

EXPERIMENTAL GRAPHS OF
 FREQUENCY-STRESS LEVEL RELATION OF THE
 AXIALLY LOADED SPACE FRAME STRUCTURE



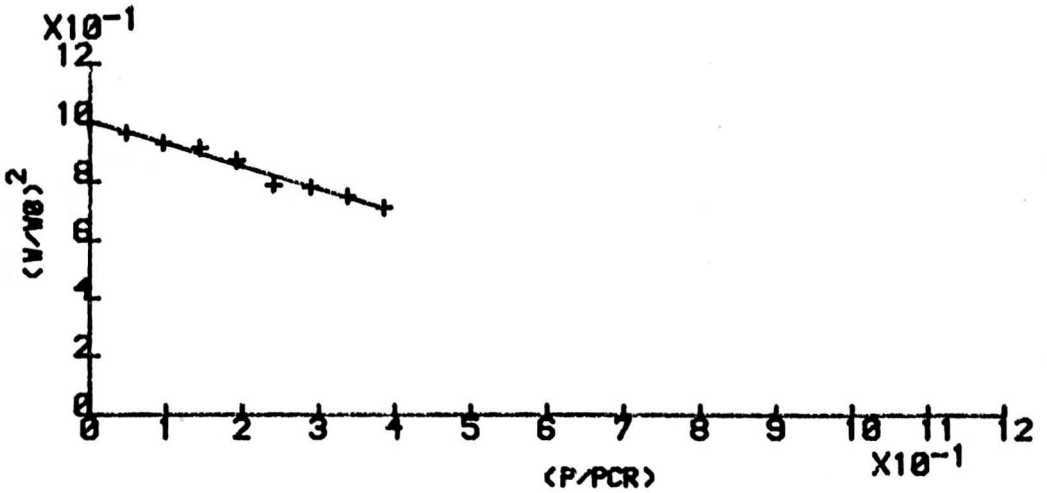
EXPERIMENT NO.15



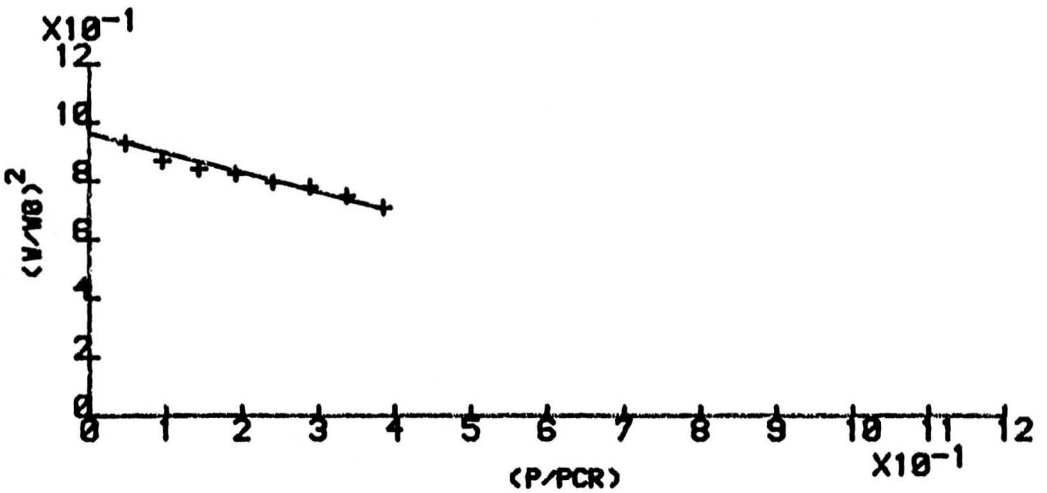
EXPERIMENT NO.16

FIGURE NO. A3-8

EXPERIMENTAL GRAPHS OF
FREQUENCY-STRESS LEVEL RELATION OF THE
AXIALLY LOADED SPACE FRAME STRUCTURE



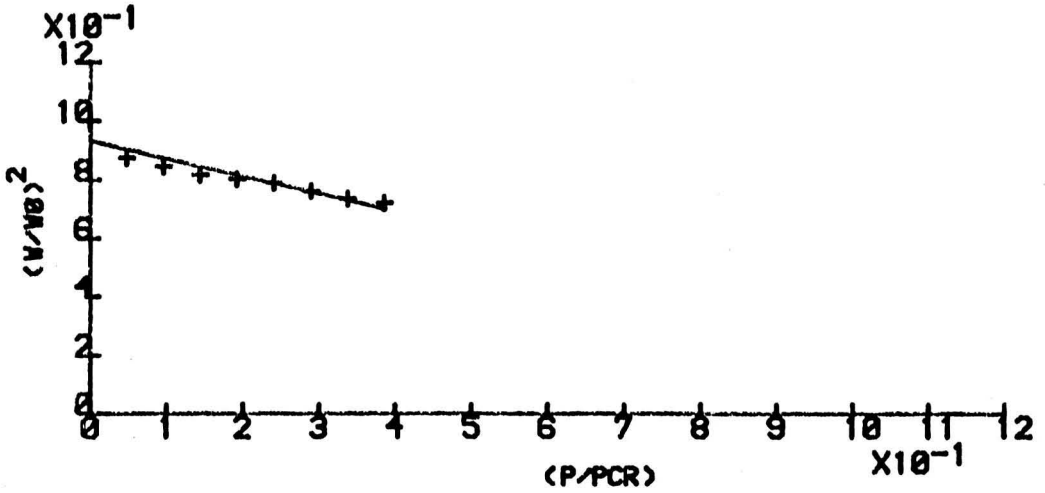
EXPERIMENT NO.17



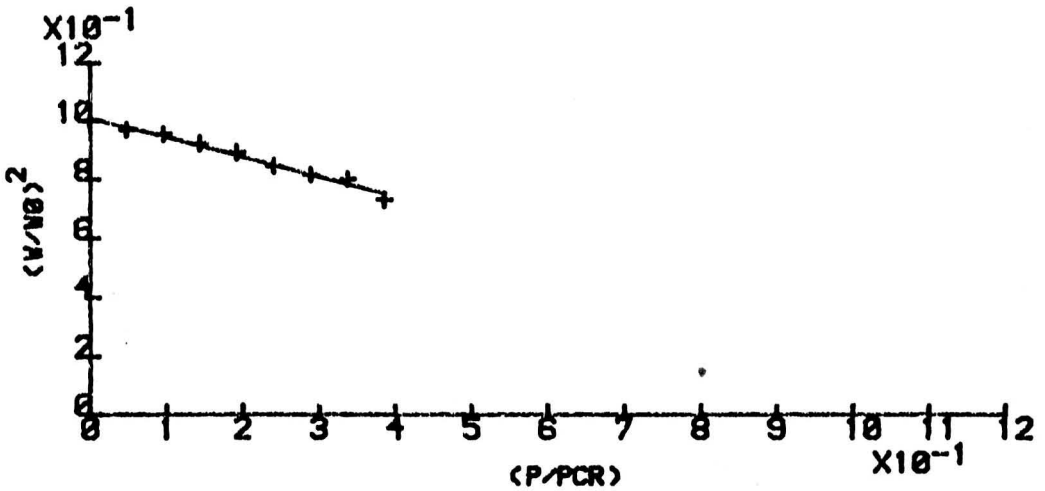
EXPERIMENT NO.18

FIGURE NO. A3-9

EXPERIMENTAL GRAPHS OF
 FREQUENCY-STRESS LEVEL RELATION OF THE
 AXIALLY LOADED SPACE FRAME STRUCTURE



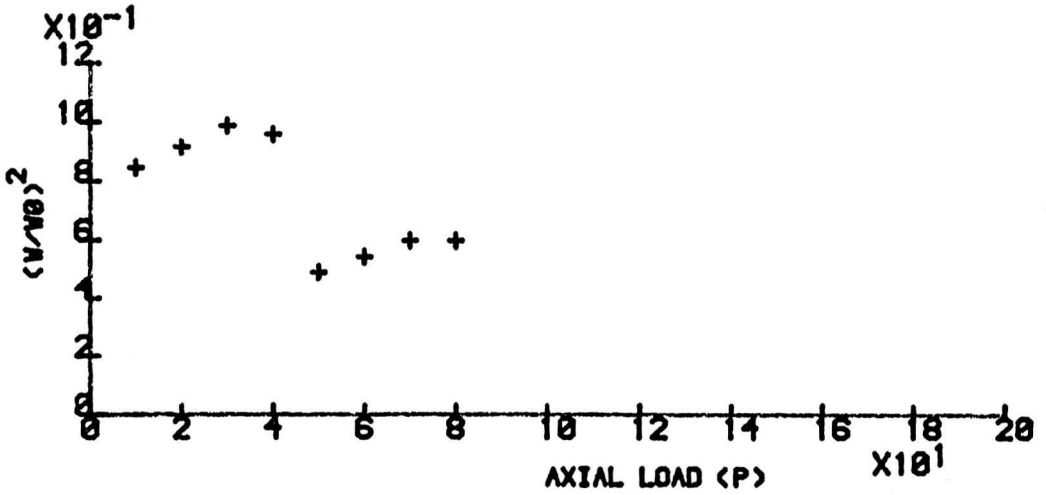
EXPERIMENT NO.19



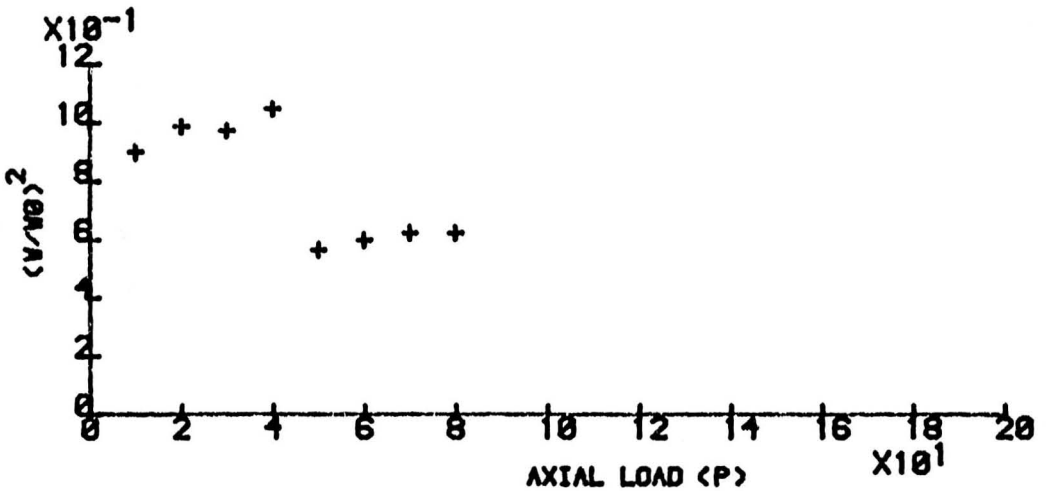
EXPERIMENT NO.20

FIGURE NO. A3-10

EXPERIMENTAL GRAPHS OF
 FREQUENCY-STRESS LEVEL RELATION OF THE
 Laterally Loaded Space Frame Structure



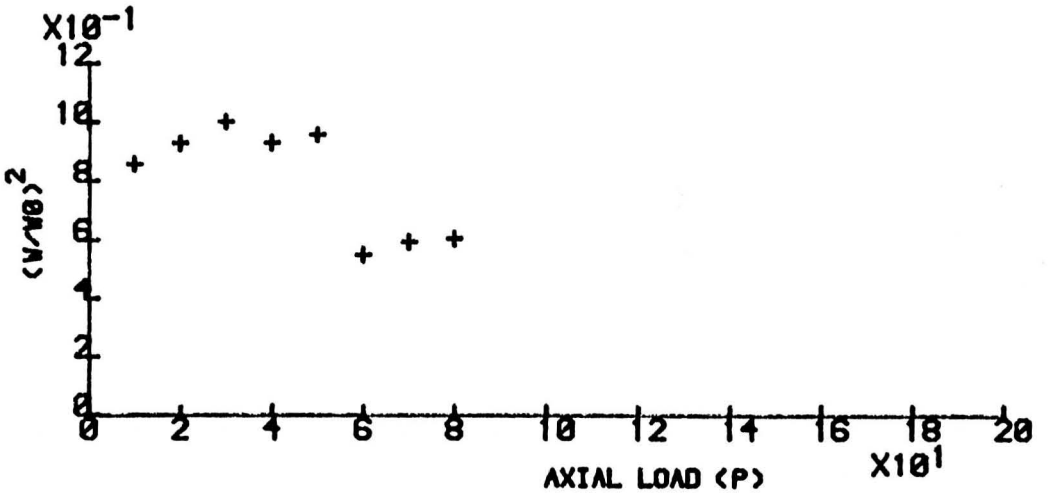
EXPERIMENT NO.21



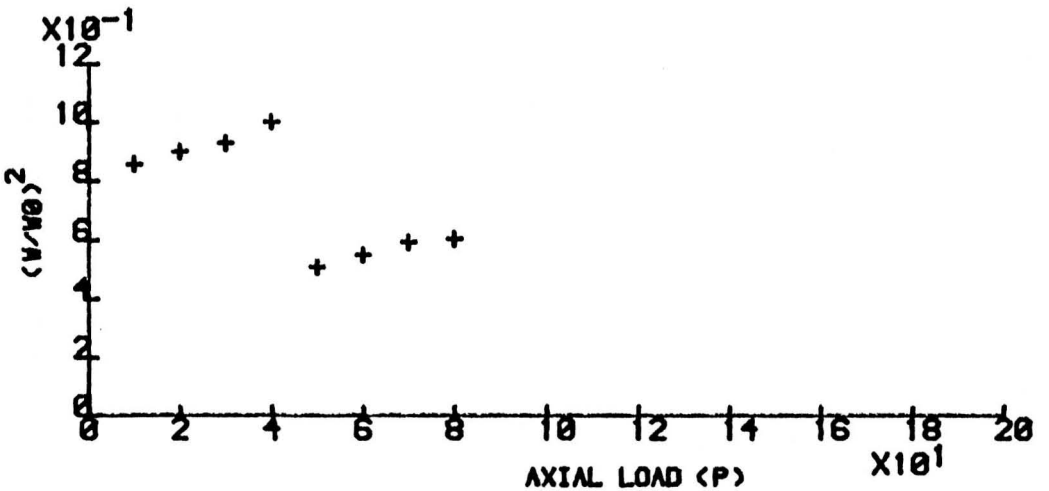
EXPERIMENT NO.22

FIGURE NO. A3-11

EXPERIMENTAL GRAPHS OF
 FREQUENCY-STRESS LEVEL RELATION OF THE
 Laterally Loaded Space Frame Structure



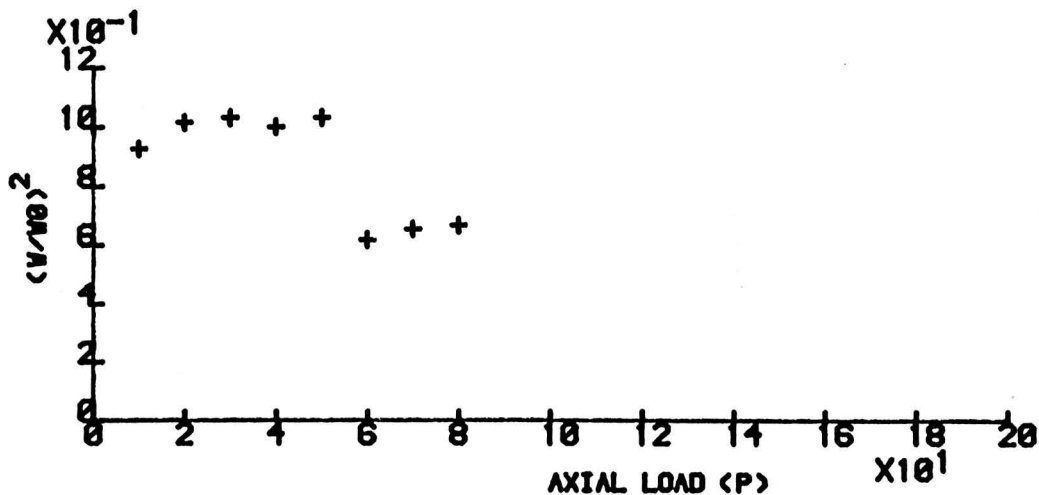
EXPERIMENT NO.23



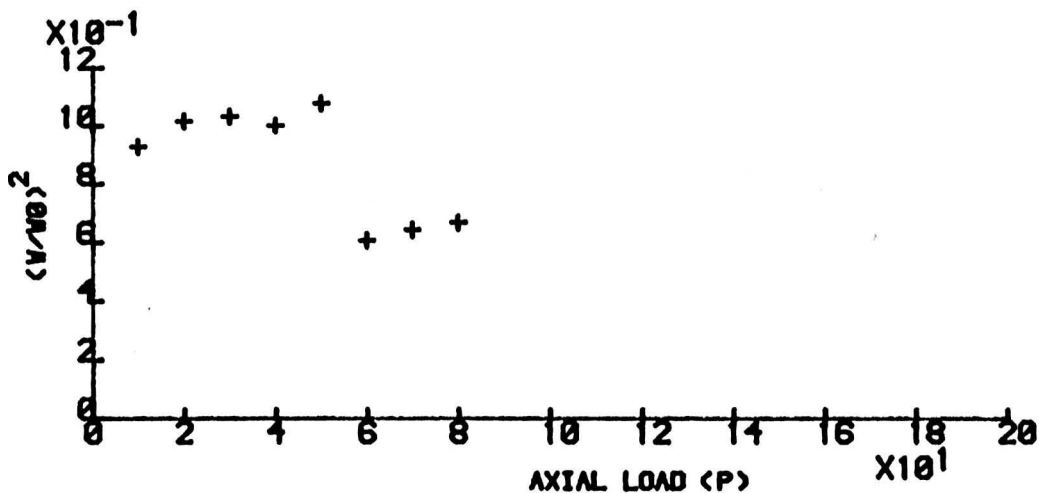
EXPERIMENT NO.24

FIGURE NO. A3-12

EXPERIMENTAL GRAPHS OF
 FREQUENCY-STRESS LEVEL RELATION OF THE
 Laterally Loaded Space Frame Structure



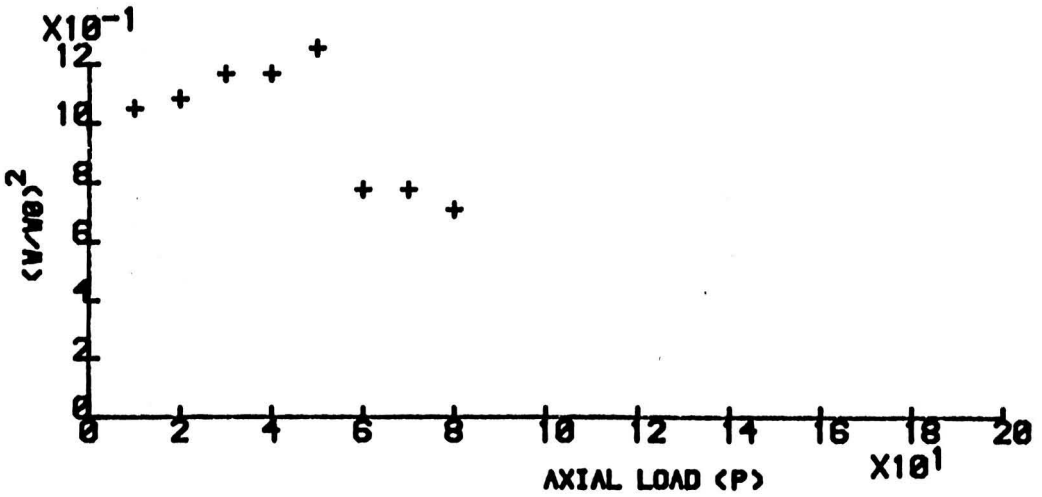
EXPERIMENT NO.25



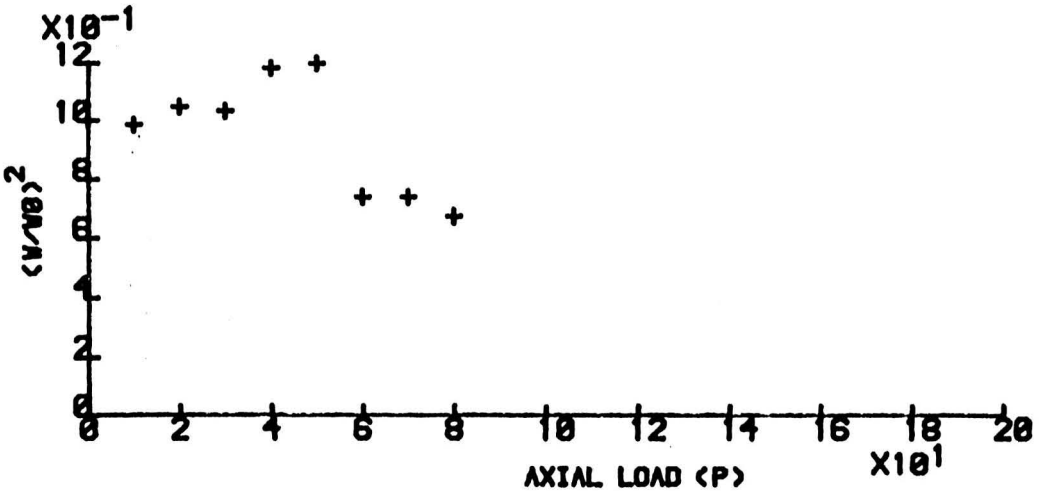
EXPERIMENT NO.26

FIGURE NO. A3-13

EXPERIMENTAL GRAPHS OF
 FREQUENCY-STRESS LEVEL RELATION OF THE
 Laterally Loaded Space Frame Structure



EXPERIMENT NO.27



EXPERIMENT NO.28

FIGURE NO. A3-14

APPENDIX 4

Results from other Sources

APPENDIX 4

RESULTS FROM OTHER SOURCES

The following graphs reported in this Appendix were produced by various authors in order to investigate the relation between the stress variation in the structure and the natural frequency of vibration (the square of the frequency), some of these graphs agree with the results obtained in the original work in this thesis, as illustrated earlier in the text, some others differ, not only in the graphs but also in the conclusions drawn.

Each graph is presented and commented upon according to the understanding of the author's conclusions.

The first graphs, figures A4-1 to A4-4 were by Lurie, see ref. [A4], in 1952 and show that a linear relationship between the axially applied load ratio to the buckling load and the square ratio of the frequency of vibration does exist for the case of two dimensional frames, neglecting the small deviations from linearity due to experimental errors, as shown in figure A4-1, curve 1. His other curves on the same figure are due to insufficient power to obtain the same level of frequency modes, as in the case of curve 2. Where inconsistencies are found, no sound reason was given, except that of stating that a higher-energy state was occurring.

In figure A4-2, curve 1 seems to be linear when considering only the first 7 data points given experimentally, but Lurie claims that it is not so due to out of plane buckling of the tested rigid-jointed truss. In curve 2 of the same figure, he carried more loads on the structure at the lowest resonant frequency to obtain a nonlinear relation between the applied loads and the square of the frequency.

In a rather similar way, he carried out experiments on a flat rectangular isotropic plate, as shown in figures A4-3 and A4-4, stating that the method is not successful for this type of structures and the nonlinearities are due to the relatively large initial deflections encountered in practice.

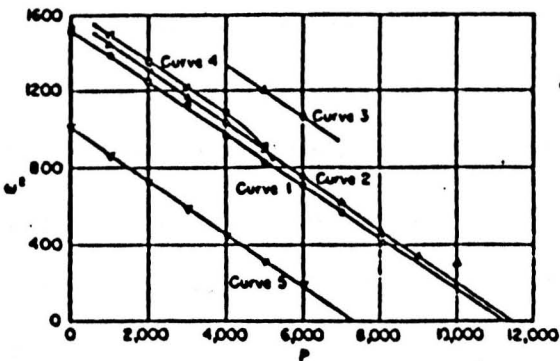


Figure A4-1
Truss - Lurie

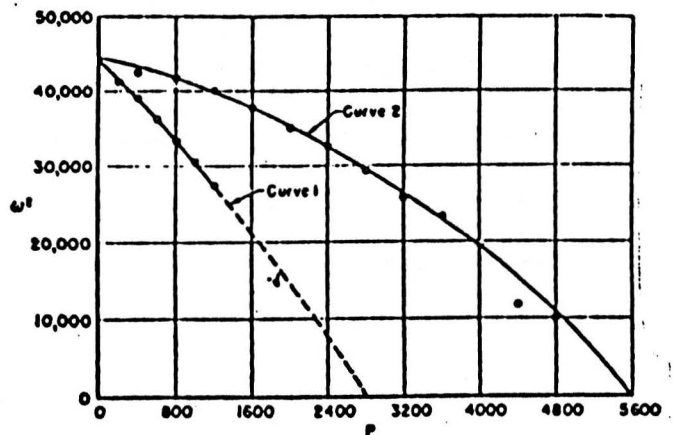


Figure A4-2
Truss - Lurie

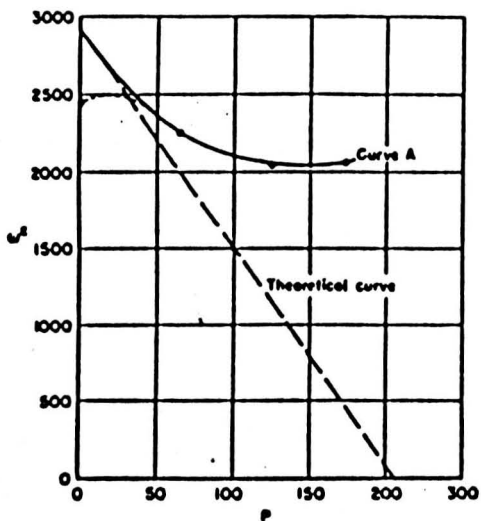


Figure A4-3

Rectangular Plate - Lurie

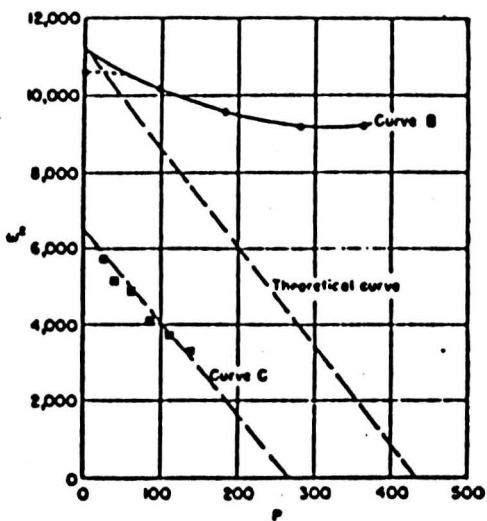


Figure A4-4

Rectangular Plate - Lurie

The graphs in figures A4- 5 and A4-6 were obtained by Kielb and Han, ref.[A2], in 1980. The first figure is for a fully clamped isotropic and rectangular plate where curves and lines are seen varyingly, depending on the aspect ratio (a/b) of the plate. The higher the aspect ratio, the closer to a linear relation is obtained between the applied loads and the square of the frequency factors. The second figure forms a summary of linear relations between the loads and the square of the frequencies for different boundary conditions around the plate. All the above results are based on theoretical grounds only.

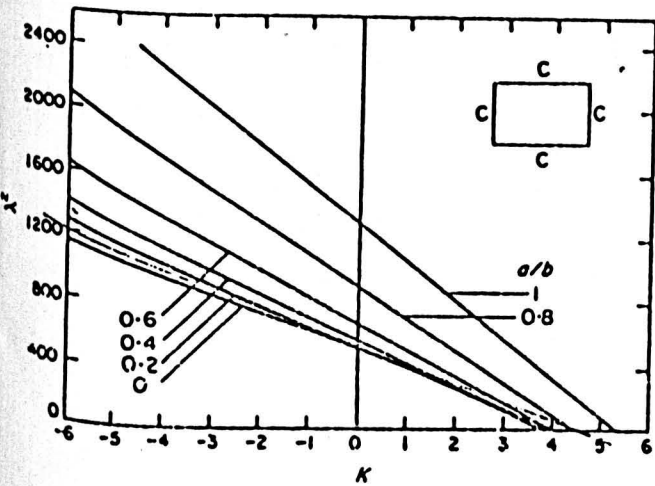


Figure A4-5
Kielb and Han

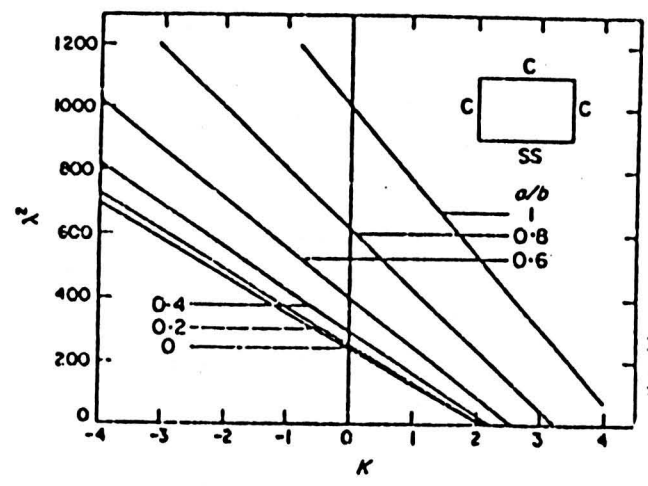


Figure A4-6
Kielb and Han

The graphs shown as figures A4-7 and A4-8 are reported by Steinert, ref.[A3], 1968 in a study of the buckling resistances of frame structures by measuring their natural frequencies, his results in figure A4-7 are linear for both symmetric and antisymmetric cases. Although his comparison with theory was not very close it indicates still the linear nature between applied loads and the square of the frequency of vibration of the frame.

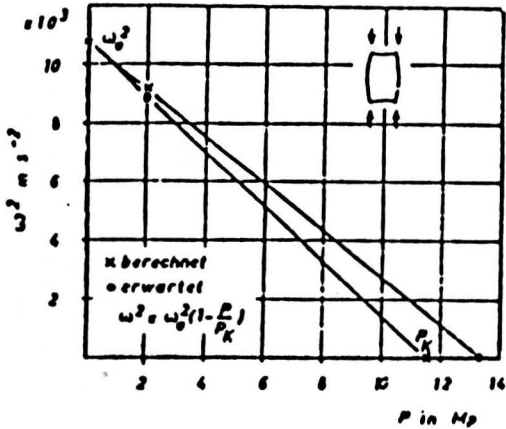


Figure A4-7

Frame - Steinert

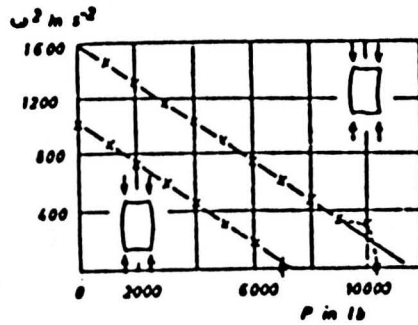


Figure A4-8

Frame - Steinert

Finally, the most recent work done by Ilanko and Tillman, ref.[A4] in 1985 on rectangular isotropic plates did not give any better clue on why this nonlinearity exists, instead, it gave the impression that the higher modes possess less energy and so they tend to be closer to the theoretical line. This statement is not feasible on both theoretical or physical grounds, since the energy should increase in the higher modes of vibration producing a wider gap between the modes of vibration and the modes of buckling. For this reason, this last work can not be a good example of progress towards the achievement of a full understanding of the relationship between the frequency ratio of vibration and the applied axial (in-plane) loads.

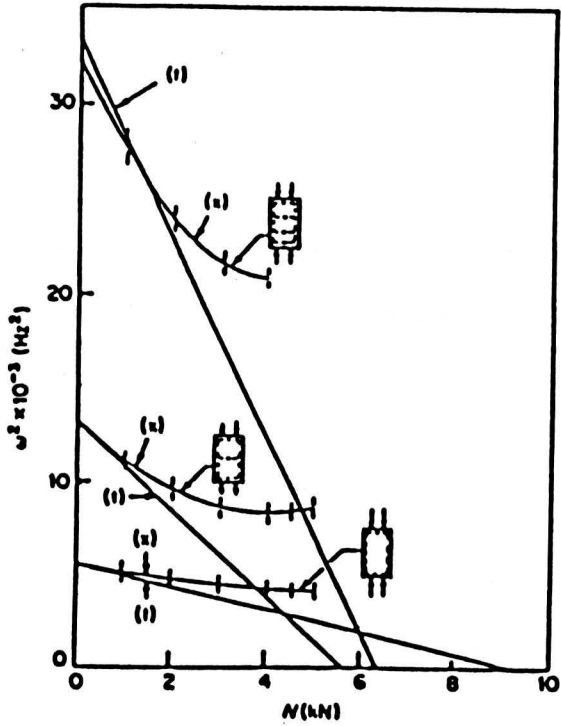


Figure A4-9

Ilanko and Tillman

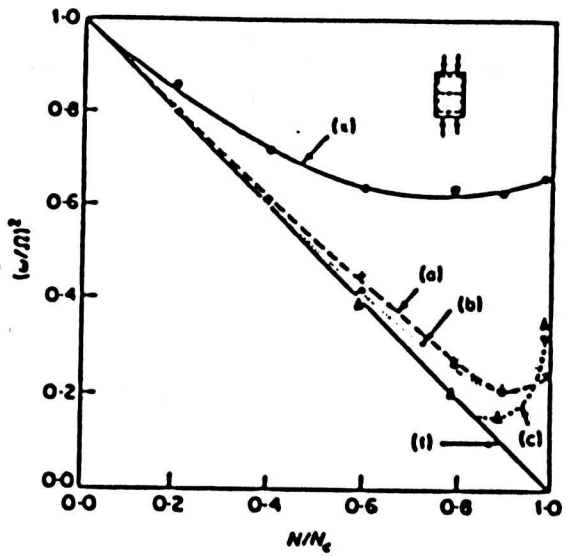


Figure A4-10

Ilanko and Tillman

To conclude, it is seen from the above graphs that there was a need for an experimental and theoretical correlation to verify the relationship between the frequency of vibration of a structure and the axial loads applied on it.

References:

A4.1) Lurie Harold," Lateral Vibrations as Related to Structural Stability," Journal of Applied Mechanics, Vol.19, 1952, pp. 195-204.

A4.2) Kielb R.E. and Han L.S.," Vibration and Buckling of Rectangular Plates Under In-plane Hydrostatic Loading," Journal of Sound and Vibration, 1980, Vol.70(4),pp.543-555.

A4.3) Steinert G.J.," Study of Buckling Resistances of Frame Structures by Measuring their Natural Frequencies," International Congress of Acoustics, Tokyo-Japan, 1968, G1-6, pp.21-24.

A4.4) Ilanko S. and Tillman S.C.," The Natural Frequencies on In-plane Stressed Rectangular Plates," Journal of Sound and Vibration, 1985, Vol.98(1),pp.25-34.

APENDIX 5

**Determination of the Elastic and
the Geometric Stiffness Matrices**

APPENDIX 5

DETERMINATION OF THE ELASTIC AND THE GEOMETRIC STIFFNESS MATRICES

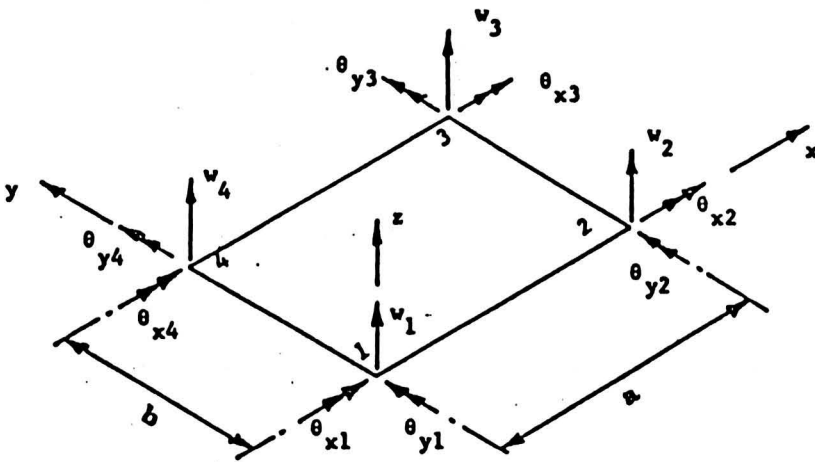


Figure A5-1

1) The Elastic Stiffness Matrix Determination:

1) Starting from a polynomial expression for the displacements,

$$\begin{aligned}
 W = & C_1 + C_2 x + C_3 y + C_4 x^2 + C_5 xy + C_6 y^2 + C_7 x^3 \\
 & + C_8 x^2y + C_9 xy^2 + C_{10} y^3 + C_{11} x^3y + C_{12} xy^3.
 \end{aligned}$$

eq.A5.1

Solving for the arbitrary constants using the following boundary conditions, note that the right hand rule is used for the vectors

$$\theta_x = \frac{\partial w}{\partial y} \quad \text{and} \quad \theta_y = - \frac{\partial w}{\partial x} \quad \text{eq.A5.2}$$

as shown in figure A5-2.

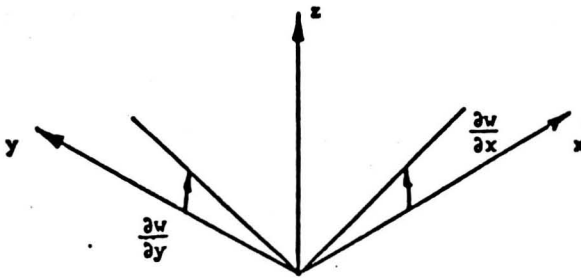


Figure A5-2

ii) The boundary conditions are represented in the following table:

Node	coordinates		displacements		
	x	y	w	θ_x	θ_y
1	0	0	w_1	θ_{x1}	θ_{y1}
2	a	0	w_2	θ_{x2}	θ_{y2}
3	a	b	w_3	θ_{x3}	θ_{y3}
4	0	b	w_4	θ_{x4}	θ_{y4}

Table-A5.1

The constants in equation A5.1 are determined as:

$$C_1 = W_1$$

$$C_2 = -a \theta_{y1}$$

$$C_3 = b \theta_{x1}$$

$$C_4 = 3 (W_4 - W_1) + a (2 \theta_{y1} + \theta_{y4})$$

$$C_5 = -W_1 + W_2 - W_3 + W_4 + a (\theta_{y1} - \theta_{y2}) - b (\theta_{x1} - \theta_{x4})$$

$$C_6 = 3 (W_2 - W_1) - b (2 \theta_{x1} + \theta_{x2})$$

$$C_7 = 2 (W_1 - W_4) - a (\theta_{y1} + \theta_{y4})$$

$$C_8 = 3 (W_1 - W_2 + W_3 - W_4) - a (2\theta_{y1} - 2\theta_{y2} - \theta_{y3} + \theta_{y4})$$

$$C_9 = 3 (W_1 - W_2 + W_3 - W_4) + b (2\theta_{x1} + \theta_{x2} - \theta_{x3} - 2\theta_{x4})$$

$$C_{10} = 2 (W_1 - W_2) + b (\theta_{x1} + \theta_{x2})$$

$$C_{11} = 2 (-W_1 + W_2 - W_3 + W_4) + a (\theta_{y1} - \theta_{y2} - \theta_{y3} + \theta_{y4})$$

$$C_{12} = 2 (-W_1 + W_2 - W_3 + W_4) - b (\theta_{x1} + \theta_{x2} - \theta_{x3} - \theta_{x4})$$

iii) Determine the shape functions by substituting for the arbitrary constants in terms of the displacements at the nodes of the element, we get:

$$W = \sum (N_{3i} - 2 W_i + N_{3i} - 1 \theta_{x1} + N_{3i} \theta_{y1}), \quad i = 1, 4.$$

eq.A5.3

where the values of N are represented in the following matrix:

$$\begin{bmatrix} N_1 \\ N_2 \\ N_3 \\ N_4 \\ N_5 \\ N_6 \\ N_7 \\ N_8 \\ N_9 \\ N_{10} \\ N_{11} \\ N_{12} \end{bmatrix} = \begin{bmatrix} -xA \{ xC + yE \} \\ bxyA^2 \\ ax^2AB \\ -xy \{ 1 + xC + yD \} \\ -bxy^2A \\ ax^2yB \\ 1 - xy + ACx^2 + BDy^2 \\ A^2Bby \\ -axAB^2 \\ -By \{ xF + yD \} \\ -by^2AB \\ -axyB^2 \end{bmatrix}$$

eq.A5.4

where,

$$\begin{array}{lll} A = 1 - y & C = 2x - 3 & E = 2y - 1 \\ B = 1 - x & D = 2y - 3 & F = 2x - 1 \end{array}$$

iv) To relate the displacements u_1, \dots, u_{12} to the displacement W we can write the following equation:

$$\{ W \} = [N_i] \{ u \}$$

eq.A5.5

where N_i matrix is previously given.

v) From the strain-displacement relations such as:

$$\begin{aligned} \epsilon_x &= -z \partial^2 W / \partial x^2 \\ \epsilon_y &= -z \partial^2 W / \partial y^2 \\ \gamma_{xy} &= -2z \partial^2 W / \partial x \partial y \end{aligned}$$

eq.A5.6

or, in matrix form of 3 X 12, the above equations could be rewritten as:

$$\underline{b} = -z \begin{bmatrix} \partial^2 N_i / \partial x^2 \\ \partial^2 N_i / \partial y^2 \\ 2\partial^2 N_i / \partial x \partial y \end{bmatrix}$$

eq.A5.7

then, the elastic stiffness matrix could be calculated from the equation:

$$K_S = \int \underline{b}^T E \underline{b} \, dv$$

eq.A5.8

The above equation is the same as equation 7.20 used in chapter 7, and the calculated elastic stiffness matrix based on the above equation is shown in section 7.3.2.

2) Geometric Stiffness Matrix determination:

We can use the same matrix N_i developed above in the equation:

$$K_g = \int \sigma_x N_i^T N_i dv \quad \text{eq.A5.9}$$

when calculated for the tested plate it gives the values of the matrix in section 7.3.1 of chapter 7.

Reference:

A5.1) Bhatt P., " Problems in Structural Analysis by Matrix Methods", The Construction Press, 1981.

